FLORIDA INTERNATIONAL UNIVERSITY

Miami, Florida

CHEMICAL PROFILING OF FENTANYL-RELATED SUBSTANCES (FRS) AND CANNABINOIDS BY GAS CHROMATOGRAPHY-INFRARED SPECTROSCOPY (GC-IR) AND GAS CHROMATOGRAPHY-MASS SPECTROMETRY (GC-MS) METHODS

A dissertation submitted in partial fulfillment of

the requirements for the degree of

DOCTOR OF PHILOSOPHY

in

CHEMISTRY

by

Kimiko Crystal Ferguson

2023

To: Dean Michael R. Heithaus
College of Arts, Sciences and Education

This dissertation, written by Kimiko Crystal Ferguson, and entitled Chemical Profiling of Fentanyl-Related Substances (FRS) and Cannabinoids by Gas Chromatography-Infrared Spectroscopy (GC-IR) and Gas Chromatography-Mass Spectrometry (GC-MS) Methods, having been approved in respect to style and intellectual content, is referred to you for judgment.

We have read this dissertation and recommend that it be approved.

Kenneth Furton

Piero Gardinali

David Becker

Shekhar Bhansali

Anthony DeCaprio, Major Professor

Date of Defense: May 30, 2023

The dissertation of Kimiko Crystal Ferguson is approved.

Dean Michael R. Heithaus
College of Arts, Sciences and Education

Andrés G. Gil
Vice President for Research and Economic Development
and Dean of the University Graduate School

Florida International University, 2023

DEDICATION

Dedicated to my late father, Noel Ferguson. I love you and I know that you are with me every day and extremely proud of me as you've always been. I hold our memories close to my heart forever. Continue to Rest in Peace.

Also dedicated to my mom, sister, and niece; the love and light in my life. I would be nothing without the love and support from you all in everything I do. I love you all.

This is for all of us!

ACKNOWLEDGMENTS

I thank God, the source of all my blessings. Thank you for keeping me safe in all aspects of my life through this entire journey.

Thank you to my initial research mentor Dr. José Almirall PhD; my dissertation and the research described herein could not have been possible without your ever valuable assistance. I owe so much of my success to you for accepting me into the research group and trusting me to conduct this important research project. Your support and guidance have been invaluable in overcoming the challenges and making sense of the message hidden within the data that I gathered. I am also grateful to the Almirall family and to former and current "A-Team" research group members for the lasting friendships we have built during my PhD. It was difficult conducting research during such an uncertain and unsettling time in the world, but we made it through. Thank you to Dr. Anthony DeCaprio for adopting me as a mentee when the need arose. I am thoroughly grateful for working with you over the past couple months in assisting me to get this far. I also want to thank my dissertation committee members, Dr. Piero Gardinali, Dr. David Becker, Dr. Kenneth Furton, and Dr. Shekhar Bhansali for providing me valuable support, criticism and encouragement during my studies through their thoughtful questions and advice.

I must also acknowledge the University Graduate School at Florida International University for its financial support through my PhD research with graduate assistantships. Thanks also to the Center for Advanced Research in Forensic Science (CARFS) through the National Science Foundation (NSF) for funding my research.

A special thank you to Analytical Solutions and Providers (ASAP) Analytical (Covington, KY) for the use of their IRD3 Detector, Essential EFTIR Software for the analysis of infrared spectra, access to the EUCLiD library, technical advice, and useful discussions. Thank you to Cerno Bioscience for providing the use of MassWorks and valuable conversations pertaining to analysis and the use of the software.

Finally, before the inception of my doctoral journey I've been blessed with a solid circle of love and support. My mother has always fostered my curiosity and independence. I am appreciative of your trust and confidence in my in all my pursuits in life; whether it be teaching, a leader in forensic science, or moving across the seas to be a student again in my adult life. I am forever indebted to you for loving me and helping to shape me as the person I am. I love you very much. My sister, words cannot express my gratitude for making me feel like the smartest person on the planet and making sacrifices you did not have to make in order for me to achieve my dreams. My love for you knows no bounds. Anyone who knows me knows how much my niece means to me. I am grateful for you and the opportunity to serve as your role model as you continue your own scientific journey. My whole life changed for the better when I found out you were coming, so thank you for influencing my positive redirection in life. I love you with my whole heart. Thank you all for laying the foundation for me to accomplish this dream I've had for a long time. This is for us!

I've been so blessed with an amazing circle of support in every aspect of my life within and without the dissertation journey, and I'm eternally grateful.

ABSTRACT OF THE DISSERTATION

CHEMICAL PROFILING OF FENTANYL-RELATED SUBSTANCES (FRS) AND CANNABINOIDS BY GAS CHROMATOGRAPHY-INFRARED SPECTROSCOPY (GC-IR) AND GAS CHROMATOGRAPHY-MASS SPECTROMETRY (GC-MS) METHODS

by

Kimiko Crystal Ferguson

Florida International University, 2023

Miami, Florida

Professor Anthony P. DeCaprio, Major Professor

Forensic laboratories are tasked with the identification of drugs like fentanyl using different confirmatory methods. Herein we report the efficacy of the identification of fentanyl-related substances (FRS) using GC-MS and GC-IR confirmation by way of newly constructed fentanyl libraries. Additionally, the utility of these libraries to the forensic community was validated through interlaboratory studies from seven (7) forensic laboratories. The efficacy of GC-MS and GC-IR for the confirmation of a small sample of phytocannabinoids and synthetic cannabinoids were also investigated. Finally, the use of MassWorks™ software to generate high resolution spectra from single quadrupole GC-MS was be explored in conjunction with high resolution QTOF-MS/MS.

New GC-MS and GC-IR libraries were created for 212 FRS and are now freely available to the forensic science community. A library search of each of the 212 FRS using the NIST

library produced 4.7% matches to the correct compound, which is not unexpected as most of the FRS were not included the NIST library. In contrast, 89.6% of the searches resulted in the correct compound within the top five candidates when using the newly created GC-MS library. Finally, when the new GC-IR library containing all 212 FRS was searched, 100% identification was achieved.

The results of the interlaboratory study showed improvement in identification of the FRS in question, increasing from ~75% using GC-MS to 100% correct when using vapor phase GC-IR analysis.

Phytocannabinoids fragment during GC-MS to produce easy to differentiate mass spectra. However, isomeric compounds of the synthetic cannabinoids resulted in some isomers being misidentified with those having similar mass spectra. This problem was resolved with the utilization of the GC-IR spectra.

In an effort to obtain high-resolution mass spectral data for fentanyl from single quadrupole GCMS data, MassWorks™ software was utilized. The accurate mass reported for the MassWorks™ data is often a fraction less than the actual value; while those generated by the high-resolution instrument are often a fraction more than the actual value. However, since the fentanyls only sparsely produce molecular ions with GC-MS, it is more useful to analyze using ESI-QTOF-MS/MS, where the molecular ion can be generated and analyzed.

TABLE OF CONTENTS

LIST OF TABLES

TABLE PAGE

LIST OF FIGURES

FIGURE PAGE

ACRONYMS AND ABBREVIATIONS

Δ^8-THC - Delta-8 Tetrahydrocannabinol

Δ^9-THC - Delta-9 tetrahydrocannabinol

AFIS - Integrated Automated Fingerprint Identification System

ASAP - Analytical Solutions and Providers

ASTM - American Society for Testing and Materials

ATR-FTIR - Attenuated Total Reflectance FTIR

BP - base peak

CBD – Cannabidiol

CBDA - Cannabidiolic Acid

CBG - Cannabigerol

CBGA - Cannabigerolic Acid

CBN - Cannabinol

CDC - Center for Disease Control

CFSRE - Center for Forensic Science Research and Education

CID - Collision Induced Dissociation

CNS - Central Nervous System

COC - Chain of Custody

CODIS - Combined DNA Index System

CSA - Controlled Substances Act

DC – Direct Current

DEA – Drug Enforcement Administration

DEA-STRL - Drug Enforcement Administration Special Testing Laboratory

EI - Electron Impact Ionization

ESI - Electrospray Ionization

EUCLiD - End User Contributed Library Identification

FAS-Kit - Fentanyl Analog Screening Kit

FIA - The Flow Injection Analysis

FIACS - Forensic Ink Analysis and Comparison System

FIU - Florida International University

FRC - Fentanyl-Related Compounds

FRS – Fentanyl-Related Substances

FTIR - Fourier Transform Infrared

GC-IR – Gas Chromatography Infrared Spectroscopy

GC-MS – Gas Chromatography Mass Spectrometry

HRMS - High resolution mass spectrometry

IBIS - Integrated Ballistic Identification System

ID - Internal Diameter

ILS – Inter-laboratory Study

IR - Infrared

KNN - k-nearest neighbor

LC – Liquid Chromatography

LOD - Limit of Detection

LOQ - Limit of Quantitation

MDBP - methylenedioxybenzylpiperazines

MMBP- methoxymethylbenzylpiperazines

m/z - mass to charge ratio

NFLIS - National Forensic Laboratory Information System

NIST - National Institute of Standards and Technology

NMR - Nuclear Magnetic Resonance

NPS - Novel Psychoactive Substances

OSAC - Organization of Scientific Area Committee

PIN - Personal Identification Number

PLSDA - partial least-squares discriminant analysis

Q-TOF - quadrupole time-of-flight

RF - Radio Frequency

SWGDRUG - Scientific Working Group for the Analysis of Seized Drugs

TOF - time of flight

USFDA – United States Food and Drug Administration

1. INTRODUCTION

"Fentanyl is the single deadliest drug our nation has ever encountered. Fentanyl is everywhere. From large metropolitan areas to rural America, no community is safe from this poison. We must take every opportunity to spread the word to prevent fentanyl-related overdose death and poisonings from claiming scores of American lives every day." – DEA Administrator Anne Milgram, 2022

1.1. Project Motivation and Significance

According to the Center for Disease Control (CDC), the number of drug overdoses recorded in 2021 was approximately 107,662 [1]. The number of fentanyl-related drug overdoses in the United States has seen an approximately eight-fold increase over the past few years, followed by deaths from prescription opioid and heroin deaths (**Figure 1**) [2]. According to CDC, between January 2021-January 2022 there was a reported 14% increase in opioid overdose from, 70,950 to 81,014 deaths reported, while deaths from synthetic opioids such as fentanyl increased 21%, from 58,908 to 71,450 [3]. The opioid epidemic in the United States is alarming because lives are being lost at an increasing rate. It is estimated that approximately 90 Americans die each day as a result of the opioid crisis, and this number continues to exponentially increase [4].

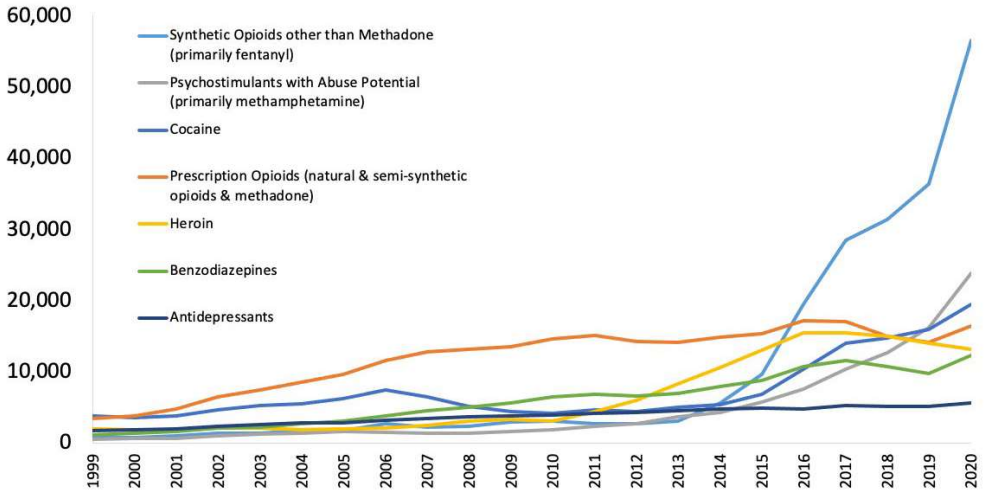

*Includes deaths with underlying causes of unintentional drug poisoning (X40–X44), suicide drug poisoning (X60–X64), homicide drug poisoning (X85), or drug poisoning of undetermined intent (Y10–Y14), as coded in the International Classification of Diseases, 10th Revision. Source: Centers for Disease Control and Prevention, National Center for Health Statistics. Multiple Cause of Death 1999-2020 on CDC WONDER Online Database, released 12/2021.

Figure 1. Number of national drug-involved overdose deaths among all ages, 1999-2020 [2].

Furthermore, the increase in fentanyl overdoses can be attributed to the increased availability of illicitly manufactured fentanyl [5]. Illicitly manufactured fentanyl includes many analogs, such as carfentanil, 2-furanyl fentanyl, acetyl fentanyl, etc., which are lethal in very small amounts [5]. It should be noted that these illicitly manufactured analogs often include those not meant for human use, for example carfentanil being used for larger animals like elephants. Hence, they are dangerous to humans in small amounts. In the past five years, there has been a steady increase in reports of seized fentanyl and fentanyl-related substances **(Figure 2)**. According to the National Forensic Laboratory Information System (NFLIS), fentanyl is now the fourth most identified drug nationally, the second most frequently analyzed by federal laboratories, and the number one reported narcotic analgesic nationally [1].

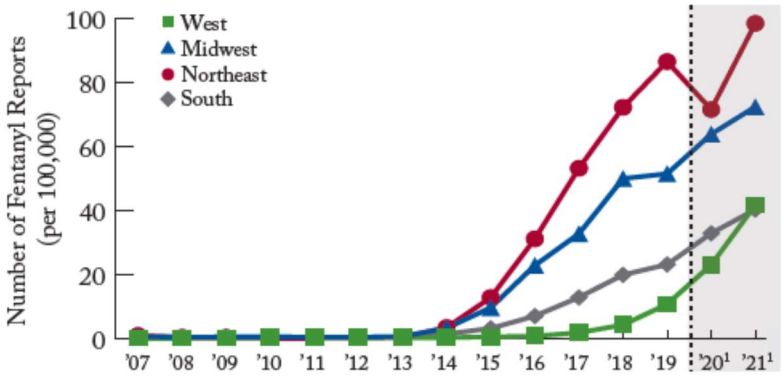

Figure 2. National and regional trend estimates of fentanyl in National Forensic Laboratory Information System (NFLIS), January 2007-December 2021 [1].

Additionally, results of the analysis of seized drugs have shown adulteration of illicit drugs such as heroin and cocaine with fentanyl without the knowledge of the user [6][7][8][9].Consequently, users are at great risk of dying from a fentanyl overdose without knowledge of the drug's presence. This adds to the already existent overdose problem, as fentanyl is lethal in even the smallest amounts [10][11][12], as little as 2 mg [12], and will most certainly result in an overdose if taken with drugs such as cocaine and heroin which are used in large amounts to achieve the high. Fentanyl is approximately 50-100 times more potent than morphine and 30-50 times more potent than heroin [13]. Since fentanyl can be absorbed through the skin, mouth, and inhaled in the air [12], it is imperative that first responders and emergency medical personnel carry Naloxone, which is an antidote to fentanyl [14]. Such exposures are dangerous to emergency responders in cases of overdose and also to those sent to seize the drugs. This uncertainty about the hazardous content of a drug seizure can quickly be alleviated if there is a method of rapid detection available without direct handling of the content. Therefore, it is imperative to develop means of rapid and safe identification of fentanyl and analogs present in a seizure. In 2021, the most

dominant form of fentanyl in the United States is *para*-fluorofentanyl [1]. This fentanyl analogue also has *ortho*-fluorofentanyl and *meta*-fluorofentanyl as related positional isomers. The identification of positional isomers of illicit drugs have often been a challenge due to the similarity in fragmentation patterns when utilizing GC-MS alone. Studies by Awad et al on the differentiation of methamphetamine and regioisomeric substances [15] have both shown the difficulty of GC-MS to differentiate isomers, while using GC-IR was effective for their differentiation.

According to the Center for Forensic Science Research and Education (CFSRE), in 2018-2022 there has been an addition of 36 new cannabinoids, second to opioids at 42 [16]. This addition of new cannabinoids often comes with the addition of positional isomers. Though GC-MS is often the gold standard in confirmatory testing in forensic laboratories, there is still the problem of the differentiation of positional isomers from each other. Studies conducted by Belal et al. on the differentiation of indole ring regioisomers of the synthetic cannabinoid JWH-007 [17] has shown the difficulty of GC-MS to differentiate the isomers. In the study, the mass spectra generated by the GC-MS were the same. However, the spectra of the GC-IR produced unique peaks allowing for differentiating the isomers from each other. In this study, the examination of the utility of GC-IR to differentiate difficult to differentiate isomeric synthetic cannabinoids will be employed. Additionally, it will be investigated if it is useful for differentiation of the phytocannabinoids.

A confirmatory analytical method which is able to provide a means of differentiation of the structure of the fentanyl analog as well as the cannabinoid in question will be useful to forensic analysis.

1.2. Hypotheses

GC-IRD data (IR in the gas phase) provides chemical information to facilitate structure elucidation and compound identification for both fentanyl and cannabinoids. The creation of a new fentanyl analogue library will facilitate more accurate identification of the FRS. A consensus-based standard method of GC-IRD analysis can be developed to improve fentanyl compound identifications using the information gathered from the inter-laboratory study results. The use of GC-IRD will also be useful for differentiating those isomers of cannabinoids which produce similar mass spectra using GC-MS. Therefore, the primary motivation for this research is to 1) build a GC-MS and GC-IR library of FRS, 2) validate the library, 3) conduct interlaboratory studies to assess the performance of the library and determine the repeatability of the GC-IR results, 4) conduct GC-MS and GC-IR studies on a small subset of synthetic and phytocannabinoids to determine if GC-IR is useful for the differentiation of their isomers, and 5) to determine if the GC-MS data obtained from the FRS can be converted to a high-resolution form which is comparable to data from an actual high-resolution mass spectrometry (HRMS) instrument.

1.3. Specific Project Goals

Aim 1: Development of a GC-IR and GC-MS Spectral Library of FRS

The original aim was to only analyze 150 fentanyl analog standards, since only these (i.e., Cayman Chemical Emergent Panels 1 and 2) were available at that time. However, and additional 62 analogs became available during the project since then (i.e., Cayman Chemical Emergent Panel 3), for a total number of 212 fentanyl related substances (FRS). A GC-IR and GC-MS spectral library was created with each of those FRS.

Aim 2: Validation of Libraries for Identification of FRS

The purpose of this aim was to test the utility of the databases using samples analyzed with their standard methods for fentanyl analysis in forensic laboratories. A second goal was to allow an understanding of the fentanyl analogs that are of most interest to these labs and assist them in the identification.

For this Aim, the Pinellas County Forensic Laboratory graciously accepted our request to visit their laboratory in order to carry out the validation, which occurred on June 10, 2021. The libraries created were shared with the lab ahead of time before our arrival. The lab director went through the list and identified which FRS are of most interest. These were then be run by GC-MS and GC-IR using their normal method. Since the laboratory already had the Analytical Solutions and Providers (ASAP) Analytical Essential Fourier Transform Infrared (FTIR) software, it was just a matter of utilizing the libraries we shared with them to conduct the search. The libraries will be tested for their ability to accurately identify the compounds selected by noting the number of compounds correctly ranked first and those in the top five.

In addition to Pinellas County, the Drug Enforcement Administration Special Testing Laboratory (DEA-STRL) also agreed to participate in the validation.

Aim 3: Interlaboratory Study for Analysis and Identification of FRS

The inter-laboratory study design aimed to assess the inter-laboratory repeatability of the GC-IR methods and the performance of the libraries developed. Seven (7) laboratories agreed to participate and a prerequisite to participation is the possession of the Fentanyl

Analog Screening Kit (FAS-Kit) and the four Emergent Panels from Cayman Chemical. Twenty samples from the kit were selected for analysis and communicated to a designated official from the laboratory who prepared the blind samples; at least eight (8) sets of isomers were included. Participants analyzed the samples by both GC-MS and GC-IR using each laboratory's specific standard method for analysis, with analysis done by an analyst not involved with the sample preparation. The resulting spectra generated were utilized for searching with our Agilent MSD Chemstation library and the FIU ASAP FTIR library. The performance was assessed based on the number of correct identifications. Each of these will be converted to a percentage.

Aim 4: GC-IR and GC-MS Analysis of Phytocannabinoids and Synthetic Cannabinoids

Based on the success of the performance of the GC-IRD to differentiate the positional isomers of the FRS, the same analytical method will be used for the analysis of cannabinoids. For this study, a sample of phytocannabinoids will be analyzed as well as positional isomers of select synthetic cannabinoids. Spectra will be acquired using GC-IR and GC-MS and a library of the cannabinoids will be created. The library will be searched to assess if there are any difficulties in identification of samples analyzed by GC-MS. If so, the GC-IR library will be searched to see if it provides correct identification of the compound in question.

Aim 5: Use of Cerno Bioscience's MassWorks™ Software to Convert Single Quadrupole GC-MS Data of FRS to High Resolution Data Capable for Use in Spectral Accuracy

This aim was added after all previous experiments were complete. It aims to explore the usefulness of the software in converting the single quadrupole data to high resolution data,

creating better distinguished GC-MS spectra for some hard-to-differentiate positional isomers. Furthermore, the MS spectra produced by the MassWorks software will be compared with those generated from a high-resolution mass spectrometry instrument to verify the accuracy. Their values will be compared to each other as well as to the exact mass value.

Aims 4 and 5 were not original aims but were added as the research progressed.

1.4. Dissertation Overview

Chapter 2 will give a general overview of literature on fentanyl and its analysis. Fentanyl chemical structures and analysis will be covered. Furthermore, difficulties with the analysis of these chemical structures will also be discussed.

Chapter 3 will detail the background of the instruments utilized in the research completed. This includes details of the use of gas chromatography-mass spectrometry (GC-MS) and gas chromatography-infrared spectroscopy (GC-IR), their configuration and use in drug analysis and identification.

The details of the materials and methods used in the scientific investigations will be elaborated in Chapter 4.

Chapter 5 discusses the utility of GC-IR libraries for the differentiation of positional isomers of fentanyl-related substances (FRS). This includes details of the design of the study, the results of the library searches, and the limit of detection (LOD) and limit of quantitation (LOQ) results.

Chapter 6 presents specifics on the inter-laboratory study (ILS) for fentanyl analysis done. Details of the inter-laboratory instructions as well as the ILS results are presented and discussed.

Chapter 7 explores the analysis of cannabinoids by GC-MS and GC-IR. The usefulness of the analytical methods for the analysis of phytocannabinoids and synthetic cannabinoids will be discussed. Additionally, the limit of detection (LOD) and limit of quantitation (LOQ) results of each sample will be detailed.

In Chapter 8, the use of the MassWorks™ software in producing high-resolution mass spectra and its spectral accuracy performance will be explored. Additionally, the high-resolution spectra produced from the software will be compared those produced from an actual high-resolution mass spectrometry instrument; the ESI-QTOF-MS/MS.

Finally, in Chapter 9 the overall conclusions and possible future directions of the research project will be elaborated.

2. INTRODUCTION TO THE ANALYSIS OF CONTROLLED SUBSTANCES; REVIEW OF LITERATURE

2.1 Controlled Substances in the U.S.

Drugs are substances introduced into the body which affect the function of the body. Some drugs help the body to function properly and are available with prescription from a medical provider, however, they may have the potential to be abused outside of their prescribed use. For this reason, the United States has adopted the practice of scheduling drugs. Under the Controlled Substances Act (CSA), substances are placed under five schedules based on the following [18]: potential for abuse, known scientific evidence of beneficial medical and pharmacological effects, current scientific knowledge of the substance, history and current pattern of abuse, duration and significance of abuse, risk to public health, psychic or psychological dependence liability, and whether the substance is an immediate precursor of an already scheduled substance [18]. Schedule I is the most restrictive and includes drugs with high potential for abuse/addiction and no medical use e.g. heroin, with the potential for abuse/addiction decreasing and medical use increasing as the schedule increases to Schedule V (e.g., cough suppressants) [19] . The Federal Analog Act, under the US Controlled Substances Act, was passed 1986 in response to the causative agent in numerous overdoses by fentanyl analogs. This allowed for controlled substances analogues to be treated as Schedule I substances and established criminal penalties for the possession of controlled substances [10][18]. From the 1990's to today, the majority of federal drug legislation has addressed concerns over synthetic drugs including fentanyl [18] and the work continues with the constantly evolving drugs trade.

2.2. History and Predominance of Fentanyl

Fentanyl, a synthetic opioid, was first synthesized in 1960 by Paul Janssen in Belgium as a medicine used to treat pain, and was approved by the United States Food and Drug Administration (USFDA) as an intravenous anesthetic in 1972 under the name Sublimaze® [10]. Today, the Drug Enforcement Administration (DEA) has determined that two primary routes of illicit manufacture of fentanyl exists – The Janssen synthesis route and the Siegfried method [20]. The Janssen route is patented for original synthesis of fentanyl and is beyond the skill of clandestine manufacturers; however the detection of the benzylfentanyl impurity from the analyzed product is an indicator of the Janssen route of manufacture. The Siegfried method involves the use of N-phenethyl-4-piperidone (NPP) as the starting material which is used to produce the immediate precursor to fentanyl, 4-anilino-N-phenethyl-4-piperidone (ANPP). The presence of ANPP without the presence of benylfentanyl is an indicator of the Siegfried method of manufacture.

Since being approved, there has been a steady increase in consumption of licit fentanyl, in addition to proliferation of illicit manufacture and overdose from fentanyl and its analogues [10]. The drug has evolved rapidly with the development of several analogs, with the prescription and veterinary-use fentanyl analogs now DEA Schedule II [10]. Fentanyl is powerfully addictive due to its intense euphoric effects [21], causing severe physical and psychological withdrawal symptoms in its user. The addict becomes a danger in their communities when their desire for the drug outweighs their aversion to criminal activities. The popularity of the drug is fueled both by higher quality product, cheaper prices and wider proliferation. Studies have also linked an over-prescription of opiate-derived pain medications as the main gateway to fentanyl use [22]. Recreational use of pain medication

gives way to habitual use and, ultimately, to addiction [5]. Opioids like fentanyl are depressants of the central nervous system, causing respiratory suppression and cardiac arrest during an overdose [22].

Many fentanyl analogues have since been produced for medicinal and veterinary use, as well as illicitly. In 1979, the causative agent for an outbreak of overdoses in California was deemed to be alpha-methylfentanyl, and in 1984, 3-methylfentanyl was responsible for overdoses in Pennsylvania [10]. There were at least 10 fentanyl analogs identified in the illicit market in the mid-to-late 80's which were responsible for >100 overdose deaths from 1979 to 1991 [10]. In 2013 and 2016, there was the emergence of acetyl fentanyl and butyryl fentanyl, respectively, which were responsible for numerous deaths in the northeastern United States [10]. As the number of fentanyl analogs and overdoses began to increase, there were changes in the laws to follow in order to control possession of these synthetic opioids.

According to NFLIS data from 2021, the northeastern United States continued to see a significant increase in fentanyl reports between 2020-2021, while the Midwest, West, and South increased substantially beginning in 2014 [1]. The West reported the highest percentage of fentanyl (77%) reports, followed by the Midwest and Northeast (60% each) [1]. Of the narcotic analgesics reported, fentanyl (60%) accounted for more than half, while the precursor ANPP (6%), fluorofentanyl (4%), and *para*-fluorofentanyl (3%) were included in >25% of the cases [1]. In 2019, neither fluorofentanyl nor its associated isomers appeared in the top 25 drugs; however, by 2021, fluorofentanyl was the 12th most frequently reported drug and the 6th most frequently reported narcotic analgesic, while

para-fluorofentanyl was the 16th most frequently reported drug and the 7th most frequently reported narcotic analgesic [1].

2.3. Chemistry of Fentanyl and FRS

Fentanyl is a synthetic opioid used for treating severe pain in clinical settings. However, due to its high potential for abuse as a Schedule II drug, it is produced using illicit manufacture processes for sale in the illegal drug trade.

The basic structure of fentanyl consists of an amide group, a piperidine ring, an aniline ring, and an N-alkyl chain, each of which provides the regions of substitutions that alter the structure of illicit fentanyl analogs **(Figure 3)** [23]. These substitution regions are altered by producers on the illicit market and contribute to the diversity of fentanyl analogs currently in existence. Currently, there is an emerging trend of fluorofentanyl proliferating the United States illicit market [1] resulting from substitution of fluorine on the aniline ring of the structure.

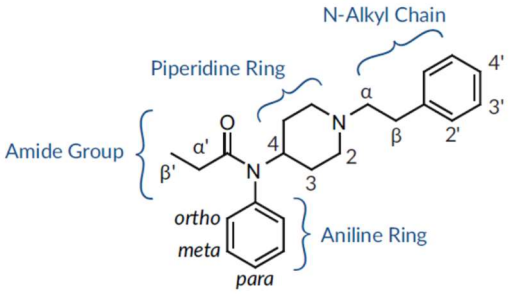

Figure 3. Regions of potential substitutions on the fentanyl scaffold [23].

The pharmacological action of opioids like fentanyl and heroin is through the interaction with G protein-coupled opioid receptors in the central nervous system (CNS) [24]. Here, fentanyl is an agonist primarily for the mu (μ) receptor, closing Ca^{2+} channels on

presynaptic nerve terminals reducing neurotransmitter release and opening K^+ channels inhibiting postsynaptic neurons [25], [26]. Stimulation of the μ receptor produces effects such as euphoria, analgesia, respiratory depression, etc. [25] , characteristic of depressants like opioids. The fentanyl is then metabolized to norfentanyl and excreted from the body [27].

2.3.1. Chemical Structure and Implications on Analysis of FRS

The structure of fentanyl and FRS determine the spectra produced using the respective analytical methods involved in their structural elucidation. There are steps involved in the sample acquisition and preparation processes for FRS before analysis in forensic laboratories. These are detailed below as well as information on how the chemical structure of fentanyl affects analysis using GC-MS and some remediation methods used to overcome these problems.

2.3.1.1. Analytical workflow of FRS in a forensic laboratory

The privilege of observation of the work flow of fentanyl analysis was provided by a visit to the Pinellas County Forensic Laboratory Drug Analysis Unit. An overview of the steps involved in fentanyl analysis was obtained through observation of the working of an actual case.

The first step, as in any forensic laboratory, is the inspection of packaging at the evidence management area. Here, the package is inspected to ensure that there is no breach in the heat sealed transparent plastic evidence bags. The information from the Chain of Custody (COC) on the evidence bag is barcoded at the laboratory for easy identification in their

laboratory information management system. The electronic COC matches with the evidence being brought in and is signed electronically with a personal identification number (PIN) used by laboratory employees; only non-lab employees submitting and receiving evidence need a written signature since they do not have the PIN assigned for laboratory employees.

When the evidence reaches the analyst in the laboratory, the barcode is scanned and the COC is inspected for the request for analysis. The analyst ensures the details on the evidence matches those in the database, accurately describing the evidence in the database. The analyst then obtains the gross weight of the evidence brought in. The bag is then transferred under the hood and a composite sampled from all four corners and the center is obtained as the net weight is recorded. This sample is what will go into the analytical tubes for dilution and subsequent analysis.

The samples are then taken for screening and confirmatory tests. The first screening test is the Marquis test, which presumptively identifies alkaloids and which is also used as a presumptive test for opiates and opioids. A color change to a deep purple denotes an opiate or opioid, while an orange coloration indicates possible fentanyl [28]. Next, the cobalt thiocyanate/stannous chloride test (Young's test) is performed. This test is principally for cocaine and gives a blue coloration indicating positivity. Confirmatory tests such as thin layer chromatography, GC-MS, and gas phase GC-IR are then performed, followed by a library search to determine the possible identity of the drug in question. The GC-MS and gas phase GC-IR analytical methods are detailed in the following subchapter.

2.3.1.2. Presumptive tests of FRS

Presumptive tests for opioids indicate that opioid alkaloids may be present but are not specific, as many other compounds give similar color results using the test reagents. Therefore there is a requirement of additional confirmatory techniques [29].

The Marquis test, consisting of 40% formaldehyde added to 10 mL concentrated sulfuric acid, is widely used as an opioid field test and can also be used as a field test for fentanyl. For common opiates and opioids, a purple color indicates a positive test result; however, for fentanyl an orange color indicates the presence of fentanyl [28].

One abnormality in the presumptive test of fentanyl is recorded in literature. The cobalt thiocyanate test gives anomalous results when used on fentanyl. This test, when used on cocaine containing substances, produces a blue color which is indicative of the presence of cocaine [30]. Cocaine contains unshared electrons on its nitrogen atom which form a coordination compound with the cobalt thiocyanate, forming a blue color [30]. Fentanyl, when tested with cobalt thiocyanate, produces the same characteristic blue color as does cocaine hydrochloride [30], leading to a false positive for cocaine. To increase the specificity of the test for cocaine, a second step involving addition of aqueous stannous chloride solution is added (collectively referred to as the Young's test). The blue color remains if cocaine is present and disappears if procaine, lidocaine, or tetracaine is present [30]. .

To further increase the specificity of the test for cocaine, the Scott's test may be performed. The Scotts reagent is made of deionized water, cobalt thiocyanate, and glycerol. In the first step, a small amount of the Scotts reagent is added to the test material and will develop

a blue color if cocaine is present [28]. In the second step, one drop of hydrochloric acid is added, and a disappearance of the blue color indicates a positive for cocaine [28]. In the final step, five drops of chloroform is added, and if the blue color reappears in the lower chloroform layer this indicates a positive for cocaine [28]. The Scott's test for cocaine which truly shows a negative for fentanyl, due to the disappearance of the blue color after adding the hydrochloric acid.

There are numerous other field test kits which are used to presumptively test for fentanyl. There are some which are largely useful for toxicology purposes for analysis in body fluids in healthcare settings such as those utilized in the study by Wharton, et al [31]. Additionally, drug users may do presumptive testing on their own utilizing rapid fentanyl test strips in an effort to avoid fentanyl overdose through inadvertent adulteration of their drug of choice with fentanyl [32]. These single-use immunoassay tests involve placing a diluted portion of the drug in the test well and reading the results; test reads positive (single red line) or negative (two red lines) for the presence of fentanyl [32]. If the result is positive, the drug user knows there is adulteration with fentanyl which can be fatal.

Confirmatory testing follows presumptive testing to definitely identify the compounds in question. A common method of confirmatory testing for drugs employs GC-MS methods as detailed below.

2.3.2. GC-MS Analysis of Fentanyl

Forensic chemists have the task of deciphering the structure of chemical compounds assumed to be drugs which are provided to the laboratory for analysis. To accomplish this, there are numerous analytical chemistry methods employed. One such method is gas

chromatography mass spectrometry (GC-MS). This method ionizes compounds and separates them by mass to charge ratio. One of the first reports of the use of GC-MS for the analysis of fentanyl was in 1981 by the Department of Anesthesiology at the University of Texas Medical School [24], [33]. Though GC-MS is considered the gold standard for analysis in forensic laboratories, it is not without its limitations for fentanyl analysis.

A recent publication from Cayman Chemical reports on the difficulty of unambiguous identification of some of the fentanyl analogues by MS, due to the ambiguous fragmentation information and the common absence of molecular ion peaks [23]. Additionally, some fentanyl analogs differ so slightly that they have the same mass spectra, making identification by GC-MS alone difficult.

Law enforcement often depends on MS spectral libraries for the characterization of seized drugs, but these are useless if some of the drugs, like fentanyl analogs, are continuously being produced and not characterized as yet. In fentanyl, the molecular ion is not produced in the spectra, therefore the molecular weight is not easily identified [23]. In order to help discern the molecular weight of the FRS, there are four (4) common fragmentation patterns reported by Cayman Chemical:

Pattern 1:

Cleavage between the α and β carbons of the ethyl heterocyclic linker, resulting in the base peak (BP) ion:

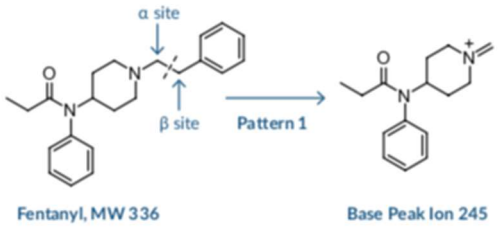

Figure 4. Fragmentation Pattern 1. Cleavage between the α and β carbons of the ethyl heterocyclic linker, resulting in base peak (BP) ion [23].

In this case, the BP corresponds to the primary cleavage of the compound, with occurs between the α and β carbons on the phenethyl moiety or similar chain [23]. For example, the presence of m/z 91, the tropylium ion, in the spectra strongly indicates a phenethyl group and the molecular weight of the compound will be equal to the addition of m/z 91 to the BP [23]. If a group other than a phenethyl is attached to the piperidine ring, an ion fragment at m/z 81 is seen and not m/z 91 [23]. For substituted fentanyl with a hydroxyl group in the β position, such as β-hydroxy fentanyl, primary cleavage occurs at the α and β carbons, but a smaller fragment will be observed as the molecular ion minus 18 for the loss of water from the molecule [23]. An exception to this pattern occurs when the phenethyl moiety is replaced with a N-benzyl or N-methyl moiety, such as in benzyl fentanyl, where the molecular ion is noticeable along with the BP of m/z 91, resulting from the cleavage between the piperidine ring and the benzyl group [23].

Pattern 2:

Additional cleavage of the BP ion occurs along the piperidine ring and at the amide C-N bond [23]:

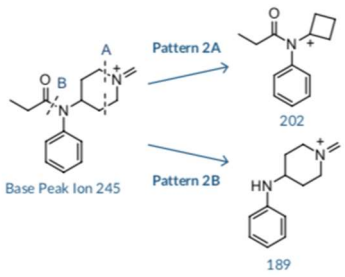

Figure 5. Fragmentation Pattern 2. Additional cleavage of the BP ion occurs along the piperidine ring and at the amide C-N bond [23]

The BP ion first undergoes cleavage along the piperidine ring (Pattern 2A), eliminating the nitrogen and two carbons to form a cyclobutyl group of m/z 202 [23]. The second cleavage occurs along the C-N amide bond to produce a peak with an abundance of 30-60% of the BP (Pattern 2B) [23]. These masses will be different depending on the substitutions on the piperidine group, amide group, or aniline ring [23]. Subtracting the mass of this fragment from the BP will give the mass of the acylium ion [23].

Pattern 3:

Subsequent cleavage at either the piperidine ring or the amide C-N bond of the secondary fragments results in a third characteristic fragment [23]:

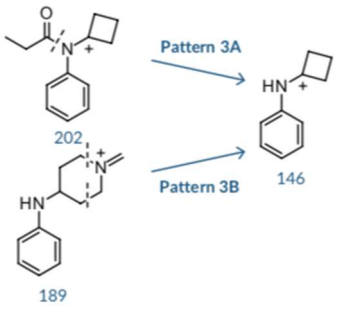

Figure 6. Fragmentation Pattern 3. Subsequent cleavage at either the piperidine ring or the amide C-N bond of the secondary fragments results in a third characteristic fragment [23].

This fragmentation pattern results from cleavage along the amide bond and additional cleavage within the piperidine ring [23]. In the example of the fragment of fentanyl in Figure 6, cleavage of the amide C-N bond of m/z 202Pattern 3A, forms fragment 146 and cleaving the piperidine ring of ion 189 amu, Pattern 3B, yields ion 146amu [23]. The ratio between 146 amu and 189 amu is almost always > 1, unless there is a branched alkyl group or closed alkyl ring system present [23]. Therefore, if the 146 and 189 peaks are present in the spectra, the unknown will most likely be a fentanyl-like compound without substitutions on the piperidine or aniline regions. If those peaks are absent, this indicates a substitution on the aniline or piperidine ring [23].

Pattern 4:

Cleavage at the amide C-N bond will generate the BP if a highly stabilized or highly substituted group is present in the acyl region [23]:

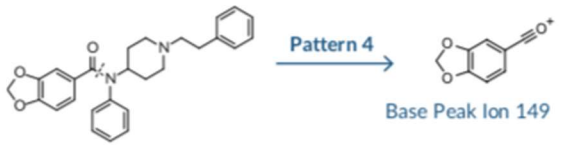

Figure 7. Fragmentation Pattern 4. Cleavage at the amide C-N bond will generate the BP if a highly stabilized or highly substituted group is in the acyl region [23]

If the primary cleavage occurs along the amide C-N bond to generate the BP instead of between the α and β carbons, then a highly resonance-stabilized group is likely substituted in the R_1 position [23].

These observations offer assistance in interpreting the possible structure of an observed fentanyl molecule based on the fragmentation pattern. However, since isomeric forms of fentanyl may have similar fragmentation patterns, another unambiguous means of identification must be employed to offer confirmation of the compound in question. One analytical method that offers greater discriminating power and offers more structural information is GC-IR. This method will be explored in detail in Chapter 3.

In studies done by Feeney, et al., spectral trends observed in GC-EI-MS data of fentanyls were studied [34]. The BP ions produced are often linked to the structure and regions of substitution. BP ions of 245 m/z and 259 m/z result from the breaking the bond between the phenethyl chain and piperidine ring (with the base peak of 259 retaining the methyl group on the fragment ion, while that containing 245 losing the methyl group) [34]. Those with a base peak ion of 91 m/z have a N-benzyl or N-methyl substitution at the core structure, while those with an ion of 95 m/z undergo cleavage of the bond along the amide C-N bond [34].

These fragmentation patterns often produce confounding compound identifications that must be overcome by forensic analysis. One method utilized was the mass spectral mapping of fentanyl analogs of Type I fentanyl analogs (those molecules differing from fentanyl be a single modification) [35]. This library searching technique allows for the correct identification of unknown fentanyls which belong to Type I, but are inaccurate for those belonging to Type II [35]. As a result, there needs to be a more inclusive library searching tool available to the forensic community.

2.4. Chemistry of Cannabinoids

Cannabinoids may be of natural or man-made origin. The natural cannabinoids are known as phytocannabinoids (plant cannabinoids) and endocannabinoids (brain-derived), while the man-made cannabinoids are known as synthetic cannabinoids. The study focuses on the phytocannabinoids and synthetic cannabinoids..

Herbal cannabis includes the parts of the plant (except seeds and woody stalk material) *Cannabis sativa*, which can be grown in all parts of the world [25]. The active substance in *Cannabis sativa* is cannabinoids, which is mainly concentrated in the resin of the plant particularly in the flowering area, leaves, and stem [25]. The main psychoactive cannabinoids concentrated in the cannabis and cannabis resin is Δ^9-tetrahydrocannabinol (Δ^9-THC), with cannabinol (CBN) and cannabidiol (CBD) also among the main components [25]. CBN is a major breakdown product of Δ^9-THC and cannabinol is a pre-cursor to Δ^9-THC [25]. Cannabigerol (CBG) is found in high concentrations in younger plans but in lower concentrations in more mature plants [36]. These cannabinoids bind to

specific G-protein-coupled cannabinoid receptors (CB1 receptors in the brain, lung, and kidney, and CB2 receptors in the immune system and in the hematopoietic cells), with Δ^8-tetrahydrocannabinol (Δ^8-THC) having a lower affinity for the CB1 receptor than Δ^9-THC [25]. Binding of THC to the receptor results in inhibition of adenylate cyclase and in calcium ion channel inhibition and potassium channel activation, producing a feeling of euphoria and heightened sensory awareness and distortion of time, sound, and color followed by a feeling of relaxation [25].

Synthetic cannabinoids are not found in nature, but are synthesized in a laboratory. They have similar biological effects as the phytocannabinoids and bind to the same cannabinoid receptors in the body [37]. However, these are more potent than the phytocannabinoids. These chemicals are often sprayed on plant material and smoked, and are commonly known as "spice" or "K-2". There are a wide range of synthetic cannabinoids as will be detailed later on in the chapter.

2.4.1 Structure and Chemistry of Phytocannabinoids

Cannabis use is often linked to the effects of the psychoactive phytocannabinoids present. Though there are a variety of phytocannabinoids in existence, only the most commonly encountered phytocannabinoids will be explored in this section of the dissertation. Additionally, the analytical methods routinely utilized in their analysis will be discussed. There are >100 cannabinoids found in cannabis, which are further divided into 10 subclasses [36]. In order to remain within the scope of the phytocannabinoids studied, the focus will be on the phytocannabinoids listed in **Table 1**.

Table 1. Phytocannabinoids involved in this study and their structure

Phytocannabinoid	Structure
CBD	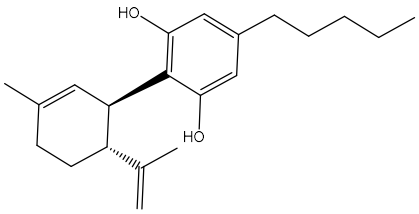
CBG	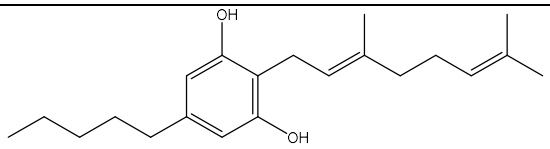
CBN	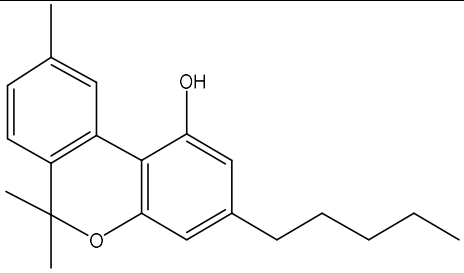
Δ^8-THC	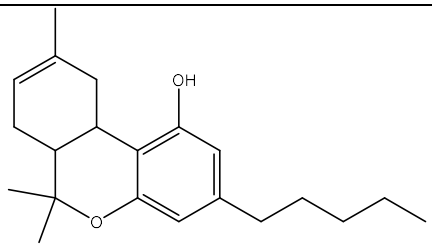

Δ^9-THC	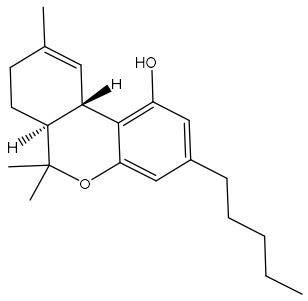

CBD's structure was first elucidated in 1963 by Mechoulam and Shvo. CBD and its corresponding acid, cannabidiolic acid (CBDA), are the most abundant cannabinoids in industrial hemp [36]. CBG was the first cannabinoid identified, and its precursor cannabigerolic acid (CBGA) was discovered as the first biogenic cannabinoid formed in the plant, which are pharmacologically useful as antibiotics, antifungals, and analgesics [36]. CBN is mainly an oxidation artifact of THC and CBD, respectively, with main pharmacological characteristics consisting of sedative, antibiotic, and anticonvulsant effects [36]. The Δ^8-THC is considered a Δ^9-THC artifact, being 20% less active than Δ^9-THC [36]. Finally, Δ^9-THC is the main psychoactive compound in cannabis, with THC acid A being the main biogenic precursor and first structurally identified in 1964 [36].

2.4.2 Structure and Chemistry of Synthetic Cannabinoids

According to the 2022 second quarter trend report from the Center for Forensic Science Research and Education (CFSRE), opioids account for 17% of novel psychoactive substances (NPS) tested and synthetic cannabinoids account for 3% [38]. Synthetic cannabinoids were first synthesized in the 1970's in an effort to develop treatments for cancer pain [37]. Their diversity in structure lead to grouping them into classes known as

classical cannabinoids, non-classical cannabinoids, hybrid cannabinoids, aminoalkylindoles, eicosanoids, and others [37].

The classical cannabinoids are based on a dibenzopyran ring and include compounds that are structurally similar to those which occur naturally in the cannabis plant like Δ^9-THC; examples including HU-210 and others from the HU series [37]. The non-classical cannabinoids include bicyclic and tricyclic structures and analogs and include compounds that are quite similar to the classical cannabinoids with regards to the alkyl chain attached to the central phenol moiety of the compound. Examples include the CP family of cannabinoids [37]. Hybrid cannabinoids have a combination of classical and non-classical structural features; examples include AM-4030 because it has the dibenzopyran ring that is common to classical cannabinoids and an aliphatic hydroxyl group common in the CP family of the non-classical cannabinoids [37]. The structures of classical, non-classical, and hybrid cannabinoids are shown in **Figure 8**.

The aminoalkylindoles are structurally dissimilar to Δ^9-THC but maintain cannabimimetic properties and are often the most common synthetic cannabinoids encountered in illicit products [37]. The class is further divided into:

1. Naphthoylindoles – e.g. JWH-015, JWH-018, JWH-073, JWH-122, JWH-200
2. Phenylacetylindoles – e.g. JWH-250, JWH-251
3. Benzoylindoles – e.g. AM-694, RSC-4
4. Naphthylmethylindoles – e.g. JWH-184, JWH-196, JWH-192
5. Cyclopropoylindoles – e.g. UR-144, XLR-11
6. Adamantoylindoles – e.g. AB-001, AM-1248

7. Indole carboxamides – e.g. APICA, 5F-APICA.

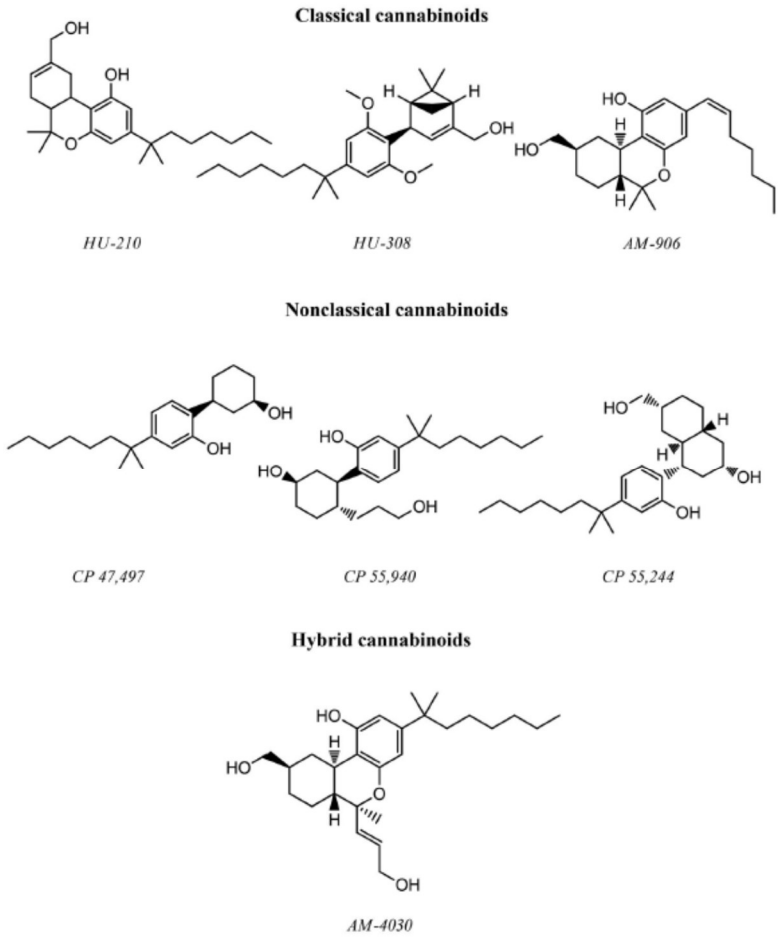

Figure 8. Chemical structure of some examples of classical cannabinoids, nonclassical cannabinoids, and hybrid cannabinoids. Figure taken from [37].

Eicosanoids are synthetic analogs of endocannabinoids, such as anandamide (e.g. methanandamide) [37]. Those cannabinoids which do not fit in the previously mentioned classes are grouped into "other"; e.g. diarylpyrroles (e.g. SR141716A), naphthoylpyrroles (e.g. JWH-307) and naphthtylmethylindenes (e.g. CRA-13) [37]. **Table 2** below provides examples of the structures of the classes previously mentioned.

Table 2. The main classes of synthetic cannabinoids, detail of their structure, and examples. Table derived from [37].

Synthetic Cannabinoid Class		Examples
Classical Cannabinoids	Similar structure to Δ9-THC; Derivatives of dibenzopyran	HU-210; HU-211; HU-208; HU-311; AM-906, AM-411, O-1184
Nonclassical Cannabinoids	Structure quite similar to classical cannabinoids; Derivatives of cyclohexylphenol; Bicyclic and tricyclic analogs to Δ9-THC	CP 47,497 and its analogs; CP 55,940, CP-55,244
Hybrid Cannabinoids	Combine structural features of both classical and nonclassical cannabinoids	AM-4030
Aminoalkylindoles	No structural similarity with Δ9-THC	WIN 55,212-2; AM-1241, JWH-015
Eicosanoids	Synthetic analogs of endocannabinoids such as anandamide	methanandamide
Others	Cannabinoids constituting no classes in their own right: diarylpyrazoles, naphtoylpyrroles, naphthoylpyrroles and naphthylmethylindenes.	SR141716A; SR144528

Due to the constantly ever changing nature of illicit manufacture of synthetic cannabinoids, the classes are constantly evolving, with a new class possibly being developed in the near future.

2.4.3 Presumptive Tests of Cannabinoids

2.4.3.1. Phytocannabinoids

The same principle used for choosing analytical methods for fentanyl analysis applies to the analysis of phytocannabinoids. Category A, B, and C methods are used individually or in combination for presumptive or confirmatory testing. The presumptive tests for phytocannabinoids include the Fast Blue B salt test and the Duquesnois-Levine test. The Fast Blue B test can be performed on a filter paper: fold two filter papers over each other and open to form a funnel; place a small amount of sample into the center of the upper paper and add two drops of petroleum ether, allowing the liquid to penetrate the lower filter paper; discard the upper filter paper and allow the lower filter paper to dry; add a very small amount of Fast Blue B salt (1% w/w diluted with anhydrous sodium sulphate) to the center of the filter paper and then add two drops of sodium bicarbonate (10% w/w in

aqueous solution) [39]. A purple-red color is indicative of cannabinoid being present; THC gives a red color, CBN gives a purple color, and CBD gives an orange color [39].

The Duquenois-Levine test can be performed in a test tube. A small amount of the material in question is placed in a test tube and shaken with 2 mL of acetaldehyde and vanillin mixture (0.5 mL of acetaldehyde and 0.4 g of vanillin in 20 mL ethanol) for 1 min; add 2 mL of concentrated hydrochloric acid allowing the mixture to stand for 10 min; if a color develops, add 2 mL of chloroform and mix gently [39]. If the chloroform layer (lower) becomes violet in color then this indicates the presence of cannabinoids [39].

2.4.3.2. Synthetic cannabinoids

Synthetic cannabinoids are presumptively tested mostly using immunoassay-based tests. Immunoassays fall into the Category C analytical method. In these type of tests, a small sample is placed in a sample well and the presence or absence of the drug in question is noted by the presence or absence of a line in the test result region (whichever is specific to that test).

2.4.4. Challenges in the Analysis and Confirmatory Methods of Analysis of Cannabinoids

Presumptive analysis is often not enough to ensure proper identification of a drug in question. Though GC-MS is often the gold standard in confirmatory testing in forensic laboratories, there is still the problem of the differentiation of positional isomers from each other. Studies conducted by Belal et al. on the differentiation of indole ring regioisomers of the synthetic cannabinoid JWH-007 [17] have shown the difficulty of GC-MS to differentiate isomers. In the study, the mass spectra generated by the GC-MS were the

same. However, the spectra of the GC-IR produced unique peaks, allowing for differentiating the isomers from each other. However, one disadvantage of GC-IR is that sensitivity is lower than that of GC-MS. Hence, GC-IR can be used as a complement to the GC-MS in the differentiation of isomeric compounds.

In this study, the examination of the utility of GC-IR to differentiate difficult isomeric synthetic cannabinoids will be employed. Additionally, it will be investigated if this approach is useful for differentiation of the phytocannabinoids.

Drug isomers often pose a problem using GC-MS analysis as well, and this poses a problem since law enforcement and the judiciary would benefit from unambiguous identification of isomers. Since structurally isomeric compounds often produce similar mass spectra, identification may be accomplished with the use of alternative methodologies, such as using another analytical instrument which has the ability to provide spectral information that can be used to differentiate isomers which produce similar mass spectra. In the chapter to follow, the instruments utilized in this study for this purpose will be explored.

3. INSTRUMENTATION BACKGROUND

3.1. Scientific Working Group for the Analysis of Seized Drugs (SWGDRUG) Classification of Analytical Techniques

The Scientific Working Group for the analysis of Seized Drugs (SWGDRUG) classifies analytical methods into three categories (Categories A, B, or C) based on their discriminating power, with increasing selectivity in the order of Category C, B, and A [40] (**Figure 9**).

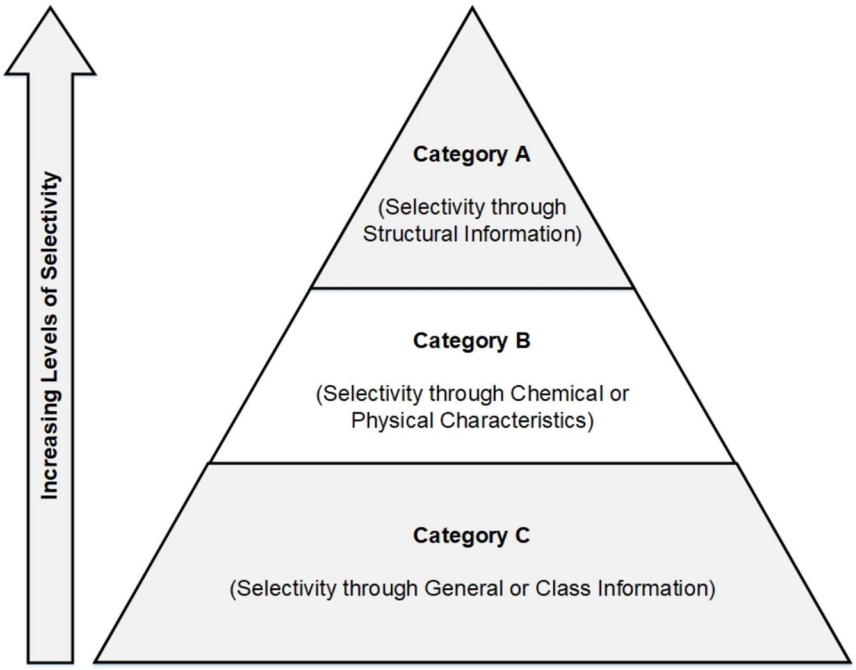

Figure 9. Categories of methods of analysis and their levels of selectivity in analysis [40].

Category A methods have the greatest selectivity, due to their ability to provide structural information about the compound in question; e.g. mass spectrometry and infrared spectroscopy. Category B provides selectivity through elucidation of the physical or chemical properties of the compound in question; e.g., gas chromatography and liquid chromatography. Category C provides selectivity through general or class information;

e.g., color tests [40]. Further examples of analytical methods for the different categories is shown in **Table 3.**

Table 3. The categories and examples of analytical methods utilized in analytical chemistry [40] .

Category A (Selectivity through Structural Information)	Infrared Spectroscopy
	Mass Spectrometry
	Nuclear Magnetic Resonance Spectroscopy
	Raman Spectroscopy
	X-ray Diffractometry
Category B (Selectivity through Chemical and Physical Characteristics)	Capillary Electrophoresis
	Gas Chromatography
	Ion Mobility Spectrometry
	Liquid Chromatography
	Microcrystalline Tests
	Supercritical Fluid Chromatography
	Thin Layer Chromatography
	Ultraviolet/Visible Spectroscopy
	Macroscopic Examination (Cannabis only)
	Microscopic Examination (Cannabis only)
Category C (Selectivity through General or Class Information)	Color Tests
	Fluorescence Spectroscopy
	Immunoassay
	Melting Point
	Pharmaceutical Identifiers

In forensic analysis of drugs, the methods selected determine if the analytical scheme is useful for presumptive or confirmatory testing. According to the Organization of Scientific Area Committee (OSAC), in order to conduct confirmatory testing, two methods of analysis must be chosen, with at least one being from Category A. Alternatively, three methods can be chosen, with two being Category B and one being Category C. Using Category C alone is only useful for presumptive testing. Hyphenated methods such as GC-

MS count as two methods, with GC being Category B and MS being Category A. In the following section, details of the analytical methods will be provided.

3.2 Gas Chromatography – Mass Spectrometry (GC-MS)

Gas Chromatography – Mass Spectrometry (GC-MS), as mentioned before, utilizes both Category B (GC) and Category A (MS) analytical methods. This method is used in a wide cross section of industries which employ the use of analytical instrumentation. The instrument is composed of the gas chromatograph and a mass spectrometer. The GC-MS separates chemicals into its individual components (using gas chromatograph) and identifies/quantifies the components at a molecular level (using the MS detector) [41].

The gas chromatograph contains a chromatographic column (stationary phase) which facilitates the separation of the vaporized analytes carried by the inert carrier gas which is often helium. The driving force behind the separation is the interaction of the analyte with the stationary phase which is generally tied to its polarity; this affects the retention time of the analyte elution.

Once separated by the GC, the vaporized sample moves to the mass spectrometer. Here, ionization of the molecule occurs through electron ionization (EI) by the bombardment of the molecule with free electrons emitted from a heated filament [41]. The ionized molecule then enters the mass analyzer. The mass analyzer consists of four hyperbolic metal rods parallel in a radial array [41]. A pair of the opposite rods has a negative potential while the other pair has a positive potential, and a combination of direct current (DC) and radio frequency (RF, ~1 MHz) electric field applied to the four rods induces an oscillatory

motion of the ions [41]. The oscillating trajectories are mass dependent and ions with one particular mass to charge ratio (m/z) can be transmitted to the detector when a stable trajectory through the rods is obtained [41]. When the ions reach the detector, their abundances are measured and are reported as a numerical value respective to the particular m/z ion, resulting in the spectra characteristic to the compound in question.

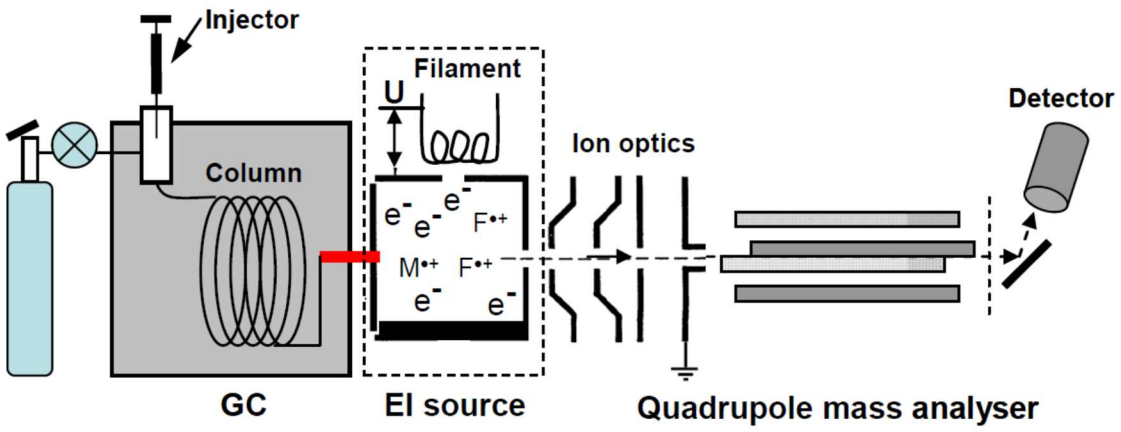

Figure 10. Schematic diagram of a GC-MS with EI ionization source [41].

Though it has a vast variety of uses for analysis, GC-MS is widely used in forensic chemistry for drug analysis, and is considered the gold standard for drug analysis. Psychoactive drugs such as cannabinoids, methamphetamines, fentanyl, and heroin are routinely analyzed by GC-MS in forensic laboratories. The unique quality that makes it so useful for drug analysis is the high sensitivity. Drugs turned in to the laboratory for analysis tend to be in low concentrations; hence an analytical method able to detect at such concentrations is very advantageous.

As described previously, determination of the molecular weight and structure of fentanyl analogs via GC-MS is rather difficult. Furthermore, some isomeric forms of fentanyl will also produce similar mass spectra, further complicating analysis by GC-MS. Therefore, another analytical method is necessary which could positively identify each isomer from the other.

3.3 Gas Chromatography – Infrared Spectroscopy (GC-IR)

In this study we propose to use gas chromatography vapor phase infrared spectroscopy (GC-IR) for the differentiation of the fentanyl analogs (**See in Figures 11 & 12)**. **Figure 11** is a picture of the interior of the of the IRD3 detector used in the studies conducted. In **Figure 12** is a schematic of the functional parts within the detector. In GC-IR, the compound is injected in the inlet of the GC and separated by polarity as the vaporized compound passes through the stationary phase of the GC column. Once separated, the analyte then enters the IR portion of the instrument through the lightpipe (keeps sample vaporized) which is 120mm long and 1mm internal diameter (ID) [42]. An interesting feature of the light pipe is 1mm ID which matches the 1mm cavity of the IRD light source resulting in a concentrated energy flux, resulting in the light pipe's maintenance of maximum sample concentration [42]. This structure of the light pipe minimizes noise and maximizes signal in a phenomenon known as the Hirshfeld Advantage [42]. Simultaneously the IR source produces a beam of infrared radiation, and by means of the interferometer and mirrors, interacts with the vaporized sample maintaining its characteristic geometry while generating unique spectral results after passing through the

detector [43]. This method explained employs the Fourier transform infrared (FTIR) detection. In this method, an interferogram is generated which is then converted to spectra in the detector by means of a Michelson interferometer. A major advantage of GC-IR is that no two compounds will generate the same spectra [43]. Hence, the spectra generated is much like a unique fingerprint for that particular compound.

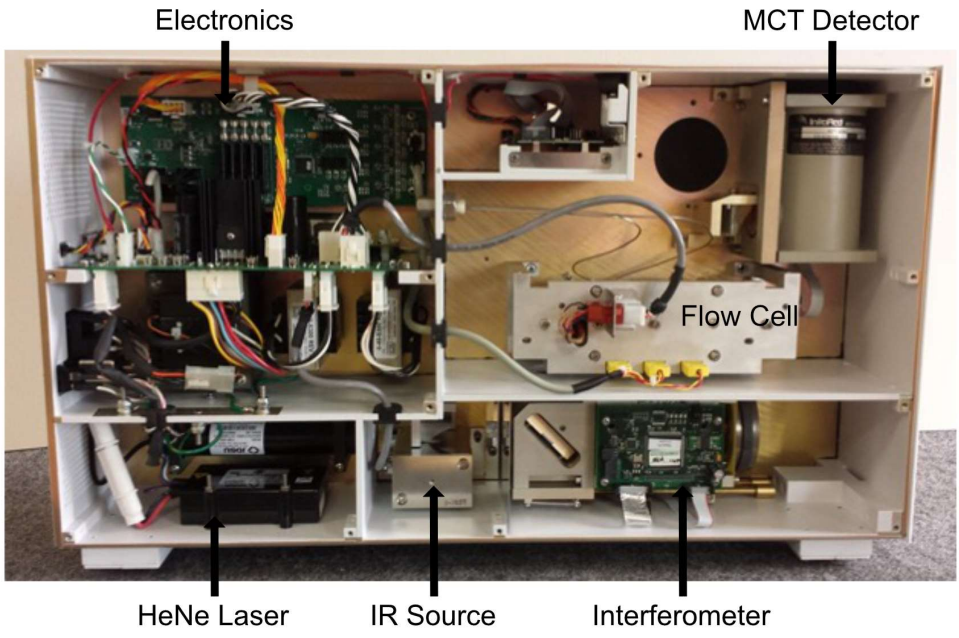

Figure 11. The internal view of the GC-IR instrument.

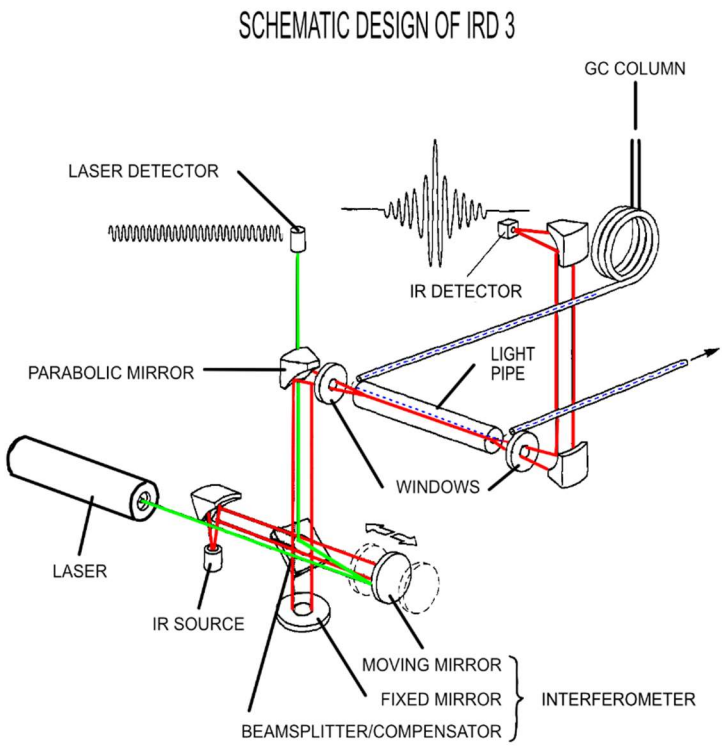

Figure 12. Schematic diagram of GC-IR instrument [41].

In condensed phase/solid phase GC-IR, the compound is first separated on the GC just as in gas phase GC-IR. However, the difference lies in the fact that in solid phase GC-IR, the eluent off the column are deposited on to a rotating IR transparent disc which is cooled to approximately -100 to 50ºC [44], which stimulates condensation of the compound being analyzed. After deposition, the infrared beam passes through each condensed spot and the detector automatically collects spectral data [44]. Studies using the GC-Solid Phase IR for isomer differentiation of novel psychoactive substances have also been as successful as GC- Vapor Phase IR [45].

Vapor phase IR and solid phase IR both have the advantage of measurement of frequencies simultaneously in a single scan. This provides a wide range of information about the types

of chemical bonds which exists in a single molecule. One phenomenon which exists when comparing drug compounds whose spectra are generated from vapor phase IR versus solid phase IR is polymorphism. In polymorphism, there is a difference in the spectra produced as a result of differences in molecular interactions existing in the different crystalline forms. As a result, vibrations of one or more of the molecules can interact in such a way to increase the number of bands or shift their frequencies [46]. In studies done by Donahue, et. al., the comparison of the vapor phase IR spectra of a hypothetical carbon dioxide molecule with a solid phase IR spectra of the carbon dioxide molecule yielded alteration of the spectral features generated [46]. In the vapor phase form, the molecule was free of outside molecular interactions; however, in the solid phase form the molecular interactions of the resulting crystalline structure caused change in the symmetry of the molecule which altered the spectral features.

Attenuated Total Reflectance FTIR (ATR-FTIR) is another method of FTIR utilized for drug analysis. Sample preparation for solid samples involves grinding the material to a fine powder and dissolving into a liquid mineral oil to create a paste which is spread between two Mid-Infrared transparent windows e.g. potassium bromide (KBr) [47]. Liquid samples are analyzed as thin films, mostly of Teflon® in cells; a cell consisting of two transparent IR windows [47]. The principle behind ATR-FTIR is the measurement of the changes that occur in a totally internally reflected infrared beam when the beam comes into a sample [47]. An infrared beam is directed onto an optically dense crystal with a high refractive index at a certain angle; the internal reflectance creates an evanescent wave that extends into the sample held in contact with the crystal [47]. In regions of the infrared spectrum where the sample absorbs energy, the evanescent wave will be attenuated; the

attenuated energy from each evanescent wave is passed back to the IR beam, which then exits the opposite end of the crystal and is passed to the detector which produces an infrared spectrum [47] using the same principle of FTIR explained above.

Studies conducted by Belal et al. on the differentiation of indole ring regioisomers of the synthetic cannabinoid JWH-007 [17] and Awad et al on the differentiation of methamphetamine and regioisomeric substances [15] have both shown the difficulty of GC-MS to differentiate isomers. In both studies, the mass spectra generated by the GC-MS were the same. However, the spectra of the GC-IR produced unique peaks allowing for differentiating the isomers from each other. However, one disadvantage of GC-IR is sensitivity of GC-IR is lower than that of GC-MS. Hence, GC-IR can be used as a complement to the GC-MS in the differentiation of isomeric compounds.

Methods complementary to GC-MS, such as gas chromatography Fourier-transform infrared spectroscopy (GC-IR) are often employed in forensic laboratories. GC-IR is considered a confirmation method due to their uniqueness of infrared spectra, whereby no two compounds though similar can have the same spectra [43]. The GC-IR method was successful in the identification of fentanyl analogs[48][49] isomeric ethoxyphenthylamines and methoxymethcathinones [50], methylenedioxybenzylpiperazines (MDBPs) and methoxymethylbenzylpiperazines (MMBPs) [51], and methamphetamine and regioisomeric substances [15]. Though it is successful in differentiation of isomers, one of the limitations of the GC-IR is its low sensitivity in comparison to GC-MS [52] whereby mass loadings of less than 25ng on column generally produces undefined spectra [48].

The fentanyl crisis is only a few years in existence and as such there are not many means of characterizing the constantly evolving fentanyl analogs. The United States Drug

Enforcement Administration's Special Testing and Research Lab (DEA-STRL) has recently embarked on a fentanyl signature profiling research initiative. As of December, 2017, fentanyl and 29 other fentanyl-related compounds (FRCs) have been identified in DEA casework [53], with limited reporting in recent literature [53]. According to the National Forensic Laboratory Information System (NFLIS) 2020 mid-year report, fentanyl is the fourth most identified drug reported by the forensic laboratories taking part in the NFLIS survey, up from being fifth in previous years [54]. The spectra obtained from each of the 212 fentanyl analog standards can be obtained using Fourier-transform infrared spectroscopy (FTIR). FTIR is regarded as a Category A analytical technique having maximum discriminating power for drug analysis according to the Scientific Working Group for the Analysis of Seized Drugs (SWGDRUG) recommendations [55]. The gas-phase GC-IR reference library will be made readily available to any forensic laboratory as part of supplementary material in a peer-reviewed publication for use by operational laboratories to search during analysis of seized street samples.

The use of databases has been vital to the success of the field of forensic science. This is evident in the use of the Integrated Ballistic Identification System (IBIS) for bullets and cartridge cases, the Integrated Automated Fingerprint Identification System (AFIS) for fingerprints, and the Combined DNA Index System (CODIS) for DNA as databases for matching data from a suspect/victim and crime scene. The rapidly evolving new drugs entering the illicit market prompted the forensic community to begin development of controlled databases. These databases include spectral information from a wide variety of analytical techniques such as GC-MS, GC-IR, NMR, and Raman [56][57] to name a few.

Based on previous data in the use of GC-IR to differentiate isomeric methamphetamines and synthetic cannabinoids [17][15], GC-IR can be a useful tool for differentiation of isomeric fentanyl compounds. Therefore, the generation of a GC-IR library of fentanyl analogues provides chemical information to facilitate structure elucidation and compound identification. The creation of this library will facilitate identification of compounds. The library will be a useful tool to other laboratories for their fentanyl confirmation. Currently, forensic laboratories utilize GC-IR for fentanyl confirmation but lack the spectral information of the 212 analogs contained in the FAS-Kit. Therefore, the library can be used in validation studies to determine its usefulness. Hence, inter-laboratory tests can be performed to develop a consensus-based standard of GC-IR analysis to improve fentanyl compound identifications.

A GC-MS analysis followed by spectral library searching has been the acceptable mode of making drug identifications in complex mixtures [58]. To the author's knowledge, this is the first reporting of a gas-phase infrared (GC-IR) as well as GC-MS library of fentanyl analogs. The purpose is to present a novel gas phase infrared spectral library specific for fentanyl analogs. The utility for the differentiation of fentanyl analog isomers will also be explored.

4. MATERIALS AND METHODS

4.1. Utility of GC-MS and GC-IR Libraries in Differentiating Positional Isomers of Fentanyl-Related Substances (FRS)

Some sections published in: K Ferguson, J Perr, S L.Tupik, H Haddad, M Gilbert, R Newman and JR Almirall. Utility of Gas Chromatography Infrared Spectroscopy (GC-IR) for the Differentiation of Positional Isomers of Fentanyl Related Substances. *Forensic Chemistry*.(2022) 29, 100425. https://doi.org/10.1016/j.forc.2022.100425

4.1.1. Materials

The Fentanyl Analog Screening (FAS) Kit including Emergent Panels 1-3, (**see Appendix Table for a complete listing)**, contained 200 µg of each of the 212 FRS in individual vials and was obtained from Cayman Chemical (Ann Arbor, MI). A 500 µL aliquot of HPLC grade methanol (Fisher Scientific, Atlanta, GA) was pipetted into each vial to create an approximate 400 µg/ml (or 400 ppm) concentration. Each vial was vortexed at medium speed for a minimum of 15 minutes and stored at 0 °C.

4.1.2. Instrumentation

GC-IR studies were conducted using three different instruments, an Agilent Technologies 6890N Network GC System coupled to an IRD3 detector obtained from Analytical Solutions and Providers (ASAP) installed at Florida International University (FIU), an Agilent Technologies 7890B GC System coupled to an IRD3 detector obtained from Analytical Solutions and Providers (ASAP) installed at the Drug Enforcement Administration's (DEA) Special Testing and Research Laboratory, and an Agilent 7890B

GC with an ASAP IRD 3 detector obtained from Analytical Solutions and Providers (ASAP) installed at the Pinellas County Forensic Laboratory.

The GC at FIU was operated in splitless mode with high purity helium as the carrier gas at a flow rate of 1.5 mL/min. The column used was a 30 m x 0.32 mm coated with 0.25 µm (OV-5) purchased from Ohio Valley Specialty Company (Marietta, OH). The oven program consisted of an initial temperature of 100 °C without hold ramped at a rate of 30 °C/min to a final temperature of 310 °C with a final hold of 9 min. The GC inlet temperature was 270 °C with an injection volume of 3 µL (for a total of 1.2 µg of analyte mass loading). The IRD detector at FIU was operated at light pipe and transfer line temperatures of 250 °C and all spectra were collected in the 500-4000 cm^{-1} range with a resolution of 8 cm^{-1}. Each library standard was analyzed in triplicate using an autosampler.

The Special Testing and Research Laboratory's GC-IR used a 30 m x 0.32 mm column with 0.25 µm HP-5 stationary phase and was operated using a 2:1 split ratio with a 2.0 mL/min constant flow of high purity helium as the carrier gas. The oven program consisted of a starting temperature of 65 °C with an initial 1.5-min hold ramped at a rate of 20 °C/min to a final temperature of 310 °C and a final hold of 5 min. The GC inlet temperature was 280 °C with an injection volume of 2 µL. The IRD detector was operated at light pipe and transfer line temperatures of 280 °C and all spectra were collected from 550-4000 cm^{-1}.

The GC at the Pinellas County Forensic Laboratory was operated in splitless mode with high purity helium as the carrier gas at a flow rate of 1.7 mL/min with a splitless hold time of 1.2 min. The column used was a 30 m x 0.32 mm Agilent HP5 with a film thickness of 0.25 µm. The oven program consisted of an initial temperature set at 80 °C for 1.2 minutes

ramped at 30 °C/min to 320 °C with a final hold time of 4 min. The GC inlet temperature was 250 °C with an injection volume of 3 µL. The IRD light pipe was operated at 250 °C and the transfer lines at 275 °C and all spectra were collected in the range 500-4000 cm^{-1} with a resolution of 8 cm^{-1}. Each library standard was analyzed in triplicate using an autosampler.

GC-MS studies at FIU were conducted using an Agilent Technologies 7890A GC System coupled to an Agilent Technologies 5975C inert mass spectrometer (MS). The GC was operated using a 5:1 split with high purity helium as the carrier gas at a flow rate of 1.5 mL/min. A 30 m x 0.25 mm column coated with 0.25 µm-thick sorbent DB-5MS column from Agilent Technologies was used. The oven program consisted of the same used for GC-IR studies. The GC inlet temperature was 270 °C with an injector volume of 1 µL (for a total of 400 ng of analyte mass loading). The MS was operated in scan range 34-600 amu with the electron ionization at 70 eV while the source temperature was set at 230 °C, and the quadrupole temperature was set to 150 °C. Each library standard was analyzed in triplicate.

At the Special Testing and Research Laboratory, the analysis was performed using two GC-MS systems – an Agilent Technologies 7890B GC System coupled to an Agilent Technologies 5977A MS using high purity helium as the carrier gas and an Agilent Technologies Intuvo 9000 GC System coupled to an Agilent Technologies 5977B MS using high purity hydrogen as the carrier gas.

The 7890B GC used a 30 m x 0.25 mm column with a 0.25 µm DB-5 film thickness and was operated using a 25:1 split with at a constant flow rate of 1.5 mL/min. The oven

program started at 100 °C with an initial 1-min hold then ramped at a rate of 12 °C/min to a final temperature of 280 °C holding for 9 min. The GC inlet temperature was 280 °C with an injector volume of 1 µL. The MS was operated in scan range 30-550 amu with the electron ionization at 70 eV while the source temperature was set at 230 °C and the quadrupole temperature was set to 150 °C.

The 9000 Intuvo GC used a 20 m x 0.18 mm column with a 0.18 µm HP-5MS film thickness and was operated using a 60:1 split with a constant flow rate of 1.0 mL/min. The oven program started at 80 °C holding for 0.5 min, then ramped at a rate of 80 °C/min to 180 °C with a 2-min hold, then ramped 40 °C/min to 270 °C with a 1-min hold, and finally ramped at 100 °C/min to 310 °C with a 2 min hold. The GC inlet temperature was 260 °C with an injector volume of 1 µL. The MS was operated in scan range 40-500 amu with the electron ionization at 70 eV while the source temperature was set at 230 °C and the quadrupole temperature was set to 150 °C.

GC-MS studies at the Pinellas County Laboratory were conducted using an Agilent Technologies 7890A GC System coupled to an Agilent Technologies 5975C inert mass spectrometer (MS). The GC was operated using a 50:1 split with high purity helium as the carrier gas at a flow rate of 1.0 mL/min. A 20 m x 0.18 mm (DB-5MS) column coated with 0.18 µm-thick sorbent from Agilent Technologies was used. The oven program consisted of an initial temperature of 120 °C with an initial hold time of 2 min, ramped to 320 °C at a rate of 35 °C/min, with a final hold time of 3.3 min. The GC inlet temperature was 250 °C with an injection volume of 1 µL. The MS was operated in scan range 40-500 AMU with the electron ionization at 70 eV while the source temperature was set at 230 °C, and

the quadrupole temperature was set to 150 °C. Each library standard was analyzed in triplicate.

Tables 4 and 5 lists the instrumental parameters and analytical conditions for the three participating laboratories in this study.

Table 4. Instrumental parameters and the gas chromatography and infrared analytical conditions for the three participating laboratories in the study.

Instrumental and Analytical Conditions	FIU Research Laboratory	DEA Special Testing and Research Laboratory	Pinellas County Forensic Laboratory
Gas Chromatography			
GC Instrument Model	Agilent 6890N	Agilent 7890B	Agilent 7890B
Carrier Gas	Helium	Helium	Helium
Gas Flow Rate	1.5 mL/minute	2.0 mL/minute	1.7 mL/minute
Injector Split Ratio	Splitless	2:1 Split	Splitless
Column Type (All used 30m x 0.32 mm with 0.25µm film coating)	Ohio Valley Specialty Company OV-5	Agilent HP-5	Agilent HP-5
Initial Temperature	100 °C no hold	65 °C for 1.5 minutes	80 °C for 1.2 minutes
Ramp Rate	30 °C/minute	20 °C/minute	30 °C/minute
Final Temperature	310 °C	310 °C	320 °C
Hold Time	9 minutes	5 minutes	4 minutes
Inlet Temperature	270 °C	280 °C	250 °C
Injection Volume	3 µL	2 µL	3 µL
Infrared Spectroscopy			

IR Instrument Model	ASAP IRD3	ASAP IRD3	ASAP IRD3
Light Pipe Temperature	250 °C	280 °C	250 °C
Transfer Line Temperature	250 °C	280 °C	275 °C
Spectral Range	500-4000 cm^{-1}	550-4000 cm^{-1}	500-4000 cm^{-1}
Spectral Resolution	8 cm^{-1}	8 cm^{-1}	8 cm^{-1}

Table 5. Instrumental parameters and the gas chromatography and mass spectrometry conditions for the three participating laboratories.

Instrumental and Analytical Conditions	FIU Research Laboratory	DEA Special Testing and Research Laboratory	Pinellas County Forensic Laboratory
Gas Chromatography			
GC Instrument Model	Agilent 7890A	Agilent 7890B	Agilent 7890A
Carrier Gas	Helium	Helium	Helium
Gas Flow Rate	1.5 mL/minute	1.5 mL/minute	1.0 mL/minute
Injector Split Ratio	5:1	25:1	50:1
Column Type	Agilent Technologies DB-5MS (30m x 0.25 mm with 0.25µm film coating)	Agilent Technologies DB-5 (30m x 0.25 mm with 0.25µm film coating)	Agilent Technologies DB-5MS (20m x 0.18 mm with 0.18µm film coating)
Initial Temperature	100 °C no hold	100 °C for 1 minute	120 °C for 2 minutes
Ramp Rate	30 °C/minute	12 °C/minute	35 °C/minute
Final Temperature	310 °C	280 °C	320 °C
Hold Time	9 minutes	9 minutes	3.3 minutes
Inlet Temperature	270 °C	280 °C	250 °C

Injection Volume	1 µL	1 µL	1 µL
Mass Spectrometry			
MS Instrument Model	Agilent Technologies 5975C	Agilent Technologies 5977A	Agilent Technologies 5975C
Source Temperature	230 °C	230 °C	230 °C
Quadrupole Temperature	150 °C	150 °C	150 °C
Scan Range	34-600 amu	30-550 amu	40-500 amu
EI voltage	70eV	70eV	70eV

4.1.3. FIU Fentanyl Library Construction for MS Spectra

The MS spectra generated from all 212 compounds were used to create a library using Agilent's MSD Chemstation version E.02.01.1177 at FIU and shared with the DEA Special Testing and Research Laboratory and the Pinellas County Forensic Laboratory. This library consists solely of spectra from FRS. All spectra were collected in triplicate.

4.1.4. Library Construction for FTIR Spectra using Analytical Solutions and Providers (ASAP) Analytical Software

All spectra acquired by the GC-IR method were converted to .spc files and a library of all the analyzed FRS was created at FIU and shared with the DEA Special Testing and Research Laboratory and the Pinellas County Forensic Laboratory. All spectra were collected in triplicate. ASAP's End User Contributed Library Identification (EUCLiD) [59] was also obtained and utilized in the search studies at FIU. The EUCLiD library

consists of 1,400 spectra of different compounds contributed by end users, including 32 FRS compounds contained in the FAS-Kit.

4.1.5. Library Evaluation Performed by FIU

The FIU MS Library, the NIST08 MS library, the EUCLiD library, and the FIU Fentanyl IR libraries were assessed. All 212 FRS were searched, in triplicate, using each of the two IR libraries (the EUCLiD library and the new FIU vapor-phase IR Fentanyl library) for a total of 636 searches. The NIST08 MS library and the FIU MS Library were searched in the same manner. The following criteria were followed to ensure spectra of good quality were added to the library:

(i) Chromatographic peaks with a signal to noise ratio of equal to or greater than three (3) produced mass spectra with clearly defined base peaks and reproducible fragmentation for MS and smooth (not noisy) absorption peaks in the IR.

(ii) The spectral searches were deemed correctly identified after they were searched in triplicate against the created library and the resulting "match" was number one in the match for at least two out of the three searches.

(iii) The quality score needed to be equal to or greater than 90 for the MS and equal to or greater than 0.95 for the IR.

Additional library evaluation occurred when the Special Testing and Research Laboratory analyzed 20 blind samples. The GC-IR analyst was instructed to select the best library spectra using the FIU generated vapor phase IR library only. A GC-MS analyst, independent of the GC-IR analyst, was instructed to select the best library spectra on mass

spectral data only using in house available libraries (National Institute of Standards and Technology (NIST)20 library, the CaymanSpectralLibrary_092220 library) and the FIU generated mass spectral library.

4.1.6. Determination of the Limit of Detection (LOD) and Limit of Quantitation (LOQ) of the GC- IR

A calibration curve was constructed at both FIU and the Special Testing and Research Laboratory laboratories using peak areas to determine the approximate LOD and LOQ of the GC-IR instrumental systems using the methods described above. Fentanyl was used for the LOD/LOQ studies since it is the parent compound to the fentanyl-related compounds of interest. Seven different concentrations of fentanyl ranging from 10 ppm to 1000 ppm were analyzed in triplicate with 1 µL injections using the same instrument programming as detailed in the section 2.2.

4.1.7. Summary of Study

The main goals of this study were to describe the process of the creation of new gas-phase mass spectral and infrared libraries of FRS at FIU, the evaluation of the utility of these libraries to differentiate between positional isomers of FRS at FIU and to evaluate the usefulness of the libraries by two external laboratories (DEA STRL and Pinellas County Forensic Laboratory). The performance of the libraries was evaluated using a blind study of twenty (20) FRS that were distributed to the two external laboratories. The 20 different FRS isomers were selected on the basis of similarity of mass spectral fragmentation patterns and are shown in **Table 6** below.

Table 6. The identity of the 20 FRS used in the blind study along with the rationale of why these were selected.

Currently in the NIST Library
1. Sufentanil
2. Alfentanil
Not in the NIST Library but readily distinguishable by MS spectra
3. Thiophene fentanyl
4. Remifentanil
5. Ocfentanil
6. Fentanyl carbamate
7. α-methyl Butyryl fentanyl
8. 2, 3-seco-Fentanyl
9. Acrylfentanyl
10. Senecioylfentanyl
Not in the NIST Library and not readily distinguishable by MS spectra but readily distinguishable by IR spectra
11. Furanyl fentanyl
12. ortho-methyl Furanyl fentanyl
13. Valeryl fentanyl
14. meta-Fluorofentanyl
15. para-methyl Fentanyl
16. para-Chlorobutyryl fentanyl
17. FIBF
18. Crotonyl fentanyl
19. ortho-methyl Cyclopropyl fentanyl
20. ortho-methyl Acetyl fentanyl

The analysts in the external laboratories were asked to analyze the 20 blind FRS samples and to search the FIU-generated MS and IR libraries to determine compound identity using the criteria defined in section 2.5.

4.2. Inter-laboratory Studies for Fentanyl Analysis

Some sections are submitted for publication and can be found in: K Ferguson, J Perr, S Tupik, M Gilbert, R Newman, A Winokur, I Vallejo, S Hokanson, M Pothier, B Knapp, M Icard, K Kramer, and JR Almirall. "An Interlaboratory Study to Evaluate the Utility of Gas Chromatography Mass Spectrometry (GC-MS) and Gas Chromatography Infrared Spectroscopy (GC-IR) Spectral Libraries in the Forensic Analysis of Fentanyl Related Substances (FRS)". Journal of Forensic Science, In press. 2023

4.2.1. Materials

Each laboratory was instructed to use the Fentanyl Analog Screening Kit (FAS Kit), obtained from Cayman Chemical (Ann Arbor, MI), and reconstituting the respective reference material to the specification in the accompanying instructions. For GC-IR studies, each sample was recommended to be reconstituted to a final concentration of 400µg/ml (or 400 ppm). For GC-MS studies, each sample was to be further diluted to a final concentration of 100µg/ml (or 100 ppm).

4.2.2. Instrumentation

Tables 7 and 8 lists the instrumental parameters and analytical conditions for the seven participating laboratories in this study.

Table 7. Instrumental parameters and the gas chromatography and infrared analytical conditions for Laboratories #1-7 in the ILS.

Instrumental and Analytical Conditions	**Laboratory #1**	**Laboratory #2**	**Laboratory #3**	**Laboratory #4**	**Laboratory #5**	**Laboratory #6**	**Laboratory #7**
Gas Chromatography							
GC Instrument Model	Agilent 7890	Agilent 7890B	Agilent 7890A	Agilent 7890B	Agilent 7890B	Agilent 7890A	Agilent 6890N
Carrier Gas	Helium	Helium	Helium	Helium	Helium	Helium	Helium
Gas Flow Rate	2.0 mL/min	2.0 mL/min	5.2204 mL/min	1.7 mL/min	3.0 mL/min	1.8 mL/min	1.5 mL/min
Injector Split Ratio	1:1 to 20:1	2:1	Splitless	Splitless	Splitless	5:1	Splitless
Column Type	Rtx-1 15.0 m x 0.32 mm x 0.25 µm	Agilent HP-5 30 m x 0.32 mm x 0.25 µm	Agilent HP-5 30 m x 0.32 mm x 0.25 µm	Agilent HP-5 30 m x 0.32 mm x 0.25µm	Agilent HP-5 30 m x 0.32 mm x 0.25 µm	Agilent DB-35MS 15 m x 0.25 mm x 0.25 µm	Ohio Valley Specialty Company OV-5 30 m x 0.32 mm x 0.25µm
Initial Temperature	100 °C	65 °C for 1.5 minutes	60 °C for 1.5 minutes	80 °C for 1.2 minutes	55 °C	225 °C	100 °C
Ramp Rate	40° C/min to 200°C, 30° C/min to 290°C	20 °C/min	45 °C/min to 200°C, 16 °C/min to 300°C	30 °C/min	30 °C/min	30 °C/min	30 °C/min
Final Temperature	290°C	310 °C	300 °C	320 °C	295 °C	315 °C	310 °C
Hold Time	5 min	5 min	2 min	4 min	10 min	10 min	9 min
Inlet Temperature	290°C	280 °C	225 °C	250 °C	270 °C	270 °C	270 °C
Injection Volume	1.5 µL	2 µL	2 µL	3 µL	3 µL	3 µL	3 µL
Infrared Spectroscopy							
IR Instrument Model	Analytical Solutions and Providers (ASAP) IRD3	ASAP IRD3	ASAP IRD3	ASAP IRD3	ASAP IRD3	Spectra Analysis DiscovIR	ASAP IRD3
Light Pipe Temperature	290°C	280 °C	250 °C	250 °C	295 °C	N/A	250 °C
Transfer Line Temperature	290°C	280 °C	250 °C	275 °C	295 °C	325 °C	250 °C
Spectral Range	550-4000 cm^{-1}	550-4000 cm^{-1}	550-4000 cm^{-1}	500-4000 cm^{-1}	500-4000 cm^{-1}	650-4000 cm^{-1}	500-4000 cm^{-1}
Spectral Resolution	8 cm^{-1}	8 cm^{-1}	8 cm^{-1}	8 cm^{-1}	8 cm^{-1}	4 cm^{-1}	8 cm^{-1}

Table 8. Instrumental parameters and the gas chromatography and mass spectrometry conditions for laboratories #1-7 in the ILS.

Instrumental and Analytical Conditions	**Laboratory #1**	**Laboratory #2**	**Laboratory #3**	**Laboratory #4**	**Laboratory #5**	**Laboratory #6**	**Laboratory #7**
Gas Chromatography							
GC Instrument Model	Agilent 6890N	Agilent 7890B	Agilent 7890A	Agilent 7890A	Agilent 7890B	Agilent 7890B	Agilent 7890A
Carrier Gas	Helium	Helium	Helium	Helium	Helium	Helium	Helium
Gas Flow Rate	0.8 mL/min	1.5 mL/min	3.0 mL/min	1.0 mL/min	2.0 mL/min	1.5mL/min	1.5 mL/min
Injector Split Ratio	5:1	25:1	3:1	50:1	10:1	20:1	5:1
Column Type	ZB-1 MS (12.0m x 0.20mm x 0.33µm film coating)	Agilent Technologies DB-5 (30m x 0.25 mm x 0.25µm film coating)	Agilent Technologies DB-1 (30m x 0.25 mm x 0.25µm film coating)	Agilent Technologies DB-5MS (20m x 0.18 mm x 0.18µm film coating)	Agilent Technologies DB-CSI #6 (15m x 0.25 mm x 0.25µm film coating)	Agilent Technologies DB-35MS (15m x 0.25 mm x 0.25µm film coating)	Agilent Technologies DB-5MS (30m x 0.25 mm x 0.25µm film coating)
Initial Temperature	100 °C	100 °C for 1 minute	90 °C for 2.73 minutes	120 °C for 2 minutes	280 °C for 5.33 minutes	270°C	100 °C no hold
Ramp Rate	65°C/min to 220°C, 40°Cmin to 290°C	12 °C/min	35 °C/min to 200 °C, 16 °C/min to 300 °C	35 °C/min	30 °C/min	5°C/min to 285 °C, 30°C/min to 300 °C	30 °C/min
Final Temperature	290 °C	280 °C	300 °C	320 °C	310 °C	300 °C	310 °C
Hold Time	6.15 min	9 min	3.88 min	3.3 min	4 min	1 min	9 min
Inlet Temperature	290 °C	280 °C	275 °C	250 °C	270 °C	290 °C	270 °C
Injection Volume	1 µL	1 µL	1 µL	1 µL	2 µL	1 µL	1 µL
Mass Spectrometry							
MS Instrument Model	Agilent Technologies 5975B	Agilent Technologies 5977A	Agilent Technologies 5975C	Agilent Technologies 5975C	Agilent Technologies 5979B	Agilent Technologies 5977A	Agilent Technologies 5975C
Source Temperature	230 °C	230 °C	230 °C	230 °C	230 °C	230 °C	230 °C
Quadrupole Temperature	150 °C	150 °C	150 °C	150 °C	150 °C	150 °C	150 °C
Scan Range	50-525 amu	30-550 amu	40-550 amu	40-500 amu	34-550 amu	14-500 amu	34-600 amu
EI voltage	70eV	70eV	70eV	70eV	70eV	70eV	70eV

Laboratory #2 also performed GC-MS analysis using hydrogen as the carrier gas. This was done using an Agilent Technologies Intuvo 9000 GC System coupled to an Agilent Technologies 5977B MS using high purity hydrogen as the carrier gas. The 9000 Intuvo GC used a 20 m by 0.18 mm column with a 0.18 µm HP-5MS film thickness and was operated using a 60:1 split with a constant flow rate of 1.0 mL/min. The oven program started at 80 °C holding for 0.5 minute, then ramped at a rate of 80 °C/min to 180 °C with a 2-minute hold, then ramped 40 °C/min to 270 °C with a 1-minute hold, and finally ramped at 100 °C/min to 310 °C with a 2-minute hold. The GC inlet temperature was 260 °C with an injector volume of 1 µL. The MS was operated in scan range 40-500 amu with the electron ionization at 70 eV, source temperature at 230 °C, and quadrupole temperature at 150 °C.

Post analysis evaluation of the laboratory-analyzed 20 blind samples was performed by searching the spectra against the specified libraries. The GC-IR analyst was instructed to select the best matched library spectra using the FIU generated vapor phase IR library only. A GC-MS analyst, independent of the GC-IR analyst, was instructed to select the best library matched spectra on mass spectral data only using in-house available libraries (if available) and the FIU generated mass spectral library.

Summary of Study

The purpose of the interlaboratory study was the evaluation of the utility of GC-MS and GC-IR for the differentiation of FRS that were analyzed by 7 different laboratories. The performance of the newly generated GC-MS and GC-IR fentanyl libraries was evaluated using a blind study of 20 FRS that were analyzed by external laboratories. The twenty (20)

different FRS, shown in **Table 9,** were selected based on their presence in the current NIST mass spectral GC-MS library and/or their structurally similar isomeric forms exhibiting close spectral fragmentation patterns. The reason for the inclusion of those already in the NIST library was to have a compound present which is already established as included.

Table 9, as seen below, lists the 20 FRS selected for the ILS grouped by category of choice for ease of use in identification. The 3 identification categories are: 1) Currently in the NIST Library, 2) Not in the NIST Library but may be readily distinguishable by MS spectra, and 3) Not in the NIST Library and may not be readily distinguishable by MS spectra, but readily distinguishable by IR spectra. The standardized name and average retention time in minutes (for lab #7 as an example, n=3 analytical runs) for each FRS is also listed.

Table 9. Twenty (20) FRS used in the blind study grouped by selection criteria**.** The retention time is representative of data obtained using the analytical parameters of Laboratory #7.

Chemical Standard (FRS)	**Standardized Name**	**Average Retention Time (min.)**
Currently in the NIST Library		
1. Sufentanil	N-[4-(methoxymethyl)-1-[2-(2-thienyl)ethyl]-4-piperidinyl]-N-phenyl-propanamide	8.33
2. Alfentanil	N-[1-[2-(4-ethyl-4,5-dihydro-5-oxo-1H-tetrazol-1-yl)ethyl]-4-(methoxymethyl)-4-piperidinyl]-N-phenyl-propanamide	9.01
Not in the NIST Library but may be readily distinguishable by MS spectra		

3. Thiophene fentanyl	N-phenyl-N-[1-(2-phenylethyl)-4-piperidinyl]-2-thiophenecarboxamide	11.35
4. Remifentanil	4-(methoxycarbonyl)-4-[(1-oxopropyl)phenylamino]-1-piperidinepropanoic acid, methyl ester	7.49
5. Ocfentanil	N-(2-fluorophenyl)-2-methoxy-N-[1-(2-phenylethyl)-4-piperidinyl]-acetamide	8.41
6. Fentanyl carbamate	phenyl[1-(2-phenylethyl)-4-piperidinyl]-carbamic acid, ethyl ester	7.81
7. α-methyl Butyryl fentanyl	N-[1-(1-methyl-2-phenylethyl)-4-piperidinyl]-N-phenyl-butanamide	8.68
8. 2, 3-seco-Fentanyl	N-[1-methyl-3-[methyl(2-phenylethyl)amino]propyl]-N-phenyl-propanamide	7.31
9. Acrylfentanyl	N-phenyl-N-[1-(2-phenylethyl)-4-piperidinyl]-2-propenamide	8.12
10. Senecioylfentanyl	3-methyl-N-phenyl-N-[1-(2-phenylethyl)-4-piperidinyl]-2-butenamide	8.65
Not in the NIST Library and may not be readily distinguishable by MS spectra, but readily distinguishable by IR spectra		
11. Furanyl fentanyl	N-phenyl-N-[1-(2-phenylethyl)-4-piperidinyl]-2-furancarboxamide	9.63
12. ortho-methyl Furanyl fentanyl	N-(2-methylphenyl)-N-[1-(2-phenylethyl)-4-piperidinyl]-2-furancarboxamide	9.96
13. Valeryl fentanyl	N-phenyl-N-[1-(2-phenylethyl)-4-piperidinyl]-pentanamide	8.74
14. meta-Fluorofentanyl	N-(3-fluorophenyl)-N-[1-(2-phenylethyl)-4-piperidinyl]-propanamide	7.87

15. para-Methylfentanyl	N-(4-methylphenyl)-N-[1-(2-phenylethyl)-4-piperidinyl]-propanamide	8.39
16. para-Chlorobutyryl fentanyl	N-(4-chlorophenyl)-N-[1-(2-phenylethyl)-4-piperidinyl]-butanamide	9.10
17. FIBF(FIBF) para-Fluoroisobutyryl fentanyl	N-(4-fluorophenyl)-2-methyl-N-[1-(2-phenylethyl)-4-piperidinyl]-propanamide	7.85
18. Crotonyl fentanyl	(2E)-N-phenyl-N-[1-(2-phenylethyl)-4-piperidinyl]-2-butenamide	8.68
19. ortho-methyl Cyclopropyl fentanyl	N-(2-methylphenyl)-N-[1-(2-phenylethyl)-4-piperidinyl]-cyclopropanecarboxamide	8.84
20. ortho-methyl Acetyl fentanyl	N-(2-methylphenyl)-N-[1-(2-phenylethyl)-4-piperidinyl]-acetamide	8.19

4.3. Analysis of Cannabinoids by GC-MS and GC-IR

4.3.1. Materials for Phytocannabinoid Studies

The cannabidiol (CBD), cannabigerol (CBG), cannabinol (CBN), and delta-8 tetrahydrocannabinol (Δ^8-THC) standards were obtained from Cerilliant Corporation® (Round Rock, TX) in individual vials. The delta-9 tetrahydrocannabinol (Δ^9-THC) standard was obtained from Restek (Bellefont, PA). A 1 mL aliquot of HPLC grade methanol (Fisher Scientific, Atlanta, GA) was pipetted into each vial to create an approximate 1000 µg/ml concentration. Each vial was vortexed at medium speed for a minimum of 15 min and stored at 0 °C.

4.3.2. Instrumentation for Phytocannabinoid Studies

GC-IR studies were conducted using an Agilent Technologies 6890N Network GC System coupled to an IRD3 detector obtained from Analytical Solutions and Providers (ASAP). The GC was operated in splitless mode with high purity helium as the carrier gas at a flow rate of 1.2 mL/min. The column used was a 30 m x 0.32 mm coated with 0.25 µm (OV-5) purchased from Ohio Valley Specialty Company (Marietta, OH). The oven program consisted of an initial temperature of 70 °C for 1 minute ramped by a rate of 20 °C/min to a final temperature of 300 °C and a final hold of 4 minutes. The GC inlet temperature was 270 °C with an injection volume of 1 µL (for a total amount of 1 µg of analyte mass loading). The IRD detector was operated at light pipe and transfer lines temperatures of 280 °C and all spectra were collected in the range 500-4000 cm^{-1} with a resolution of 8 cm^{-1}. Each standard was analyzed in triplicate using an autosampler.

GC-MS studies were conducted using an Agilent Technologies 7890A GC System coupled to an Agilent Technologies 5975C inert mass spectrometer (MS). The GC was operated using a 5:1 split with high purity helium as the carrier gas at a flow rate of 1.2 mL/min. A 30 m by 0.25 mm column coated with 0.25 µm-thick sorbent DB-5MS column from Agilent Technologies was used. The oven program consisted of the same used for GC-IR studies. The GC inlet temperature was 270 °C with an injector volume of 1 µL (for a total amount of 100 ng of analyte mass loading). The MS was operated in scan range 40-340 amu with the electron ionization at 70 eV while the source temperature was set at 230 °C, and the quadrupole temperature was set to 150 °C. Each standard was analyzed in triplicate.

4.3.3. Materials for Synthetic Cannabinoids Studies

The JWH 122 2,3,6, and 8 methylnaphthyl isomers and JWH 081 3, 6, and 7 methoxynaphthyl isomers standards were obtained from Cayman Chemical (Ann Arbor, MI) in individual vials. A 1 mL aliquot of HPLC grade methanol (Fisher Scientific, Atlanta, GA) was pipetted into each vial to create an approximate 1000 µg/ml concentration. Each vial was vortexed at medium speed for a minimum of 15 minutes and stored at 0 °C. The IR studies utilized the standards at 1000 µg/ml while the MS studies utilized the standards at 100 µg/ml.

4.3.4. Instrumentation for Synthetic Cannabinoids Studies

GC-IR studies were conducted using an Agilent Technologies 6890N Network GC System coupled to an IRD3 detector obtained from Analytical Solutions and Providers (ASAP). The GC was operated in splitless mode with high purity helium as the carrier gas at a flow rate of 1.3 mL/min. The column used was a 30 m x 0.32 mm coated with 0.25 µm (OV-5) purchased from Ohio Valley Specialty Company (Marietta, OH). The oven program consisted of an initial temperature of 70 °C for 1 minute ramped by a rate of 30 °C/min to a final temperature of 320 °C and a final hold of 8 minutes. The GC inlet temperature was 280 °C with an injection volume of 1 µL (for a total amount of 1 µg of analyte mass loading). The IRD detector was operated at light pipe and transfer lines temperatures of 280 °C and all spectra were collected in the range 500-4000 cm^{-1} with a resolution of 8 cm^{-1}. Each standard was analyzed in triplicate using an autosampler.

GC-MS studies were conducted using an Agilent Technologies 7890A GC System coupled to an Agilent Technologies 5975C inert mass spectrometer (MS). The GC was operated

using a 5:1 split with high purity helium as the carrier gas at a flow rate of 1.2 mL/min. A 30 m by 0.25 mm column coated with 0.25 µm-thick sorbent DB-5MS column from Agilent Technologies was used. The oven program consisted of an initial temperature of 80 °C and ramped by a rate of 15 °C/min to a final temperature of 320 °C and a final hold of 4 min. The GC inlet temperature was 280 °C with an injector volume of 1 µL (for a total amount of 100 ng of analyte mass loading). The MS was operated in scan range 40-400 amu with the electron ionization at 70 eV while the source temperature was set at 230 °C, and the quadrupole temperature was set to 150 °C. Each standard was analyzed in triplicate.

4.4. Accurate Mass Analysis of Fentanyl Using MassWorks™ Software and LC-QTOF-MS

4.4.1. Materials

In the MassWorks experiments, all fentanyl samples were from the FAS Kit referenced in Section 4.1.1, and were reconstituted in HPLC grade methanol (Fisher Scientific, Atlanta, GA) to 100 µg/mL (or 100 ppm) concentration and injected at a volume of 1 µL. The perfluorotributylamine (PFTBA) standard was obtained from Restek (Bellefont, PA) and was filled to approximately ¾ of the PFTBA sample bulb before being reinstalled to the mass spectrometer (MS).

In the QTOF experiments, the fentanyl was obtained from the same source as that used in the MassWorks experiment. The samples were reconstituted in HPLC grade methanol (Fisher Scientific, Atlanta, GA) to 1 µg/mL (or 1ppm) concentration and injected at a volume of 1 µL. Eluent A consisted of LC-MS grade water with 0.1% formic acid and 5

mM ammonium formate from Fisher Scientific (Fair Lawn, NJ); eluent B consisted of LC-MS grade methanol with 0.1% formic acid from Fisher Scientific (Fair Lawn, NJ).

4.4.2. Instrumentation

All samples in the MassWorks studies were analyzed using an Agilent Technologies 7890A GC System coupled to an Agilent Technologies 5975C inert mass spectrometer (MS). The GC was operated using a 5:1 split with high purity helium as the carrier gas at a flow rate of 1.5 mL/min. A 30 m x 0.25 mm column coated with 0.25 μm-thick sorbent DB-5MS column from Agilent Technologies was used. The oven program consisted of an initial temperature of 35 °C for 2 min then a first ramp of 7°C/min to 200 °C, then a second ramp of 15 °C/min to 275 °C and held for 10 min. After the hold, the column was cooled to 35 °C and held for 3 min, and the PFTBA valve opened during the final minute to introduce an internal standard calibration peak into each chromatogram. The GC inlet temperature was 270 °C with an injector volume of 1 μL (for a total amount of 400 ng of analyte mass loading). The MS was operated in scan range 34-600 amu with the electron ionization at 70 eV while the source temperature was set at 230 °C, and the quadrupole temperature was set to 150 °C.

For the Q-TOF experiments, an Agilent Technologies 1290 Infinity liquid chromatography (LC) system coupled to an Agilent Technologies 6530 Accurate-Mass quadrupole time-of-flight (Q-TOF) mass spectrometer with dual electrospray ionization (ESI) with a nozzle voltage of 500 V. The nitrogen gas was held at 200 °C with a flow of 6 L/min and a nebulizer pressure of 35 psig. Ultra-pure nitrogen used for the collision gas was generated using a nitrogen generator. The MS fragmentor and skimmer voltages were operated at

135 V and 65 V, respectively. The scan range was set to 50-1000 m/z and the collision energies were 20, 30, 40, 60, and 70 eV. The Flow Injection Analysis (FIA) screening and the FIA MS/MS were both 1-min methods. Eluent A consisted of LC-MS grade water with 0.1% formic acid and 5 mM ammonium formate from Fisher Scientific (Fair Lawn, NJ); eluent B consisted of LC-MS grade methanol with 0.1% formic acid from Fisher Scientific (Fair Lawn, NJ).

4.4.3. Data Analysis

Processing of MassWorks data was performed using MassWorks software version 6.0 (Cerno Bioscience, Reno, NV, USA). The Q-TOF data was processed using MassHunter Qualitative Analysis B.07.00.

RESULTS AND DISCUSSION

5. UTILITY OF GC-MS AND GC-IR LIBRARIES IN DIFFERENTIATING POSITIONAL ISOMERS OF FENTANYL-RELATED SUBSTANCES (FRS)

Some sections published in: K Ferguson, J Perr, S L.Tupik, H Haddad, M Gilbert, R Newman and JR Almirall. Utility of Gas Chromatography Infrared Spectroscopy (GC-IR) for the Differentiation of Positional Isomers of Fentanyl Related Substances. *Forensic Chemistry*.(2022) 29, 100425. https://doi.org/10.1016/j.forc.2022.100425

5.1. Introduction

The number of fentanyl-related drug overdoses in the United States has seen an approximate eight-fold increase over the past few years surpassing deaths from illicit use of prescription opioids and heroin [60]. In 2017, 59.8% of opioid-related deaths involved fentanyl and/or fentanyl related substances (FRS) compared to 14.3% in 2010 [61]. It is estimated that approximately ninety Americans die each day as a result of opioid abuse, and this number continues to increase at alarming levels [4]. In the past 5 years, there has been a 10-fold increase in the reporting of seized fentanyl and FRS [62]. According to the National Forensic Laboratory Information System (NFLIS) 2020 mid-year report, fentanyl is the fourth most identified drug reported by NFLIS-participating forensic laboratories, up from fifth in previous years [54].

The opioid crisis has amplified the need for identification of fentanyl and FRS. To assist with compound identification, libraries created from reference materials are needed. Forensic laboratories routinely use GC-MS as the gold standard for confirmation of seized

drugs. For the fentanyl isomers, the typical electron impact mass spectra generated results, in some cases, to no molecular ions formed and indiscriminate fragmentation for a large number of FRS positional isomers, often making identification challenging if not used in collaboration with other more discriminating analytical methods [6,7,8]. The core structure of fentanyl consists of an amide group, a piperidine ring, an aniline ring, and an *n*-alkyl chain, each of which provides regions for substitutions that alter the structure. These substitution regions are exploited by producers on the illicit market and contribute to the diversity of FRS [23].

Implementation of standard libraries has been vital to drug identification within the field of forensic chemistry. The rapidly evolving seized drugs entering the illicit market require the development and continuous maintenance of libraries containing searchable spectra of reference material. Commercial libraries exist for a wide variety of analytical techniques such as GC-MS, infrared (IR), nuclear magnetic resonance (NMR), and Raman spectroscopy [7,8]. Methods complementary to GC-MS, such as GC-IR, are being introduced into forensic laboratories as cost-effective means to distinguish FRS and other novel psychoactive substances (NPS), including cathinones and synthetic cannabinoids. GC-IR is a confirmatory technique that typically results in a unique infrared spectra, whereby no two compounds, though similar, will have the same absorbance characteristics [43]. GC-IR has been reported for the identification of FRS [10,11] isomeric ethoxyphenethylamines and methoxymethcathinones [50], methylenedioxybenzylpiperazines (MDBPs) and methoxymethylbenzylpiperazines (MMBPs) [51], and methamphetamine and regioisomeric substances [15]. Although GC-IR is successful in the differentiation of positional isomers, this technique is more limited

is terms of sensitivity compared to GC-MS [52]. Mass loadings of more than 25 ng on column for GC-IR analysis are needed to produce acceptable spectra, in comparison to sub-ng mass loadings needed for a typical GC-MS analysis [48]. GC-MS analysis with a library search of reference standards has been the routine approach for controlled substance identification in complex mixtures [58]. One recent study incorporated a targeted GC-MS method that was able to differentiate all but four compound pairs based on nonoverlapping retention time and acceptance windows or objectively different mass spectra [63].

Based upon literature searches, this appears to be the first reporting of a blind study using a FRS-specific vapor-phase infrared spectra library as well as a FRS specific mass spectra of library for 212 different FRS compounds. Studies to determine the limits of detection, limits of quantitation, and the results of library searches for the differentiation of FRS at three different laboratories are also included in this study.

5.2. Results and Discussion

5.2.1. Gas Chromatography Mass Spectrometry Results (GC-MS)

Within the 20 blind samples, six different FRS were selected based on their isomeric nature including two sets of three different structural/positional isomers. Compounds 1-3 are N-(2-methylphenyl)-N-[1-(2-phenylethyl)-4-piperidinyl]-propanamide (commonly referred to as *ortho*-methylfentanyl), N-(3-methylphenyl)-N-[1-(2-phenylethyl)-4-piperidinyl]-propanamide *(*commonly referred to as *meta*-methylfentanyl), and N-(4-methylphenyl)-N-[1-(2-phenylethyl)-4-piperidinyl]-propanamide (commonly referred to as *para*-

methylfentanyl); all have the same molecular weight of 350 amu and produce a similar fragmentation pattern containing the major ions of m/z 259, 160, and 203 (**Figure 13**). Compounds 4-6 are N-(2-fluorophenyl)-N-[1-(2-phenylethyl)-4-piperidinyl]-propanamide (commonly known as *ortho*-fluorofentanyl), N-(3-fluorophenyl)-N-[1-(2-phenylethyl)-4-piperidinyl]-propanamide (commonly known as *meta*-fluorofentoanyl), and N-(4-fluorophenyl)-N-[1-(2-phenylethyl)-4-piperidinyl]-propanamide (commonly known as *para*-fluorofentanyl; all have the same molecular weight of 354 amu and produce a similar fragmentation pattern containing the major ions of m/z 263, 164, and 207 (**Figure 14**). Note the lack of a molecular ion within all spectra, a characteristic of many of the FRS. One reason for the similarity of the fragmentation pattern is due to the cleavage of the α and β carbons of the ethyl heterocyclic linker that result in a base peak ion and a loss of the tropylium ion (C_7H_7, 91 amu) [23]. Positional isomers with indistinguishable mass spectra have been previously reported [48], [64], [65].

The blind samples of *meta*-fluorofentanyl, *para*-methylfentanyl, and *ortho*-methyl cyclopropyl fentanyl using the reported GC-MS systems operating with helium carrier gas were not correctly identified using the criteria described in section 4.1. The blind samples fluoroisobutyryl fentanyl and *ortho*-methyl cyclopropyl fentanyl using the reported GC-MS systems operating with hydrogen carrier gas were also not correctly identified using

the criteria described in section 4.1. All other blind samples were correctly identified using the criteria defined in section 4.1.

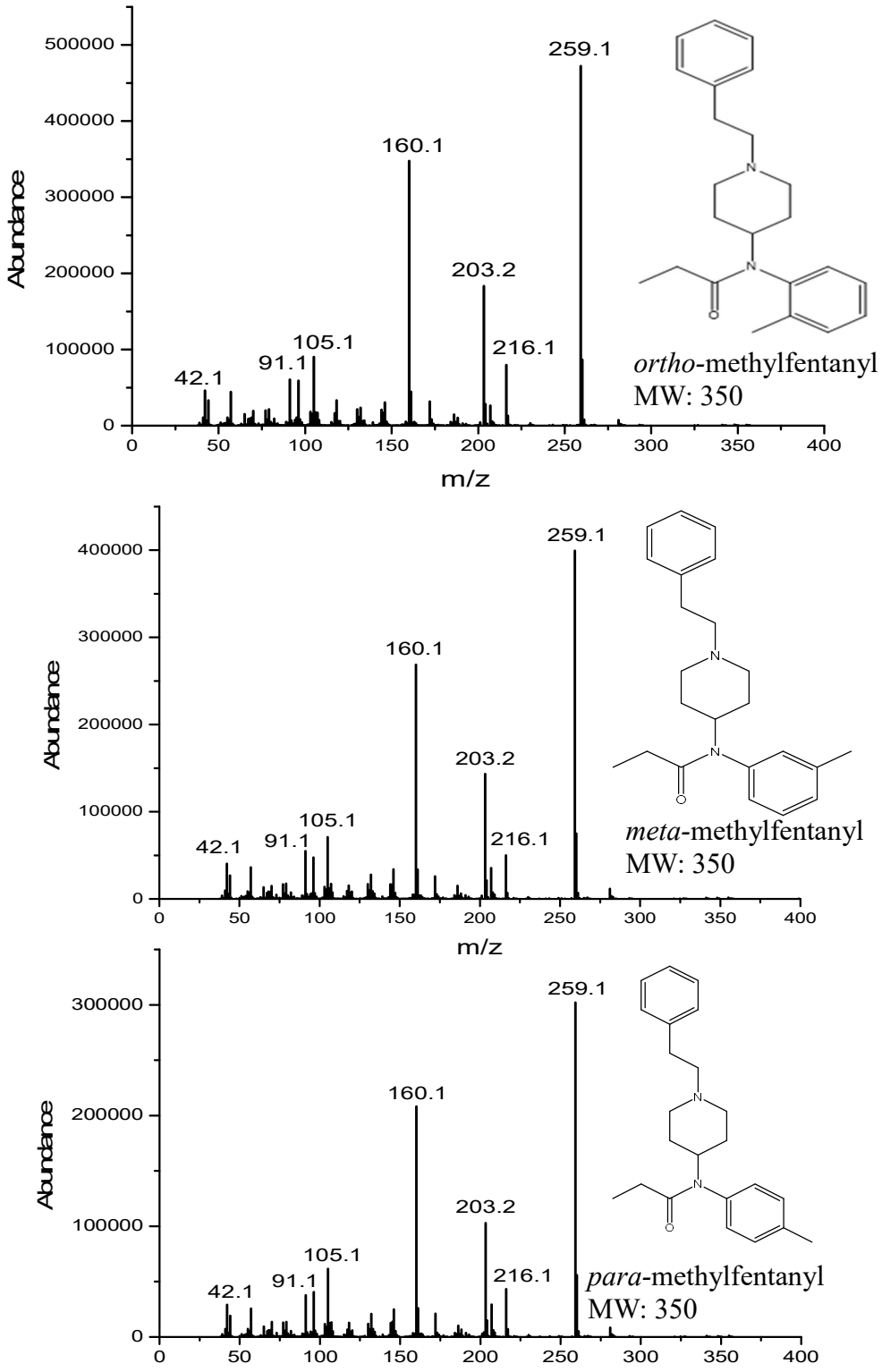

Figure 13. Mass spectra of *ortho*-methylfentanyl, *meta*-methylfentanyl, and *para*-methylfentanyl.

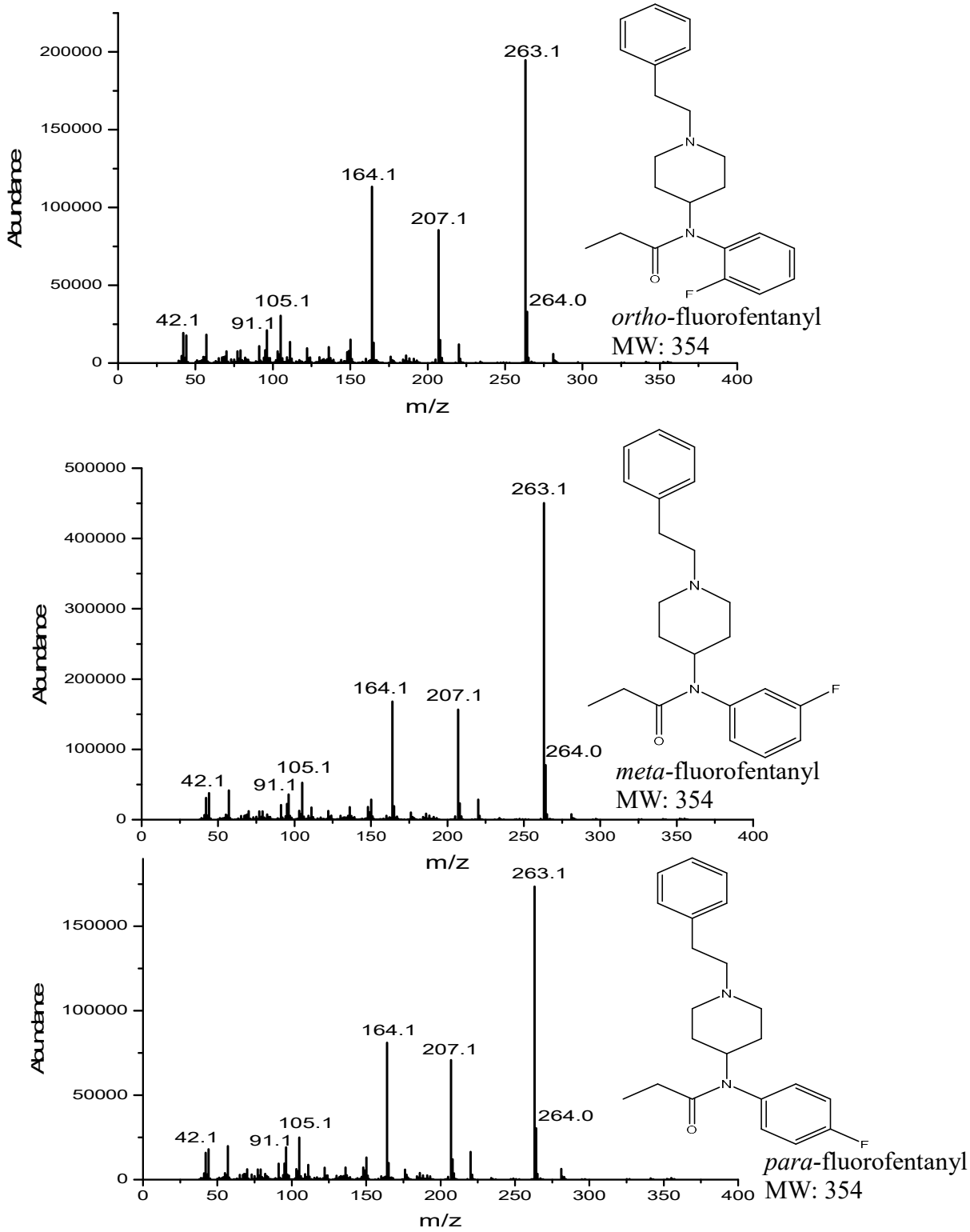

Figure 14. Mass spectra of *ortho*-fluorofentanyl, *meta*-fluorofentanyl, and *para*-fluorofentanyl.

5.2.2. Gas Chromatography Infrared Detection Results (GC-IR)

The same positional isomers from the GC-MS study were then subjected to GC-IR analysis. The vapor phase IR spectra of compounds 1-3 are shown in **Figure 15**. Similarities are noticeable in the C-H stretch region of ~3000cm^{-1}, as well as the ~1600cm^{-1} C=O region. Differences were observed both in the 1400cm^{-1} to 1350cm^{-1} ring region and in the "fingerprint region" of 1300cm^{-1} to 500cm^{-1} allowing for differentiation.

The IR spectra of compounds 4-6 are shown in **Figure 16** with similar observations for differences in the C-H stretch region, the C=O region, the ring region, as well as the fingerprint region.

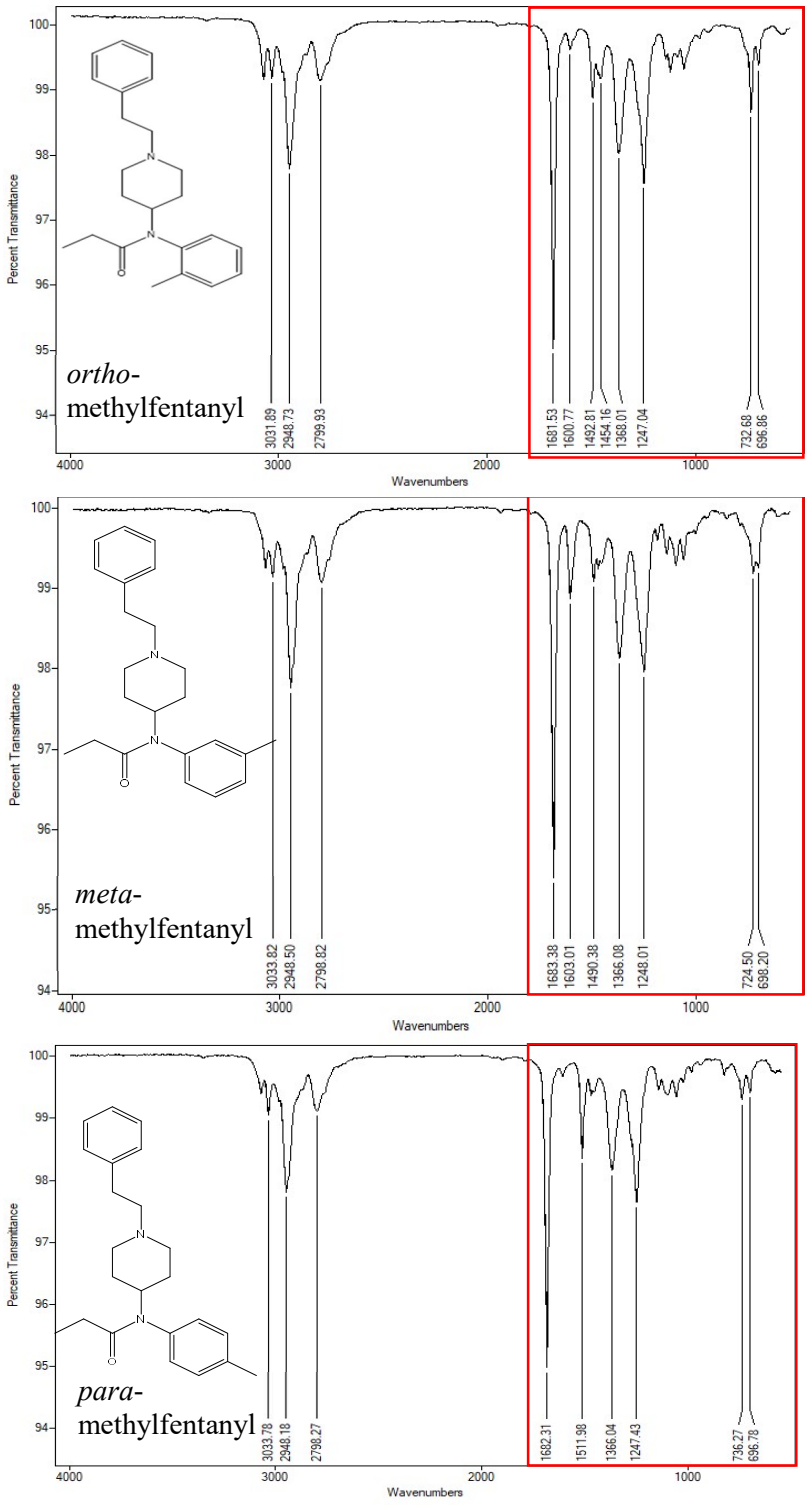

Figure 15. Vapor phase infra-red spectra of *ortho*-methylfentanyl, *meta*-methylfentanyl, and *para*-methylfentanyl. The red square depicts the "fingerprint" region of the IR spectra.

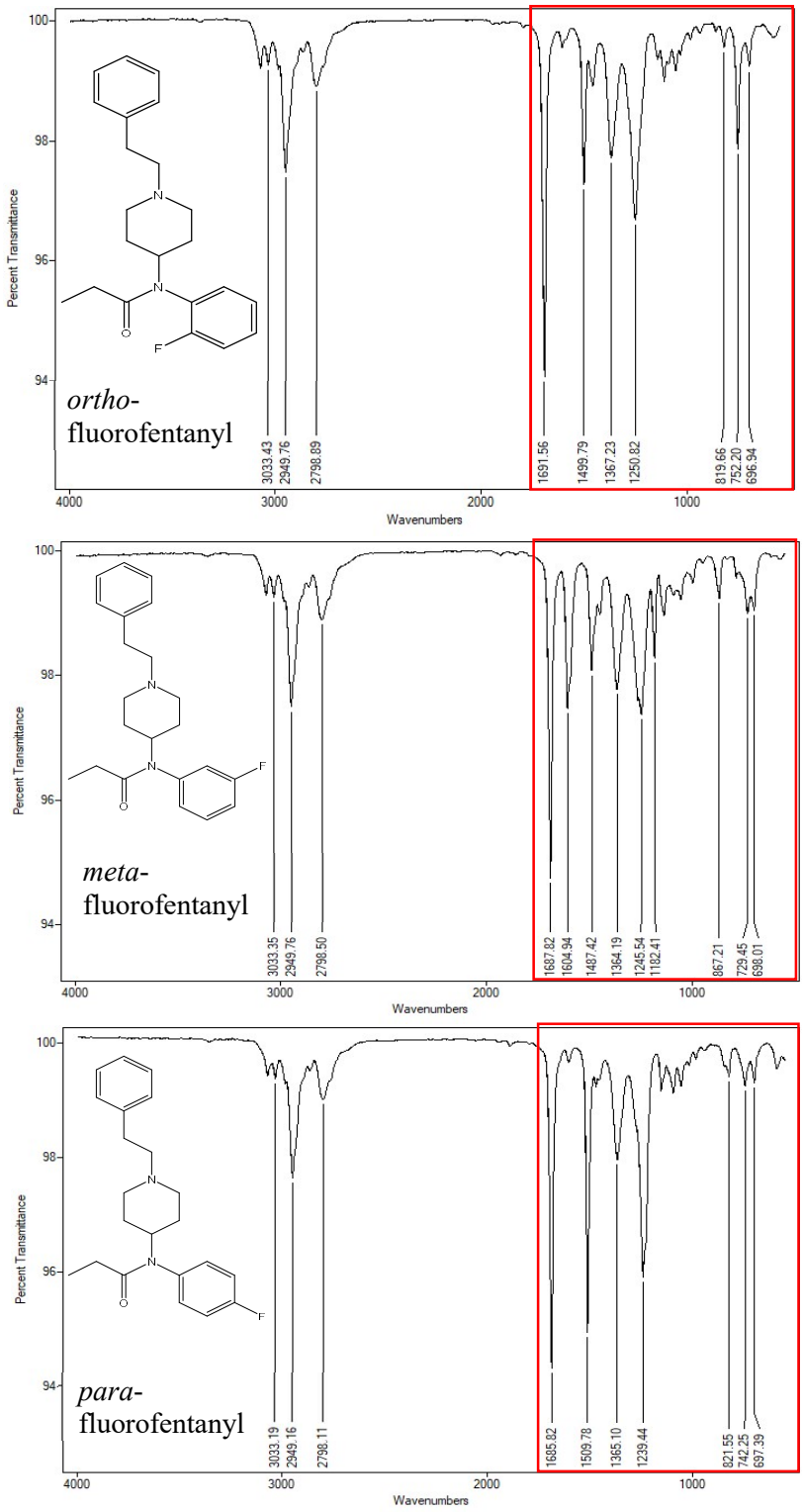

Figure 16. Vapor phase infra-red spectra of *ortho*-fluorofentanyl, *meta*-fluorofentanyl, and *para*-fluorofentanyl. The red square depicts the "fingerprint" region of the IR spectra.

5.2.3. Evaluation of the FIU FRS MS Library and FIU FRS IR Library

5.2.3.1. FIU FRS MS Library Search Results

MS spectra were searched with the Agilent MSD Chemstation software using both the National Institute of Standards and Technology (NIST) library and the FIU MS FRS library. Some of the triplicate spectra produced had minor ion differences; however, the major ions produced were similar with only slight abundance differences. Each of the 212 triplicate spectra was searched against both libraries, resulting in 212 compounds being searched three times for a total of 636 searches. The search utility uses the Probability Based Matching algorithm developed by Fred McLafferty where the significant ions and abundance spectra of unknown compounds are statistically compared to library spectra [65]. The algorithm verifies that the main peaks in the reference spectrum are also present in the unknown spectrum.

When the NIST MS library was searched, only 10 samples resulted in a primary match to the expected compound (4.7% of the searches). This was attributed to the fact that the NIST library does not contain many of the FRS contained in the FAS-Kit and Emergent Panels. When the new FIU FRS library was searched, 190 analyses resulted in a primary match to the expected compound (89.6% of the searchers). It should be noted that the FIU FRS library does contain all 212 FRS compounds. Misidentifications in the top five results were found ~ 90% of the time highlighting the similarity of MS spectra for positional isomers. For example, the results for a search of *para*-methylfentanyl yielded matches in the top five followed by its positional isomers *ortho*-methylfentanyl and *meta*-methylfentanyl also in the top five matches. A library search was also conducted for *meta*-fluorofentanyl also resulting in the top three matches, closely followed by its positional isomers *para*-

fluorofentanyl and *ortho*-fluorofentanyl in the top five matches. **Figures 13 and 14** show the similarities in the fragmentation patterns shared among the different positional isomers.

A "perfect match" was not found for ~10% of the positional isomers in the MS library given that the search algorithm utilizes the abundance of the significant ions in the reference spectrum in order to identify the unknown spectrum. Since these isomers have the same peaks in the same ratio of abundance due to similar fragmentation, it is difficult to distinguish between positional isomers, even when the reference spectra are included in the library.

5.2.3.2. FIU Fentanyl IR Library Search Results

The FIU FRS IR library generated from the analysis of the compounds in the FAS Kit (using the Essential FTIR software) and the existing EUCLiD IR Library were also evaluated. There are 32 FRS common to both libraries. When using the combination of both FIU FRS IR and EUCLiD libraries, 100% of the searches resulted in best matches to the correct compound for each of the 212 standards. *Para*-methylfentanyl and *meta*-fluorofentanyl were subsequently searched using both libraries. *Ortho*-fluorofentanyl was not searched because it is common to both the FIU Fentanyl IR Library and the EUCLiD IR library. Additionally, the same positional isomers that were searched using the MS libraries were searched again with the IR libraries. To calculate the similarity scores, ASAP uses the correlation coefficient method. This calculation is similar to the calculation of correlation coefficient in statistics to obtain the R value [66]. The x (wavenumber) and y (percent absorbance/transmittance) are collected at each point individually and calculated. The results are then compared with the reference and the unknown to determine a similarity

score. It should be noted that the *para*-methylfentanyl was not present in the EUCLiD library so it was not present in the library results after the search (**Table 10**).

Table 10. The library search results for para-methylfentanyl using FIU and EUCLiD libraries.

Sample	Metric	Name	Library	Entry
1	1.000000	020521 *Para*-Methylfentanyl 1: 3ul 400ppm	FIU	102: 020521 *Para*-Methylfentanyl 1
2	0.999647	020521 *Para*-Methylfentanyl 2: 3ul 400ppm	FIU	103: 020521 *Para*-Methylfentanyl 2
3	0.999012	020521 *Para*-Methylfentanyl 3: 3ul 400ppm	FIU	104: 020521 *Para*-Methylfentanyl 3
4	0.978178	020521 4'-Methyl Fentanyl 2: 3ul 400ppm	FIU	85: 020521 4'-Methyl Fentanyl 2
5	0.978083	020521 4'-Methyl Fentanyl 1: 3ul 400ppm	FIU	84: 020521 4'-Methyl Fentanyl 1
6	0.977495	020521 4'-Methyl Fentanyl 3: 3ul 400ppm	FIU	86: 020521 4'-Methyl Fentanyl 3
7	0.973950	032321 *Para*-Methyl Butyryl Fentanyl 3: 3ul 400ppm	FIU	341: 032321 *Para*-Methyl Butyryl Fentanyl 3
8	0.973020	020821 Orth0-Methylfentanyl 1: 3ul 400ppm	FIU	120: 020821 *Ortho*-Methylfentanyl 1
9	0.972718	020821 *Ortho*-Methylfentanyl 2: 3ul 400ppm	FIU	121: 020821 *Ortho*-Methylfentanyl 2
10	0.972533	020821 *Ortho*-Methylfentanyl 3: 3ul 400ppm	FIU	122: 020821 *Ortho*-Methylfentanyl 3

When *para*-methylfentanyl was searched against EUCLiD, the best match suggested *para*-methyl butyryl fentanyl (**Table 11**), as *para*-methylfentanyl was not contained within the EULCiD library. A comparison of the spectra of both *para*-methylfentanyl and *para*-methyl butyryl fentanyl is shown in **Figure 17**, with data being presented in absorbance units since that is the only data output which EUCLiD offers. Differences are observed in the ~1500cm^{-1} region. It should be noted that searches with the existing EUCLiD library only return 32/212 (15.1%) matches to the correct compound of the FRS searched. However, this can be explained by the lack of FRS compounds in the EUCLiD library resulting in other FRS being selected as the "best match" but with diminished confidence scores.

Table 11. Results of the EUCLiD library search for para-methylfentanyl.

Sample	Metric	Name	Library	Entry
1	0.961873	*para*-methyl Butyryl Fentanyl	Project_Euclid_v1-0-0	1167
2	0.961541	Fentanyl	Project_Euclid_v1-0-0	741
3	0.955077	N-methyl Norfentanyl	Project_Euclid_v1-0-0	1059
4	0.950822	Benzyl Fentanyl	Project_Euclid_v1-0-0	520
5	0.942833	Butyryl fentanyl	Project_Euclid_v1-0-0	558
6	0.938878	Valeryl Fentanyl	Project_Euclid_v1-0-0	1379
7	0.926652	*para*-Bromofentanyl	Project_Euclid_v1-0-0	1162
8	0.914583	Isobutyryl Fentanyl	Project_Euclid_v1-0-0	802
9	0.900042	4-Methoxy-butyryl fentanyl	Project_Euclid_v1-0-0	273
10	0.891177	*para*-Fluorofentanyl	Project_Euclid_v1-0-0	1164

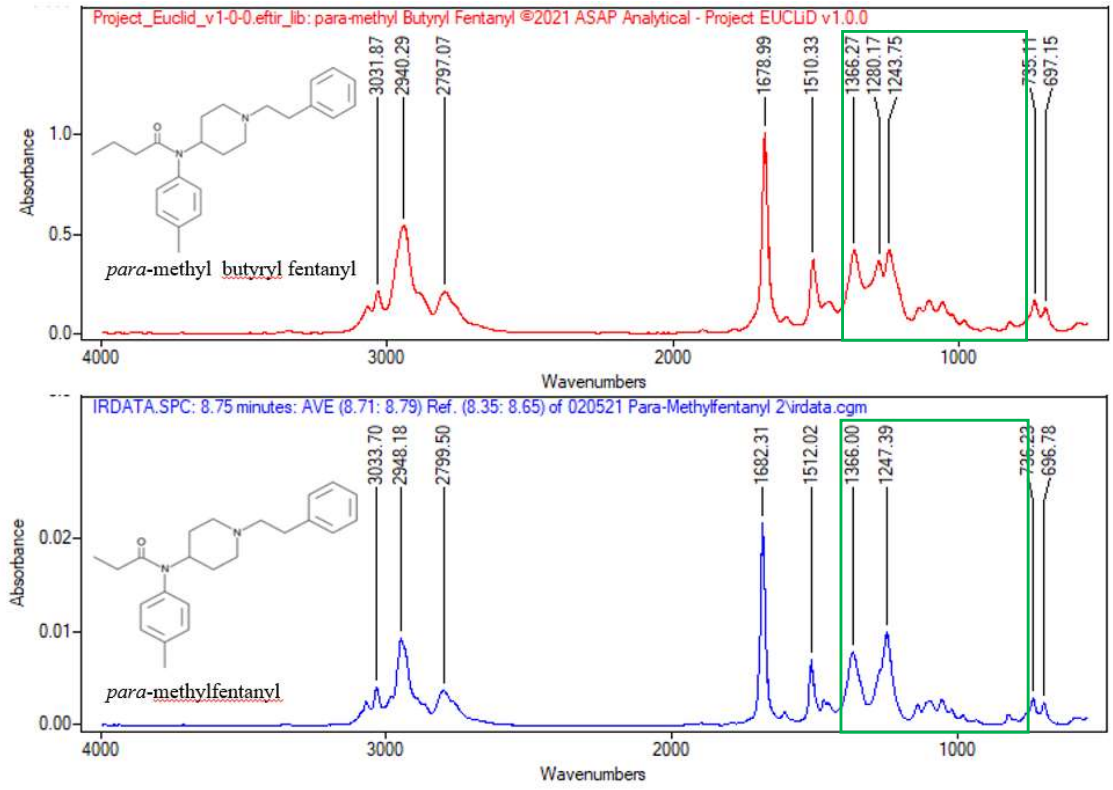

Figure 17. Comparison of spectra of *para*-methyl butyryl fentanyl (red) and *para*-methylfentanyl (blue).

For *meta*-fluorofentanyl, the search results included output from both libraries (**Table 12**). The FIU Fentanyl IR library results included the top three results correctly as *meta*-fluorofentanyl with confidence scores of 1.00, 0.99, and 0.99 respectively. The EUCLiD

library had the fourth match at a score of 0.99. It should be noted, however, that scores do not constitute an identification. The spectral comparison of the FIU Fentanyl IR library and the EUCLiD library for this compound is shown in **Figure 18**.

Table 12. The library search results for meta-fluorofentanyl using FIU and EUCLiD library for fentanyl related substances (FRS).

Sample	Metric	Name	Library	Entry
1	1.000000	020821 *Meta*-Fluorofentanyl 1: 3ul 400ppm	FIU	117: 020821 *Meta*-Fluorofentanyl 1.spc
2	0.995785	020821 *Meta*-Fluorofentanyl 2: 3ul 400ppm	FIU	118: 020821 *Meta*-Fluorofentanyl 2.spc
3	0.995247	020821 *Meta*-Fluorofentanyl 3: 3ul 400ppm	FIU	119: 020821 *Meta*-Fluorofentanyl 3.spc
4	0.989161	*meta*-Fluorofentanyl	Project_Euclid_v1-0-0	947
5	0.969818	012621 *Meta*-Fluorobutyryl Fentanyl 2: 3ul 400ppm	FIU	70: 012621 *Meta*-Fluorobutyryl Fentanyl 2.spc
6	0.969783	012621 *Meta*-Fluorobutyryl Fentanyl 3: 3ul 400ppm	FIU	71: 012621 *Meta*-Fluorobutyryl Fentanyl 3.spc
7	0.968145	012621 *Meta*-Fluorobutyryl Fentanyl 1: 3ul 400ppm	FIU	69: 012621 *Meta*-Fluorobutyryl Fentanyl 1.spc
8	0.950108	012621 *Meta*-Fluoroisobutyryl Fentanyl 3: 3ul 400ppm	FIU	74: 012621 *Meta*-Fluoroisobutyryl Fentanyl 3.spc
9	0.949963	012621 *Meta*-Fluoroisobutyryl Fentanyl 2: 3ul 400ppm	FIU	73: 012621 *Meta*-Fluoroisobutyryl Fentanyl 2.spc
10	0.949947	012621 *Meta*-Fluoroisobutyryl Fentanyl 1: 3ul 400ppm	FIU	72: 012621 *Meta*-Fluoroisobutyryl Fentanyl 1.spc

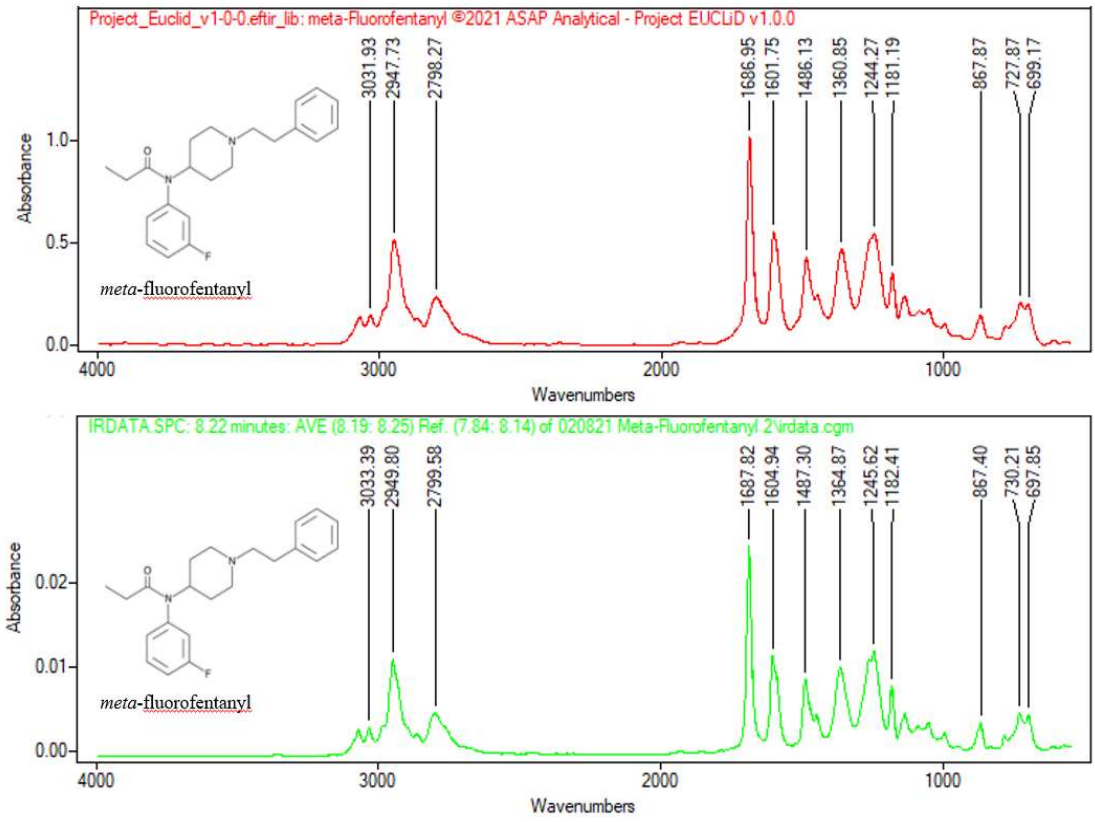

Figure 18. Comparison of spectra from EUCLiD library search (top spectra) the new FIU Fentanyl library search (bottom spectra) for *meta*-fluorofentanyl.

In **Figure 18**, the similarity in the IR spectra is evident, particularly in wavenumber region 550-1600cm^{-1}. A summary of the comparison between the different search tools (MS and IR) is shown in **Table 13** including a comparison of the search results between the GC-MS NIST library, the FIU MS library, the existing EUCLiD library and the FIU Fentanyl IR library. It should be noted that the EUCLiD user library will continue to grow, and these results are expected to improve as additional reference standards are added by users including the addition of the FIU Fentanyl IR library in the future.

Table 13. Comparison of the search results for an existing NIST GC-MS library search, a search of the new FIU MS library, the existing EUCLiD GC-IR library and the new FIU Fentanyl IR library created at the FIU laboratory.

Library	Number of Matches in the Top 5 Search Results	Percentage of Correct Matches (%)
GC-MS NIST Library	10	4.7
New FIU Fentanyl GC-MS Library	190	89.6
EUCLiD GC-IR Library (2021)	32	15.1
New FIU GC-IR FRSLibrary	212	100.0

5.2.4. LODs and LOQs of the ASAP IRD3 Detector in the GC-IR Studies

The limit of detection (LOD) and limit of quantitation (LOQ) were calculated for the ASAP IRD3 detector using fentanyl as a model compound. Each of the three participating laboratories created calibration curves using peak areas with correlation coefficients (R^2) ranging from 0.9821 to 0.9978. **Figure 19** shows the linear range of the calibration curve between 0.20 mg/mL to 1.2 mg/mL for one laboratory. The calculated LODs from the three laboratories ranged from 0.10 mg/mL to 0.19 mg/mL and the LOQs ranged from 0.30 mg/mL to 0.57 mg/mL. In comparison, the LOD and LOQ for MS calculated at FIU was

0.009 mg/mL and 0.027 mg/mL, respectively, approximately one order of magnitude better detection with the MS.

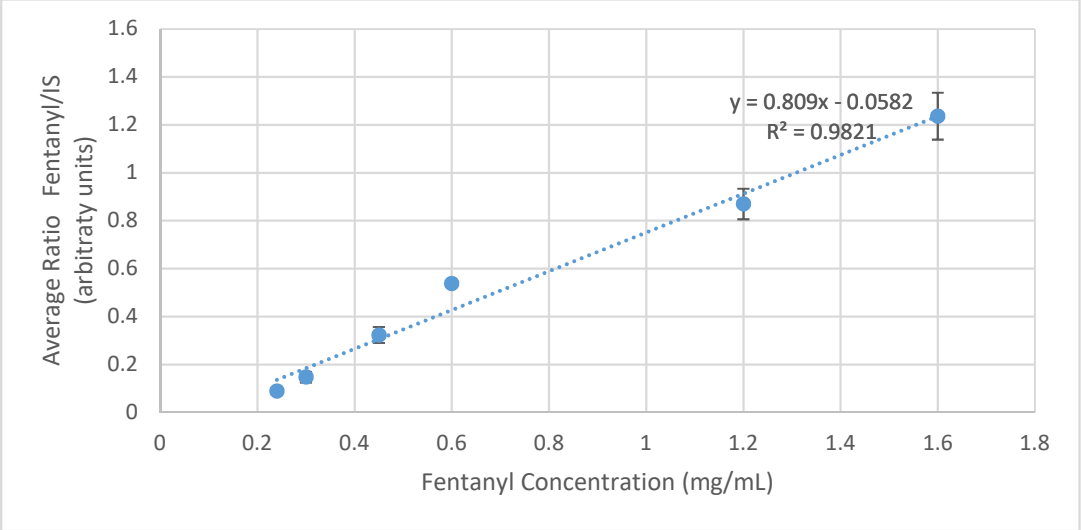

Figure 19. Calibration curve for fentanyl showing concentration (mg/mL) vs. average integrated peak area (arbitrary units).

5.2.5. Blind Study Results

A blind study was conducted to determine the utility of the MS and IR libraries to forensic laboratories for the identification of FRS. The rationale behind choosing the 20 for investigation is detailed in **Tables 6 and 9**. The laboratories are identified by numbers 1 to 3 for this paper. The results of the study are detailed in **Tables 14 and 15**.

Table 14. Results of the blind study in the identification of 20 FRS using GC-MS.

Lab Number	Number of Compounds Correctly Identified
1	20/20
2	16/20
3	16/20

Table 15. Results of the blind study in the identification of 20 FRS using GC-IR.

Lab Number	Number of Compounds Correctly Identified
1	20/20
2	20/20
3	20/20

A correct identification criteria is defined in section 4.1.5. The quality of the match must be equal to or greater than 90 for MS spectral comparison and/or must be equal to or greater than 0.95 for the IR spectral comparison. For the MS studies, laboratory #1 performed better than the other two laboratories in the identification of the compounds in question by correctly identifying all 20 compounds. Lab # 1 reported also taking into account the retention time whereas Labs # 2 and 3 solely relied on the results of the MS library search. It should be noted that when the retention time was taken into consideration for those compounds that were misidentified by MS, correct identifications of the unknown compounds were reported by the other laboratories. The use of the IR spectral comparisons performed better in the identification of the unknowns with 100% correct for all three laboratories.

5.3. Conclusion and Future Directions

GC-MS alone may not be sufficient for the identification of FRS; however, GC-IR provides an *orthogonal* confirmatory technique that differentiates between positional isomers of FRS. New GC-MS and GC-IR libraries were created with authentic reference standards, with each reference standard acquired in triplicate, for 212 FRS and are now freely available [67] to the forensic science community. Seventy-nine, or approximately 37% of the 212 analogs, did not produce a molecular ion with electron impact ionization mass

spectrometry and, as expected, positional isomers of FRS produce similar fragmentation in their mass spectra when using electron impact GC-MS. A library search of each of the 212 FRS using the NIST library produced 4.7% matches to the correct compound, which is not unexpected as most of the FRS were not included the NIST library. Only 89.6% of the searches resulted in the correct compound within the top five candidates when using the newly created GC-MS library. An existing GC-IR database (EUCLiD) that contained only 32 of the 212 FRS was also searched with 15.1% correct correlation. When the new GC-IR library containing all 212 FRS was searched, 100% identification was achieved. The three laboratories in this study searched 20 blind FRS samples using the FIU FRS Library with 100% correct match correlations.

The LODs and LOQs were also calculated for the GC-IR methods used by the three laboratories ranging in LODs between 0.10 mg/mL to 0.19 mg/mL and the LOQs from 0.30 mg/mL to 0.57 mg/mL. A larger scale interlaboratory study using a double-blind design and simulating real-world case scenarios is planned for the near future.

This study strongly supports the use of GC- IR in the analysis of unknown compounds, especially FRS, but also for all other highly manipulated drug structures with abundant isomer configurations, including cathinones and synthetic cannabinoids. The combination of GC-MS and GC-IR results in the highest confidence of isomer identification of NPS compounds.

6. AN INTERLABORATORY STUDY TO EVALUATE THE UTILITY OF GAS CHROMATOGRAPHY MASS SPECTROMETRY (GC-MS) AND GAS CHROMATOGRAPHY INFRARED SPECTROSCOPY (GC-IR) SPECTRAL LIBRARIES IN THE FORENSIC ANALYSIS OF FENTANYL-RELATED SUBSTANCES (FRS)

Some sections are submitted for publication and can be found in: K Ferguson, J Perr, S Tupik, M Gilbert, R Newman, A Winokur, I Vallejo, S Hokanson, M Pothier, B Knapp, M Icard, K Kramer, and JR Almirall. "An Interlaboratory Study to Evaluate the Utility of Gas Chromatography Mass Spectrometry (GC-MS) and Gas Chromatography Infrared Spectroscopy (GC-IR) Spectral Libraries in the Forensic Analysis of Fentanyl Related Substances (FRS)". Journal of Forensic Science, In press. 2023.

6.1. Introduction

According to the 2021 National Forensic Laboratory Information System (NFLIS) Drug Report, fentanyl remains the fourth most identified drug by forensic laboratories in the United States and the second most identified by federal laboratories [1]. This, coupled with the fact that fentanyl accounted for approximately 71,000 of the 107,000 overdose deaths reported in the United States in 2021[1], [3] highlights the fact that fentanyl related substances (FRS) continue to pose a problem for forensic analysis and to the health care system. A solution to this problem calls for a specific, unambiguous method of FRS analysis and identification that would assist the forensic community.

There are several analytical methods used in forensic laboratories for the analysis of controlled substances. Gas chromatography-mass spectrometry (GC-MS) combines chromatographic separation with unambiguous identification and is considered the drug confirmation "gold standard" in forensic science. However, this technique is not without

its limitations in confirmation of fentanyl and its positional isomers [23], [48], [68], as well as other illicit drugs and their associated isomers [50], [69], [70]. For this reason, an alternative technique for confirmation of FRS is necessary. Gas chromatography infrared spectroscopy (GC-IR) is a complementary instrumental technique to GC-MS where molecules are characterized based on the bending and stretching of chemical bonds at different wavelengths of infrared radiation to which they are exposed. This results in the formation of characteristic absorption or transmittance bands at specific wavelengths with the unique ability for "fingerprinting" based on the spectra produced by each compound [69], [70].

Several recent studies have addressed the difficulties with differentiation of regioisomeric analogs of controlled substances such as fentanyl [48], [68], phenethylamines [50], cathinones [45], and synthetic cannabinoids [70], [71] where GC-MS alone was not sufficient for their differentiation. Additionally, the product ions from tandem mass spectrometry (MS-MS) may also differentiate isomers of FRS based on the success with phenethylamines and cathinones. The immonium ions, $C_4H_{10}N^+$, (*m/z* 72) produced from collision-induced dissociation (CID) of phenethylamines, produced sufficiently different spectra which can be used in the differentiation of their regiosiomeric forms [72], [73]. Furthermore, regioisomeric forms of phenethylamines were differentiated by their CID mass spectra alone [74], [75], as well as regioisomeric forms of lysergic acid diethylamide (LSD) [76]. Finally, positional isomers of N-alkylated fluorocathinones were differentiated by their CID product-ion spectra alone [77].

When used in conjunction with GC-IR, the combination of the techniques produced sufficient information to differentiate the isomers. This current study incorporates a blind

interlaboratory exercise involving seven (7) different laboratories using GC coupled to vapor phase IR (n=6) or solid phase IR in the case of one laboratory. A previous study conducted by Jones et. al. [45] was reported as effective for differentiating positional isomers of psychoactive substances. The analogues of a new category of Novel Psychoactive Substances (NPS), 2,5-dimethoxy-N-(N-methoxybenzyl) phenethylamine (NBOMe or 25X-NBOMe), were also investigated using vapor phase GC-IR, which provided exceptional differentiation of their regioisomeric structures [78], [79]. In comparison studies of the use of GC-IR for the analysis of regioisomeric analogs of NBOMes, resulting GC-MS fragmentation patterns produced characteristic, and in some cases similar, fragment ions from the position of the substitutions were able to be confirmed using vapor phase GC-IR [80], [81]. Since these regioisomeric analogs produced similar fragment ions using GC-MS, the focus of the use of both GC-MS and GC-IR in the interlaboratory comparison studies is the main topic of this publication.

Interlaboratory studies can involve analysis of a compound or compounds by different participating laboratories for each to assess and measure variation of the results obtained. For this blind study, participants were provided 20 different samples to analyze but were not aware of the identity of the substance(s) in samples prior to the analysis although they were told that the samples contained an FRS. The participants were asked to use any existing GC-MS or GC-R libraries including in-house created libraries or the NIST library and were also provided access to 2 new libraries previously reported [67], [68]. The main purpose of this study was to determine the utility of the novel FIU GC-MS and GC-IR fentanyl libraries [67] for the identification of FRS in forensic laboratories across the United States. To evaluate this, an interlaboratory study involving 7 forensic laboratories

was organized. Twenty (20) FRS of unknown identity were analyzed by each of the seven (7) laboratories. Each substance was identified and reported to FIU by each participating laboratory. The results were evaluated for accuracy and are reported in this publication. This is the first time an interlaboratory study has been reported that compares the results of analysis of FRS amongst different forensic laboratories.

6.2. Results and Discussion

A validation study on the use of the libraries was conducted by a smaller subset of 3 laboratories and previously described by Ferguson et.al [68]. Subsequently, the interlaboratory study was extended to include four additional laboratories and now includes blind testing of 20 unknown FRS. The ability of each laboratory to correctly identify the blind samples was assessed and the results are discussed below.

6.2.1. Laboratory GC-MS Results

Each laboratory analyzed the twenty (20) blind FRS samples by gas chromatography mass-spectrometry and utilized the FIU-generated Fentanyl Mass Spectral Library for use in determining the best library match to that of the unknown substance. Each independent laboratory's results were reported, compiled, and verified. The algorithm used to identify the best matches in the FIU Fentanyl Mass Spectral library was created using the Agilent ChemStation software and used the "Probability Based Matching" (PBM) [82] where probabilities of a match are assigned using information from the mass fragments and molecular ion. However, the algorithm only utilizes a maximum of 15 to 26 peaks for compounds of molecular weight (M_r) <171 or >600, respectively; noting there is a decrease

in the probability of an exact match with increasing size and number of possible isomers [82].

Table 16 is a comparison of laboratory reported identification results for GC-MS analysis and actual FRS identity. Summaries for each participating laboratory follow.

Laboratory #1 correctly identified 16 of the 20 FRS, a result of 80% correct identification. Those incorrectly identified were Ocfentanil (also known as *ortho*-fluoro Methoxyacetyl fentanyl) which was misidentified as its positional isomer *meta*-fluoro Methoxyacetyl fentanyl; *meta*-Fluorofentanyl which was misidentified as *para*-Fluorofentanyl; *para*-Methylfentanyl which was misidentified as its positional isomer *ortho*-Methylfentanyl;; and *ortho*-methyl Cyclopropyl fentanyl which was misidentified as its positional isomer *meta*-methyl Cyclopropyl fentanyl.

Laboratory #2 correctly identified 16 of the 20 FRS. Those incorrectly identified were *ortho*-methyl Furanyl fentanyl which was misidentified as its positional isomer *meta*-methyl Furanyl fentanyl; *meta*-Fluorofentanyl which was misidentified as its positional isomer *ortho*-Fluorofentanyl; *para*-Methylfentanyl which resulted in probable matches among other possible positional isomers of methylfentanyl; and *ortho*-methyl Cyclopropyl fentanyl which also resulted in probable matches among other possible positional isomers of methyl Cyclopropyl fentanyl.

Laboratory #2's use of hydrogen as the carrier gas was also assessed to determine if it would affect the results in comparison to using helium. Using hydrogen as the carrier gas, the laboratory was able to correctly identify 16 of the 20 FRS, a result of 80% correct identification. The samples incorrectly identified were *meta*-Fluorofentanyl which was misidentified as 2'-fluoro *ortho*-Fluorofentanyl; *para*-Chlorobutyryl fentanyl which was

misidentified as *para*-Chloroisobutyryl fentanyl; FIBF which was misidentified as *ortho*-Fluorobutyryl fentanyl; and *ortho*-methyl Cyclopropyl fentanyl which was misidentified as *para*-methyl Cyclopropyl fentanyl. There was an improvement in the correct identifications of *ortho*-methyl Furanyl fentanyl and *para*-Methylfentanyl when compared to use of helium carrier gas as the carrier gas. However, previous correct identification of *para*-Chlorobutyryl fentanyl and FIBF with helium carrier gas resulted in misidentification of the two (2) FRS when hydrogen was used as the carrier gas. Using hydrogen as a carrier gas can result in its reactivity with some compounds such as aromatics and alkenes in the ion source, which can affect the resulting mass spectra [83], [84]. Though most mass spectra remain similar, there is a tendency for the quality spectral "match" to change as a result of changes in ion ratios or in extra (low abundance) peaks observed when using hydrogen carrier gas [85]. This could have been a possible reason for the misidentification of the *para*-Chlorobutyryl fentanyl and FIBF as well as the resulting correct identification of *ortho*-methyl Furanyl fentanyl and *para*-Methylfentanyl which were not observed when using helium.

Laboratory #3 correctly identified 15 of the 20 FRS, resulting in 75% correct identification. Those incorrectly identified were *ortho*-methyl Furanyl fentanyl which was misidentified as the positional isomer *meta*-methyl Furanyl fentanyl; Valeryl fentanyl which was misidentified as α'-methyl Butyryl fentanyl; *meta*-Fluorofentanyl which was misidentified as its positional isomer *ortho*-Fluorofentanyl*;* *para*-Methylfentanyl which was misidentified as its positional isomer *meta*-Methylfentanyl; and *ortho*-methyl Cyclopropyl fentanyl which was misidentified as its positional isomer *para*-methyl Cyclopropyl fentanyl.

Laboratory #4 correctly identified all 20 of the 20 FRS, resulting in 100% correct identification. This laboratory, unlike the others, leveraged the retention time data in addition to the library search data to conclude the positive identity of each FRS compound. Although mass fragmentation patterns and fragment ions produced showed similarity resulting in algorithm misidentification, inclusion of specific retention time data for all compounds proved an essential tool in FRS identification determination.

Laboratory #5 correctly identified 16 of the 20 FRS, resulting in 80% correct identification. Those incorrectly identified include Ocfentanil (also known as *ortho*-fluoro Methoxyacetyl fentanyl) which was misidentified as its positional isomer *meta*-fluoro Methoxyacetyl fentanyl; *meta*-Fluorofentanyl which was misidentified as its positional isomer *ortho*-Fluorofentanyl; *para*-Methylfentanyl which was misidentified as being either of its positional isomers *ortho* or *meta*-Methylfentanyl; and *ortho*-methyl Cyclopropyl fentanyl which was misidentified as its positional isomer *para*-methyl Cyclopropyl fentanyl.

Laboratory #6 also correctly identified 16 of the 20 FRS, resulting in 80% correct identification. Those incorrectly identified include Ocfentanil, which was misidentified as its positional isomer *meta*-fluoro Methoxyacetyl fentanyl; *meta*-Fluorofentanyl, which was misidentified as its positional isomer *ortho*-Fluorofentanyl; *para*-Methylfentanyl, which was misidentified as its positional isomer *meta*-Methylfentanyl; and Crotonyl fentanyl, which was misidentified as Cyclopropyl fentanyl.

Finally, Laboratory #7 also correctly identified 16 of the 20 FRS, resulting in 80% correct identification. Those incorrectly identified include Valeryl fentanyl, which was misidentified as α'-methyl Butyryl fentanyl; *para*-Methylfentanyl, which was misidentified as its positional isomer *ortho*-Methylfentanyl; FIBF (also known as *para*-Fluoroisobutyryl fentanyl), which was misidentified as its positional isomer *meta*-Fluoroisobutyryl fentanyl; and *ortho*-methyl Cyclopropyl fentanyl which as misidentified as *para*-methyl Cyclopropyl fentanyl.

Table 16. Chemical standard (FRS) actual identity and the laboratory reported identification for GC-MS analysis.

Chemical Standard Identity	**Laboratory Identification**						
	Lab #1	**Lab #2**	**Lab #3**	**Lab #4**	**Lab #5**	**Lab #6**	**Lab #7**
Thiophene fentanyl	Thiophene fentanyl	Thiophene fentanyl	Thiophene fentanyl	Thiophene fentanyl	Thiophene fentanyl	Thiophene fentanyl	Thiophene fentanyl
Remifentanil	Remifentanil	Remifentanil	Remifentanil	Remifentanil	Remifentanil	Remifentanil	Remifentanil
Ocfentanil (*ortho*-fluoro Methoxyacetyl fentanyl)	*meta*-fluoro Methoxyacetyl fentanyl	Ocfentanil	Ocfentanil	Ocfentanil	meta-fluoro Methoxyacetyl fentanyl	*meta*-fluoro Methoxyacetyl fentanyl	Ocfentanil
Fentanyl carbamate	Fentanyl carbamate	Fentanyl carbamate	Fentanyl carbamate	Fentanyl carbamate	Fentanyl carbamate	Fentanyl carbamate	Fentanyl carbamate
α-methyl Butyryl fentanyl	α-methyl Butyryl fentanyl	α-methyl Butyryl fentanyl	α-methyl Butyryl fentanyl	α-methyl Butyryl fentanyl	α-methyl Butyryl fentanyl	α-methyl Butyryl fentanyl	α-methyl Butyryl fentanyl
2,3-seco-fentanyl	2,3-seco-fentanyl	2,3-seco-fentanyl	2,3-seco-fentanyl	2,3-seco-fentanyl	2,3-seco-fentanyl	2,3-seco-fentanyl	2,3-seco-fentanyl
Acrylfentanyl	Acryl fentanyl	Acryl fentanyl	Acryl fentanyl	Acryl fentanyl	Acryl fentanyl	Acryl fentanyl	Acryl fentanyl
Senecioylfentanyl	Senecioylfentanyl	Senecioylfentanyl	Senecioylfentanyl	Senecioylfentanyl	Senecioylfentanyl	Senecioylfentanyl	Senecioylfentanyl
Sufentanil	Sufentanil	Sufentanil	Sufentanil	Sufentanil	Sufentanil	Sufentanil	Sufentanil
Alfentanil	Alfentanil	Alfentanil	Alfentanil	Alfentanil	Alfentanil	Alfentanil	Alfentanil
Furanyl fentanyl	Furanyl fentanyl	Furanyl fentanyl	Furanyl fentanyl	Furanyl fentanyl	Furanyl fentanyl	Furanyl fentanyl	Furanyl fentanyl
ortho-methyl Furanyl fentanyl	*ortho*-methyl Furanyl fentanyl	*meta*-methyl Furanyl fentanyl	*meta*-methyl Furanyl fentanyl	*ortho*-methyl Furanyl fentanyl	*ortho*-methyl Furanyl fentanyl	*ortho*-methyl Furanyl fentanyl	*ortho*-methyl Furanyl fentanyl
Valeryl fentanyl	Valeryl fentanyl	Valeryl fentanyl	α'-methyl Butyryl fentanyl	Valeryl fentanyl	Valeryl fentanyl	Valeryl fentanyl	α'-methyl Butyryl fentanyl
meta-Fluorofentanyl	*para*-Fluorofentanyl	*ortho*-Fluorofentanyl	*ortho*-Fluorofentanyl	*meta*-Fluorofentanyl	*ortho*-Fluorofentanyl	*ortho*-Fluorofentanyl	*meta*-Fluorofentanyl
para-Methylfentanyl	*ortho*-Methylfentanyl	undetermined (an isomer of methylfentanyl)	*meta*-Methylfentanyl	*para*-Methylfentanyl	ortho and meta-Methylfentanyl	*meta*-Methylfentanyl	ortho-Methylfentanyl
para-Chlorobutyryl fentanyl	*para*-Chlorobutyryl fentanyl	*para*-Chlorobutyryl fentanyl	*para*-Chlorobutyryl fentanyl	*para*-Chlorobutyryl fentanyl	*para*-Chlorobutyryl fentanyl	*para*-Chlorobutyryl fentanyl	*para*-Chlorobutyryl fentanyl
(FIBF)*para*-Fluoroisobutyryl fentanyl	FIBF	FIBF	FIBF	FIBF	FIBF	FIBF	*meta*-Fluoroisobutyryl fentanyl
Crotonyl fentanyl	Crotonyl fentanyl	Crotonyl fentanyl	Crotonyl fentanyl	Crotonyl fentanyl	Crotonyl fentanyl	Cyclopropyl fentanyl	Crotonyl fentanyl
ortho-methyl Cyclopropyl fentanyl	*meta*-methyl Cyclopropyl fentanyl	undetermined (*ortho* or *para* - methyl Cyclopropyl fentanyl)	*para*-methyl Cyclopropyl fentanyl	*ortho*-methyl Cyclopropyl fentanyl	*para*-methyl Cyclopropyl fentanyl	*ortho*-methyl Cyclopropyl fentanyl	*para*-methyl Cyclopropyl fentanyl
ortho-methyl Acetyl fentanyl	ortho-methyl Acetyl fentanyl	ortho-methyl Acetyl fentanyl	ortho-methyl Acetyl fentanyl	ortho-methyl Acetyl fentanyl	ortho-methyl Acetyl fentanyl	ortho-methyl Acetyl fentanyl	ortho-methyl Acetyl fentanyl
Number correctly identified	**16**	**16**	**15**	**20**	**16**	**16**	**16**

The most misidentified of the 20 FRS was *para*-Methylfentanyl, which was misidentified by 6 of the 7 laboratories. This compound has positional isomers *ortho*-Methylfentanyl and *meta*-Methylfentanyl which fragment to produce similar mass spectra [68]. The molecular weight of para-Methylfentanyl is 350 amu and fragments to produce major ions of 259, 160, and 203 *m/z*. The base peak of 259, a commonly observed base peak ion in Methylfentanyls [34], is due to the loss of the tropylium cation ($(C_7H_7)^+$, 91 amu) which results from the cleavage of the bond between the alpha and beta site of the phenthyl moiety (**Figure 20**). The lack of a molecular ion observed in the mass spectral data is somewhat characteristic of FRS, which adds to the confounding nature of FRS mass spectral analysis [23]. Closely following *para*-Methylfentanyl were *meta*-Fluorofentanyl and *ortho*-methyl Cyclopropyl fentanyl which was misidentified by 5 of the 7 laboratories participating.

A 75% - 80% rate of correct identification was reported among all laboratories that participated and did not use additional retention time data. FRS in the study with corresponding positionally related isomeric compounds listed in the instrument searchable library were often misidentified by the laboratories. This misidentification by the laboratories could be due to the algorithm that the software uses to establish identification. Since these compounds were all between 171 amu and 600 amu in molecular weight, the PBM algorithm described above uses a maximum of 26 peaks for the identification. Since these FRS spectra have well over 26 peaks, not all peaks were taken into consideration and could have been excluded in the algorithm calculation. This increases the probability of misidentification, which was observed in the results, especially of those compounds with positional isomers and similar fragmentation patterns.

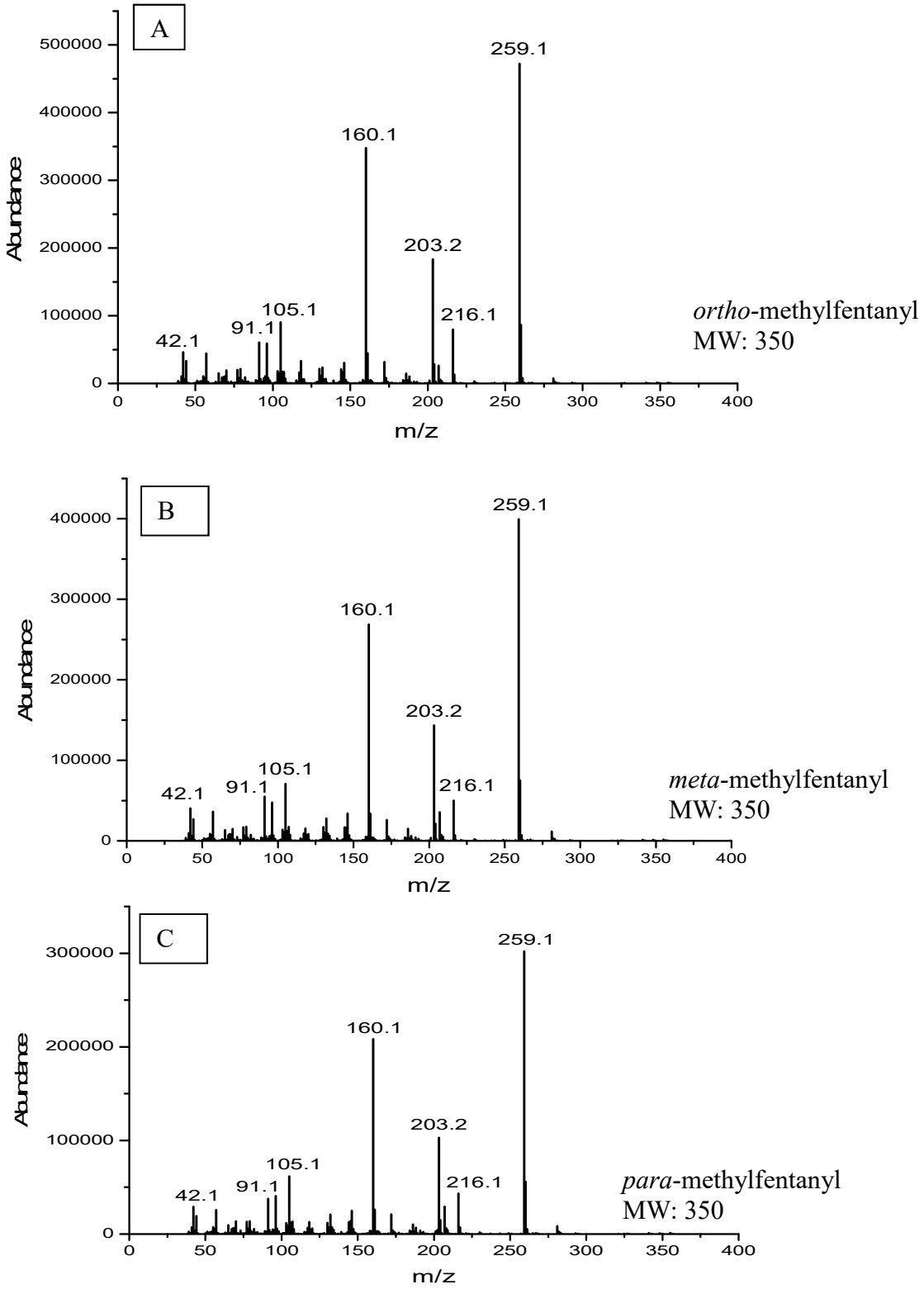

Figure 20. Mass spectra of (A) *ortho*-Methylfentanyl, (B) *meta*-Methylfentanyl, and (C) *para*-Methylfentanyl .

There were instances where the compound being searched was misidentified as its chain isomer in the library, not the positional isomer. Valeryl fentanyl was misidentified as its branched chain isomer α'-methyl Butyryl fentanyl by Laboratory #3 and Laboratory #7. The only difference in the structure is the branching of the aliphatic group next to the amide bond shown in α'-methyl Butyryl fentanyl, as opposed to existing as a straight chain in the Valeryl fentanyl. **Figure 21** shows the mass spectral fragmentation patterns. Both fragment to produce similar ions with major ions 273, 189, and 146 m/z, with minor differences in the ratio of the abundances. The 57 m/z ion is produced in both, but more abundant in the α'-methyl Butyryl fentanyl than the Valeryl fentanyl. The base peak for both is 273 m/z which is obtained from the cleavage between the alpha and beta site of the phenethyl moiety.

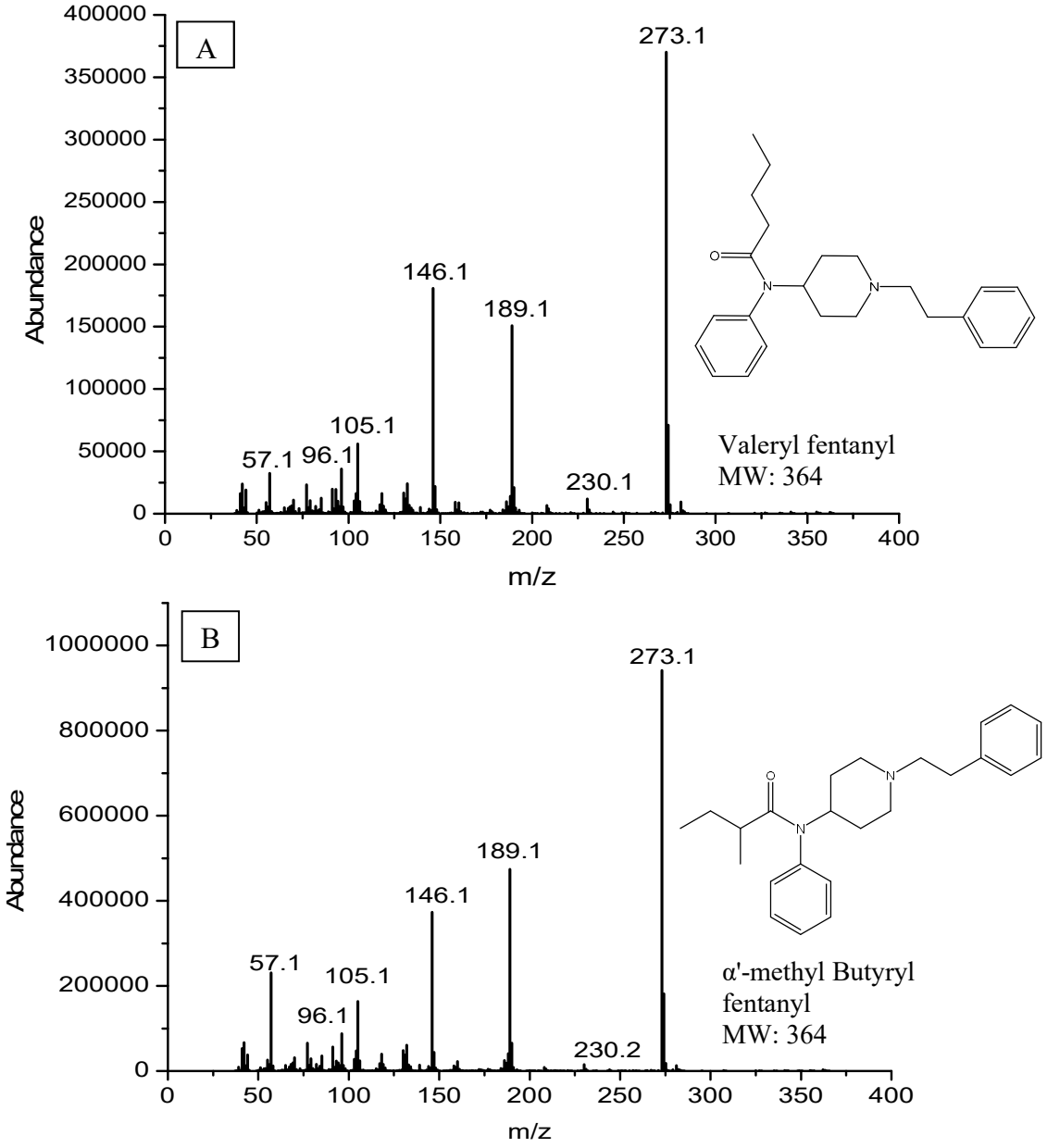

Figure 21. Mass spectra of (A) Valeryl fentanyl and (B) α'-methyl Butyryl fentanyl.

The Crotonyl fentanyl was misidentified as its cyclized isomer Cyclopropyl fentanyl by Laboratory #6. The only difference in the structure is the cyclization of the alkene group next to the amide bond shown in Cyclopropyl fentanyl, as opposed to existing as an alkene

chain in the Crotonyl fentanyl. **Figure 22** shows the fragmentation patters. They both fragment to the 257, 189, 146, and 69 m/z as the major fragment ions. The base peak of 257 m/z is also obtained through the same cleavage between the alpha and beta site of the phenthyl moiety of the structure.

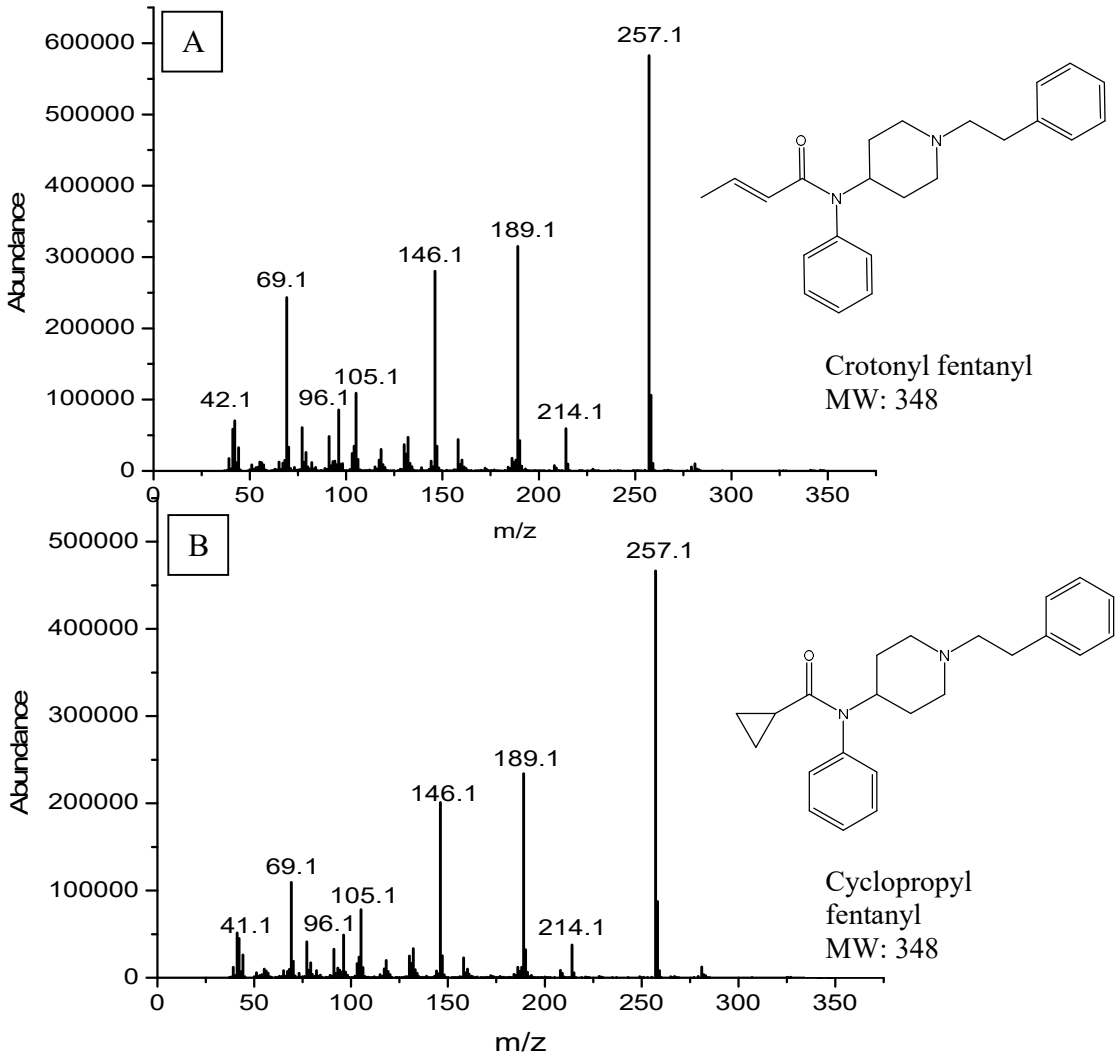

Figure 22. Mass spectra of (A) Crotonyl fentanyl and (B) Cyclopropyl fentanyl.

In the PBM utilized by the Agilent Chemstation software, the probabilities of a match are assigned using information from the base peak ion and fragments, utilizing a maximum of 15 fragments. Since the fragments in **Figures 21 and 22** produce the same base peak and similar fragments, it is evident why the algorithm might have resulted in a misidentification. A match of >90 as well as being the first in rank was deemed a "good match" for the mass spectra in the interlaboratory study, and that was also taken in to consideration when assigning if a match was made or not. Though some fulfilled the first rank and being a match of >90 they still weren't true matches upon examination (as in **Figures 21 and 22**). This just goes to show that relying on the library alone is not sufficient when assigning correct matches, there needs to be examination by an analyst for confirmation.

6.2.2. Laboratory GC-IR Results

Each laboratory analyzed the 20 blind FRS samples and used the FIU-generated Fentanyl Infrared Library to determine the identity of the compound. The Essential FTIR (eFTIR) software from Analytical Solutions and Providers (ASAP) produces the probability of a match using similarity scores generated from correlation coefficient data. This involves data collection at each point of the x-axis value (wavenumber) and the y-axis value (percent absorbance/transmittance) to use in the coefficient of determination calculation. This calculation results in an R value, similar to using the statistical method of obtaining a correlation coefficient [66].

All laboratories correctly identified all 20 FRS, resulting in 100% correct identification; except laboratory #6, which had three of the 20 correct – Thiophene fentanyl,

Senecioylfentanyl, and Sufentanil, resulting in 15% correct identification (**Table 17**). This is because all the other laboratories utilized vapor phase IR analysis while laboratory #6 utilized solid phase IR analysis in conjunction with the vapor phase generated FIU fentanyl IR library. In vapor phase IR, the light pipe of usually 1 mm internal diameter keeps the sample in the vapor phase at temperatures well above 200ºC during the acquisition time in the detector [42], [52]. In solid phase IR, the column eluent containing the sample as a gas is directly deposited onto a cryogenically cooled zinc selenide (ZnSe) disc, converted to a solid and the transmittance spectra is acquired [52]. This laboratory also compared the solid phase IR spectra of the unknowns to a library of FRS collected in the solid phase and as expected, the spectral results generated from solid and vapor phase IR were determined not interchangeable. A closer comparison of the vapor phase IR and the solid phase IR spectra of Thiophene fentanyl reveals that there are differing levels of detail between vapor phase IR spectra and solid phase IR spectra (**Figure 23**), with solid phase IR having greater resolution. In the vapor phase IR, the high temperatures reduce the dipolar interactions or intermolecular hydrogen bonding which may be present, increasing frequencies up to 30 cm^{-1} wavenumbers higher than those reported in solid phase IR [42]. This shift in wavenumber frequencies could have been a contributing factor affecting the ability of the algorithm to correctly match spectra using the FIU vapor phase library.

Table 17. Chemical standard (FRS) actual identity and the laboratory reported identification for GC-IR analysis.

Chemical Standard Identity	**Laboratory Identification**						
	Lab #1	**Lab #2**	**Lab #3**	**Lab #4**	**Lab #5**	**Lab #6**	**Lab #7**
Thiophene fentanyl	Thiophene fentanyl	Thiophene fentanyl	Thiophene fentanyl	Thiophene fentanyl	Thiophene fentanyl	Thiophene fentanyl	Thiophene fentanyl
Remifentanil	Remifentanil	Remifentanil	Remifentanil	Remifentanil	Remifentanil	Norcarfentanil	Remifentanil
Ocfentanil (*ortho*-fluoro Methoxyacetyl fentanyl)	Ocfentanil	Ocfentanil	Ocfentanil	Ocfentanil		*ortho*-Methoxy butyryl fentanyl	Ocfentanil
Fentanyl carbamate	Fentanyl carbamate	Fentanyl carbamate	Fentanyl carbamate	Fentanyl carbamate	Fentanyl carbamate	β-hydroxythioacetyl fentanyl	Fentanyl carbamate
α-methyl Butyryl fentanyl	α-methyl Butyryl fentanyl	α-methyl Butyryl fentanyl	α-methyl Butyryl fentanyl	α-methyl Butyryl fentanyl	α-methyl Butyryl fentanyl	Propyl U-47700	α-methyl Butyryl fentanyl
2,3-seco-fentanyl	2,3-seco-fentanyl	2,3-seco-fentanyl	2,3-seco-fentanyl	2,3-seco-fentanyl	2,3-seco-fentanyl	Senecioylfentanyl	2,3-seco-fentanyl
Acrylfentanyl	Acryl fentanyl	Acryl fentanyl	Acryl fentanyl	Acryl fentanyl	Acryl fentanyl	Propyl U-47700	Acryl fentanyl
Senecioylfentanyl	Senecioylfentanyl	Senecioylfentanyl	Senecioylfentanyl	Senecioylfentanyl	Senecioylfentanyl	Senecioylfentanyl	Senecioylfentanyl
Sufentanil	Sufentanil	Sufentanil	Sufentanil	Sufentanil	Sufentanil	Sufentanil	Sufentanil
Alfentanil	Alfentanil	Alfentanil	Alfentanil	Alfentanil	Alfentanil	Propyl U-47700	Alfentanil
Furanyl fentanyl	Furanyl fentanyl	Furanyl fentanyl	Furanyl fentanyl	Furanyl fentanyl	Furanyl fentanyl	*ortho*-Isopropyl furanyl fentanyl	Furanyl fentanyl
ortho-methyl Furanyl fentanyl	*ortho*-methyl Furanyl fentanyl	*ortho*-methyl Furanyl fentanyl	*ortho*-methyl Furanyl fentanyl	*ortho*-methyl Furanyl fentanyl	*ortho*-methyl Furanyl fentanyl	*ortho*-Isopropyl fentanyl	*ortho*-methyl Furanyl fentanyl
Valeryl fentanyl	Valeryl fentanyl	Valeryl fentanyl	Valeryl fentanyl	Valeryl fentanyl	Valeryl fentanyl	Propyl U-47700	Valeryl fentanyl
meta-Fluorofentanyl	*meta*-Fluorofentanyl	*meta*-Fluorofentanyl	*meta*-Fluorofentanyl	*meta*-Fluorofentanyl	*meta*-Fluorofentanyl	Senecioylfentanyl	*meta*-Fluorofentanyl
para-Methylfentanyl	*para*-Methylfentanyl	*para*-Methylfentanyl	*para*-Methylfentanyl	*para*-Methylfentanyl	*para*-Methylfentanyl	Propyl U-47700	*para*-Methylfentanyl
para-Chlorobutyryl fentanyl	*para*-Chlorobutyryl fentanyl	*para*-Chlorobutyryl fentanyl	*para*-Chlorobutyryl fentanyl	*para*-Chlorobutyryl fentanyl	*para*-Chlorobutyryl fentanyl	Propyl U-47700	*para*-Chlorobutyryl fentanyl
(FIBF)*para*-Fluoroisobutyryl fentanyl	FIBF	FIBF	FIBF	FIBF	FIBF	*para*-Fluoro tetrahydrofuran fentanyl	*FIBF*
Crotonyl fentanyl	Crotonyl fentanyl	Crotonyl fentanyl	Crotonyl fentanyl	Crotonyl fentanyl	Crotonyl fentanyl	Cyclopentenyl fentanyl	Crotonyl fentanyl
ortho-methyl Cyclopropyl fentanyl	*ortho*-methyl Cyclopropyl fentanyl	*ortho*-methyl Cyclopropyl fentanyl	*ortho*-methyl Cyclopropyl fentanyl	*ortho*-methyl Cyclopropyl fentanyl	*ortho*-methyl Cyclopropyl fentanyl	Senecioylfentanyl	*ortho*-methyl Cyclopropyl fentanyl
ortho-methyl Acetyl fentanyl	ortho-methyl Acetyl fentanyl	ortho-methyl Acetyl fentanyl	ortho-methyl Acetyl fentanyl	ortho-methyl Acetyl fentanyl	ortho-methyl Acetyl fentanyl	Isopropyl U-47700	ortho-methyl Acetyl fentanyl
Number correctly identified	**20**	**20**	**20**	**20**	**20**	**3**	**20**

A closer comparison of the vapor phase IR and the solid phase IR spectra of Thiophene fentanyl, Senecioylfentanil, and Sufentanil reveals that there is greater detail in vapor phase IR spectra than solid phase IR spectra (**Figure 23-25**). When laboratory #6 searched the 20 FRS against their in-house solid phase IR library, there was an improvement in their correct matches from three to 20 of 20 correctly identified, an improvement from 15% to 100% correct. This shows that analyses conducted using solid phase or vapor phase IR are best searched using their respective libraries. Additionally, studies conducted by Jones, et al [45] demonstrated the difficulty of differentiating isomers of novel psychoactive substances (NPS) and the ability of solid phase IR in differentiating these isomers [45], [70], [86]–[88].

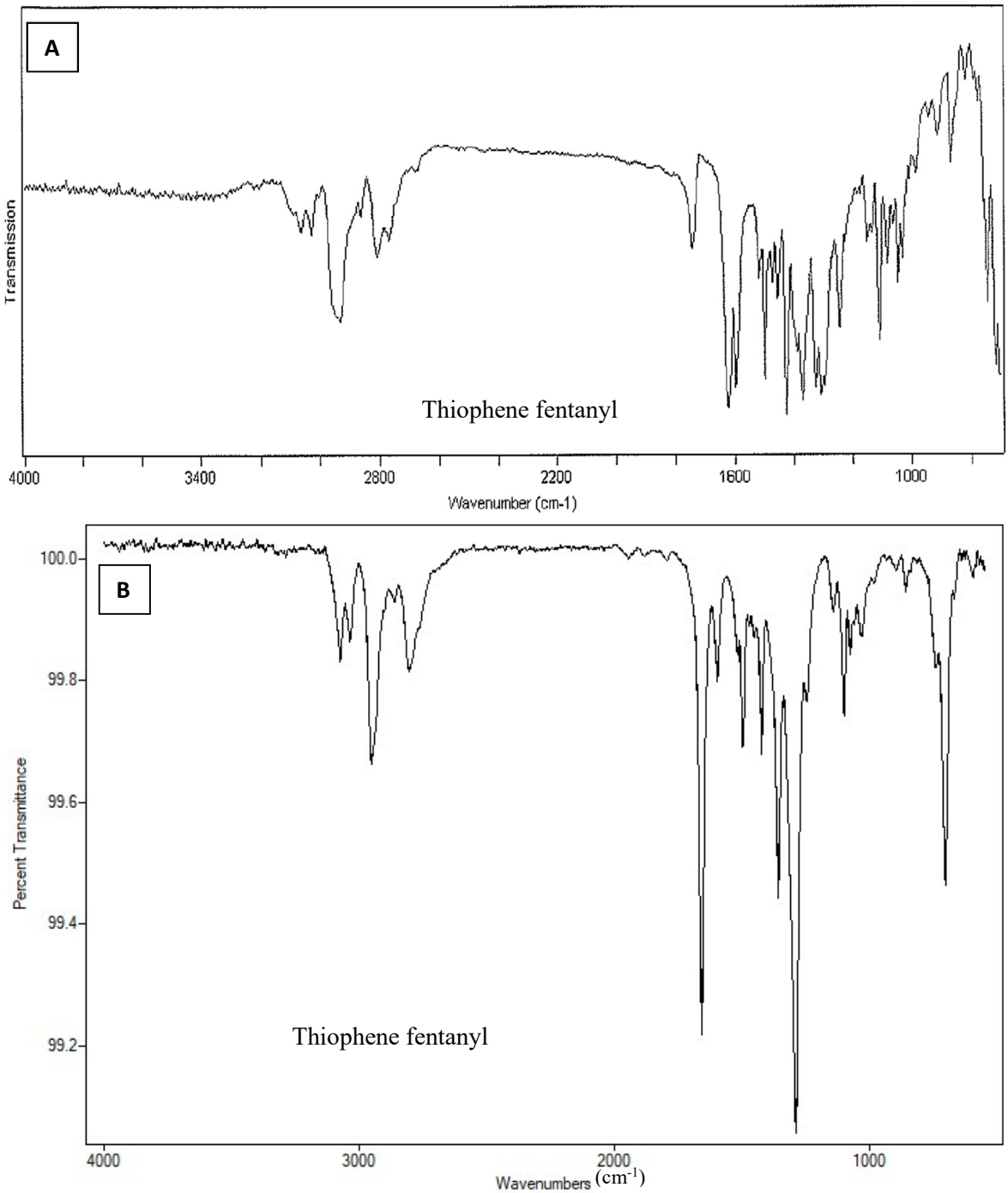

Figure 23. Thiophene fentanyl IR spectra obtained by (A) solid phase IR and (B) vapor phase IR.

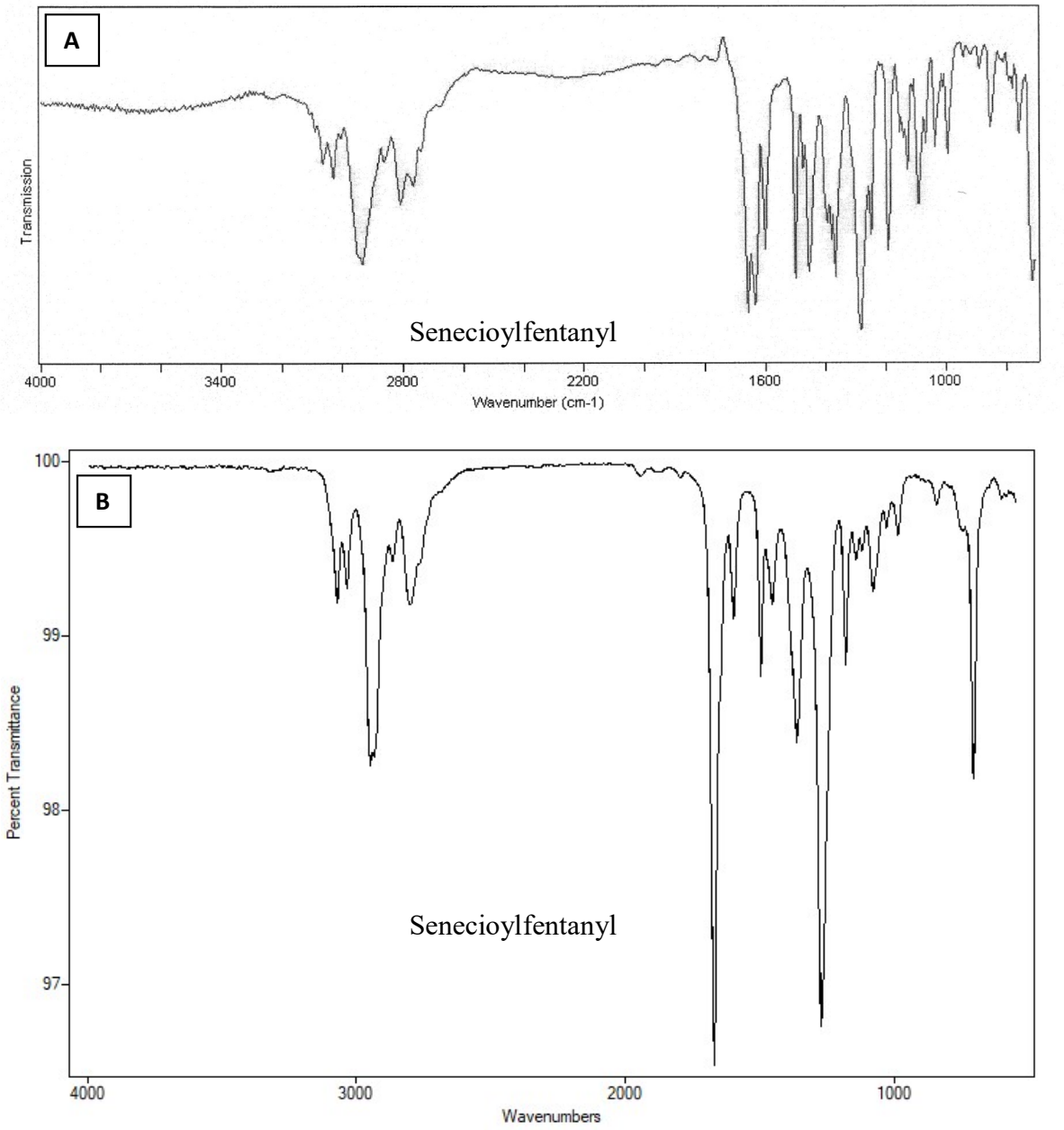

Figure 24. Senecioylfentanyl IR spectra obtained by (A) solid phase IR and (B) vapor phase IR.

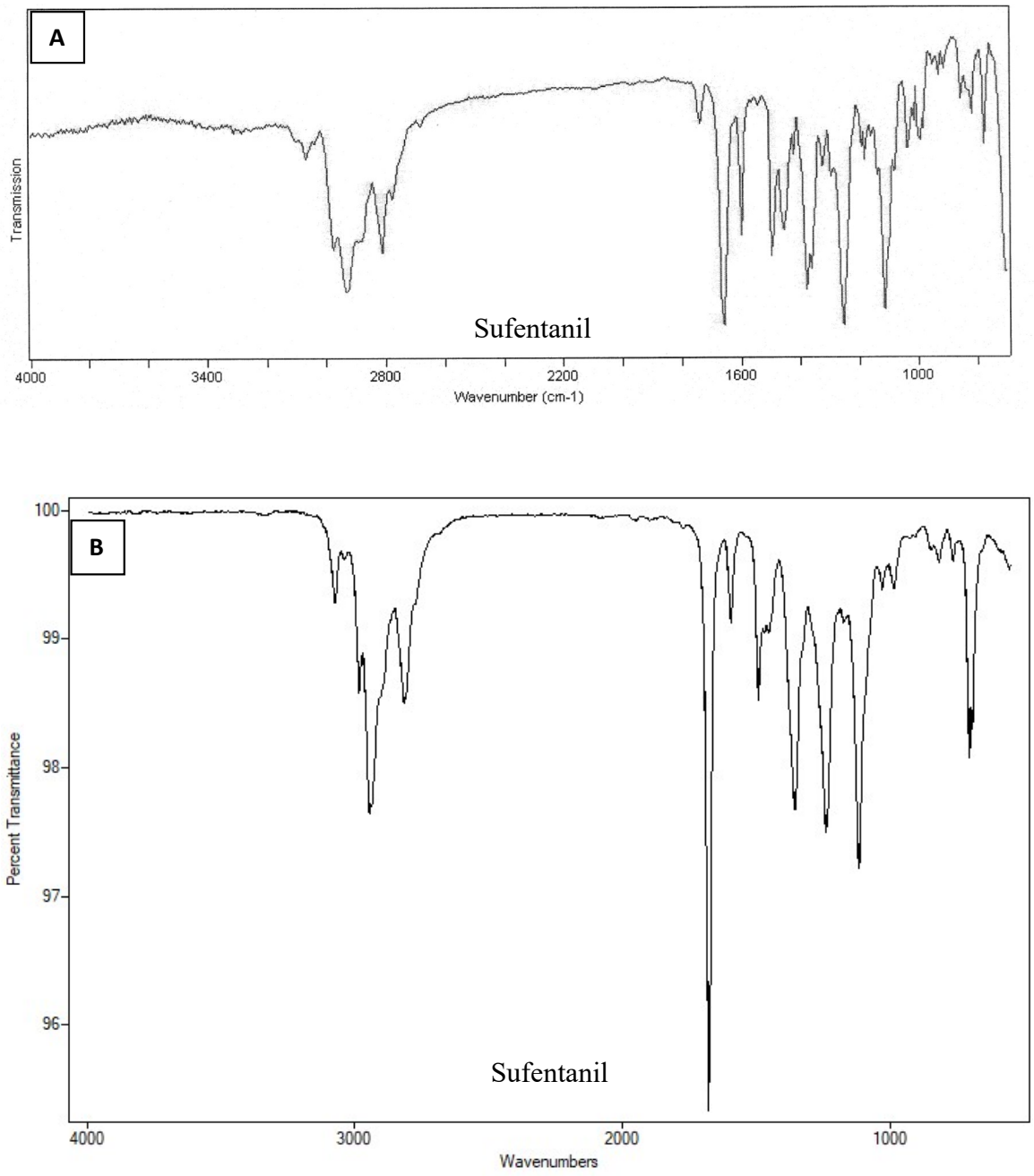

Figure 25. Sufentanil IR spectra obtained by (A) solid phase IR and (B) vapor phase IR.

Vapor phase GC-IR has been shown to be successful in differentiation of positional isomers of FRS [48], [68], phenethylamines [15], and synthetic cannabinoids [71]], which are commonly identified in forensic laboratories. The identification obtained by advantages

of using IR, as a confirmatory technique, lies in the fact that small differences in molecular structure will affect the bending and stretching within the compound structure and generate different IR spectral results. This difference is often apparent in the "fingerprint region" of these isomers which registers the vibrational changes produced because of the rearrangement of the functional groups of the positional isomers. In this study, the data demonstrated that GC-IR can be successfully applied to FRS with a high degree of confidence. It should also be noted that the correct identification is often limited by the content of the library; if the compound in question is not present in the library it can only be matched to its most similar spectra in the library. The inspection of the spectra by an analyst is necessary for confirmation of matches between comparison spectra.

The GC-MS fragmentation of positional isomers often results in similar spectra due to the regions of fragmentation being the same because of their similar structural arrangement. This results in the formation of the same base peak and fragment ions. As a result, when searched using the PBM algorithm, there is often misidentification with the isomers present in the library. This may explain the phenomena seen when the FRS with isomeric forms in the library are commonly misidentified as their isomeric form. For this reason, it is useful to include retention time data to positively identify a compound in question, as was utilized by Laboratory #4, which obtained 100% correct identification by GC-MS because of including the retention time data. Additionally, when using hydrogen as a carrier gas, the hydrogen may ionize in the ion source and react with the aromatics and olefins while in the ion source, affecting the spectra produced. This may result in a change in the quality of the spectral "match" produced because of the change in ratio of fragment ions produced. This could have been a possible reason for the misidentification of the *para*-Chlorobutyryl

fentanyl and FIBF as well as the resulting correct identification of *ortho*-methyl Furanyl fentanyl and *para*-Methylfentanyl which were not seen when using helium. The power of GC-IR being able to differentiate positional isomers lies in the fact that small differences in molecular structure will affect the bending and stretching within the compound structure and generate different IR spectral results particularly within the "fingerprint region" of the spectra. As a result, these small differences results in 100% correct identification when using the library search algorithm of the eFTIR.

6.3. Conclusion and Future Directions

GC-IR is a useful confirmatory complementary technique when used with GC-MS analysis for the differentiation and identification of FRS. Results of this blind interlaboratory study show 100% positive identification of FRS when using GC-MS in conjunction with vapor phase GC-IR analysis. Solid phase IR analysis produces spectra with different levels of detail than vapor phase IR, affecting the ability for solid phase IR spectra to be correctly searched against a vapor phase IR library. Additionally, the use of retention time data in combination with mass spectrometry data can also be useful in the identification of these compounds, as seen with Laboratory #4 obtaining 100% correct identification when reporting the GC-MS results. The results of this study can inform the development of a standard test method for the analysis of fentanyl (and fentanyl-related substances) using GC-IR in the future.

Acknowledgements

This research was sponsored by the Center for Advanced Research in Forensic Science (CARFS), an Industry University Collaborative Research Center (IUCRC) funded by the National Science Foundation (NSF) to Florida International University through award #1739805. Thank you to Analytical Solutions and Providers (ASAP) Analytical (Covington, KY) for the use of their IRD3 Detector, eFTIR Software for the analysis of infrared spectra, technical advice, and useful discussions. Students Sela Andrews and Andrea Dew are acknowledged for their assistance in data acquisition at the DEA Southeast laboratory.

7. THE UTILITY OF GC-IR FOR THE DIFFERENTIATION OF POSITIONAL ISOMERS OF CANNABINOIDS

7.1. Introduction

The abuse of cannabinoids has been recently on the rise. According to CFSRE, between the years 2018-2022 there has been an addition of 36 new cannabinoids [16]. Cannabinoids normally abused may be phytocannabinoids (natural) or synthetic cannabinoids. Both types of cannabinoids bind to the CB1 and CB2 receptors in the body. Binding to these receptors results in a feeling of euphoria and heightened sensory awareness and distortion of time, sound, and color followed by a feeling of relaxation [25]

The phytocannabinoids are the main psychoactive substances found in the *Cannabis sativa* plant. These include Δ^8-THC, Δ^9-THC, CBD, CBG, and CBN; though Δ^8-THC is more concentrated in hemp than marijuana. The main psychoactive cannabinoids concentrated in cannabis and cannabis resin are Δ^9-THC, CBD, and CBN; with CBN being both a major breakdown product of and a precursor to Δ^9-THC. CBG is found in high concentrations in younger plants but in lower concentrations in more mature plants [36].

Synthetic cannabinoids are those made in the laboratory, and they have a wide classification. These include classical cannabinoids, non-classical cannabinoids, hybrid cannabinoids, aminoalkylindoles, eicosanoids, etc. These synthetic cannabinoids are known as “spice” or “K2”, and are often sprayed on plant material and smoked. The synthetic cannabinoids, however, bind stronger to the cannabinoid receptors than the phytocannabinoids, resulting in a more intense high.

Presumptive analysis is often not enough to ensure proper identification of a drug in question. Though GC-MS is often the gold standard in confirmatory testing in forensic

laboratories, there is still the problem of the differentiation of positional isomers from each other. Studies conducted by Belal et al. on the differentiation of indole ring regioisomers of the synthetic cannabinoid JWH-007 [17] has shown the difficulty of GC-MS to differentiate isomers. In the study, the mass spectra generated by the GC-MS were the same. However, the spectra of the GC-IR produced unique peaks allowing for differentiating the isomers from each other. However, one disadvantage of GC-IR is sensitivity of GC-IR is lower than that of GC-MS. Hence, GC-IR can be used as a complement to the GC-MS in the differentiation of isomeric compounds.

In this study, the examination of the utility of GC-IR to differentiate difficult to differentiate isomeric synthetic cannabinoids will be employed. Additionally, it will be investigated if it is useful for differentiation of the phytocannabinoids.

7.2. Results and Discussion

7.2.1. Utility of GC-MS in phytocannabinoid differentiation

All phytocannabinoids were analyzed by both GC-MS and GC-IR. The purpose of the experiments was to see whether there was any similarity in the MS fragmentation patterns of the phytocannabinoids. Additionally, there was the need to investigate if the IR spectral patters produced by the phytocannabinoids had any similarity or can be used to differentiate indistinguishable MS fragmentations.

The Δ^8-THC and Δ^9-THC are both positional isomers. Upon GC-MS analysis both fragment producing similar *m/z* ions but in different ratios. For Δ^8-THC the *m/z* ions 231, 314, and 258 are the most abundant. While in Δ^9-THC the m/z ions 299, 314, and 231 are the most abundant. There was adequate enough difference in the spectra and the database

searches were enough to correctly identify each from the other. Therefore it is safe to say that GC-MS is enough to differentiate the THC isomers from each other.

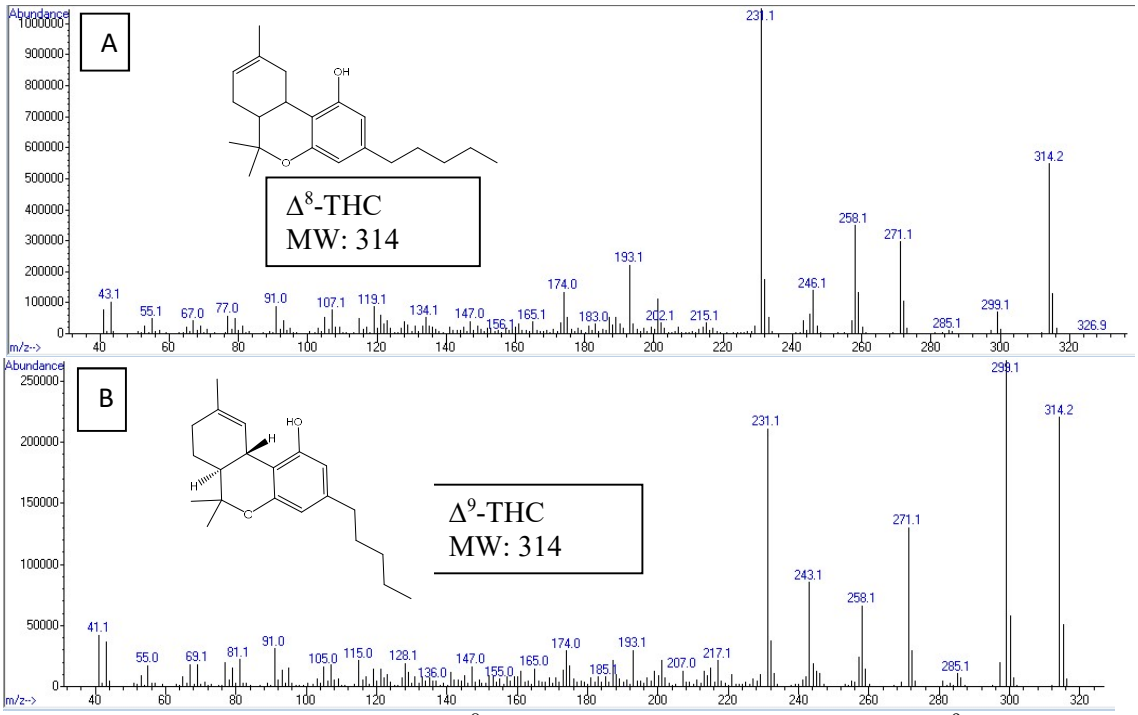

Figure 26. (A) The mass spectra of Δ^8-THC and (B) The mass spectra of Δ^9-THC.

The other cannabinoids fragmentation patters were also compared to determine if there was difficulty in differentiating them from each other. Unlike the THC isomers, the other cannabinoids studies had different *m/z* ions produced. In CBD the most abundant ions produced were 231, 232, and 246. It should also be noted that CBD is also an isomer of the Δ^8-THC and Δ^9-THC. Though they are isomeric forms, they do fragment producing the same ions but in different abundances which can be used to differentiate them. In CBG the most abundant ions produced were 193, 231, and 123. In CBN the most abundant ions

produced were 295, 296, and 238. The database searches of these cannabinoids yielded correct identification for each of the triplicate searched. Therefore, GC-MS is adequate to differentiate the phytocannabinoid compounds from each other.

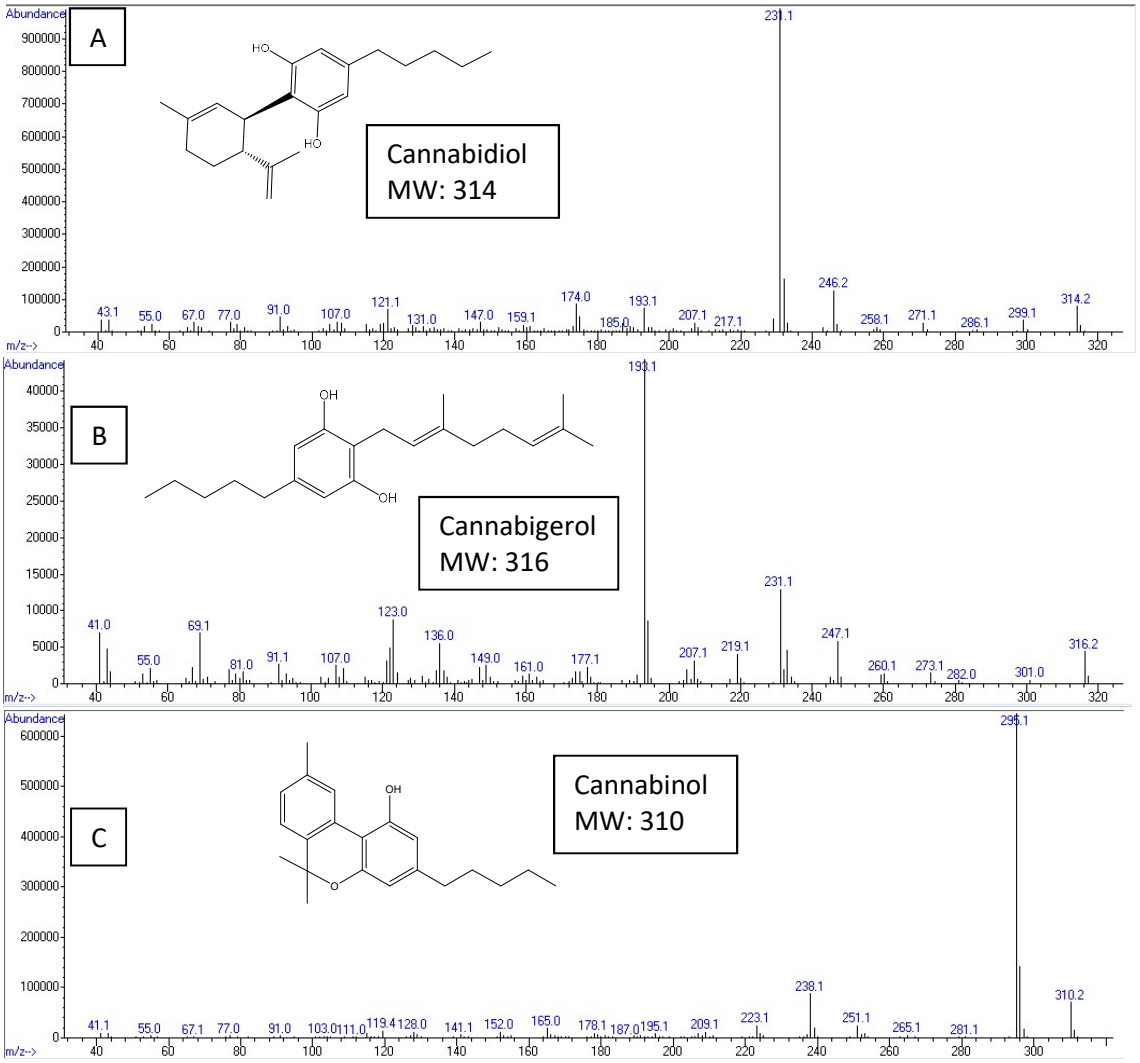

Figure 27. (A) Cannabidiol GC-MS spectra (B) Cannabigerol GC-MS spectra (C) Cannabinol GC-MS spectra

Since the GC-MS spectra were enough to differentiate each of the phytocannabinoids from each other, the GC-IR spectra were not explored as a possibility for differentiation.

However, to be certain, the spectra were still obtained and a database was created. Each search yielded the correct identification of each of the phytocannabinoids as expected.

7.2.2. Utility of GC-MS in synthetic cannabinoid isomer differentiation

2.4.4. JWH 122 isomers

The rationale for the analysis by GC-MS is to investigate if the positional isomers of JWH 122 and JWH 081 produced indistinguishable mass spectra. Similarly to the studies involving the phytocannabinoids, it was investigated whether the GC-MS or the GC-IR analysis provided better differentiation of the positional isomers of the respective compounds.

The synthetic cannabinoid JWH 122 2, 3, 6, and 8 methylnaphthyl isomers were analyzed by GC-MS. The fragmentation of all 4 positional isomers analyzed yielded similar *m/z* ions but in different abundances. The JWH 122 2-methylnaphthyl isomer had *m/z* ions 355, 298, and 168 as the most abundant. The JWH 122 3-methylnaphthyl isomer had *m/z* ions had 355, 214, and 298 as the most abundant. The JWH 122 6-methylnaphthyl isomer had the *m/z* ions 355, 214, and 298 as the most abundant. The JWH 122 8-methylnaphthyl isomer had the *m/z* ions 298, 355, and 338 as the most abundant.

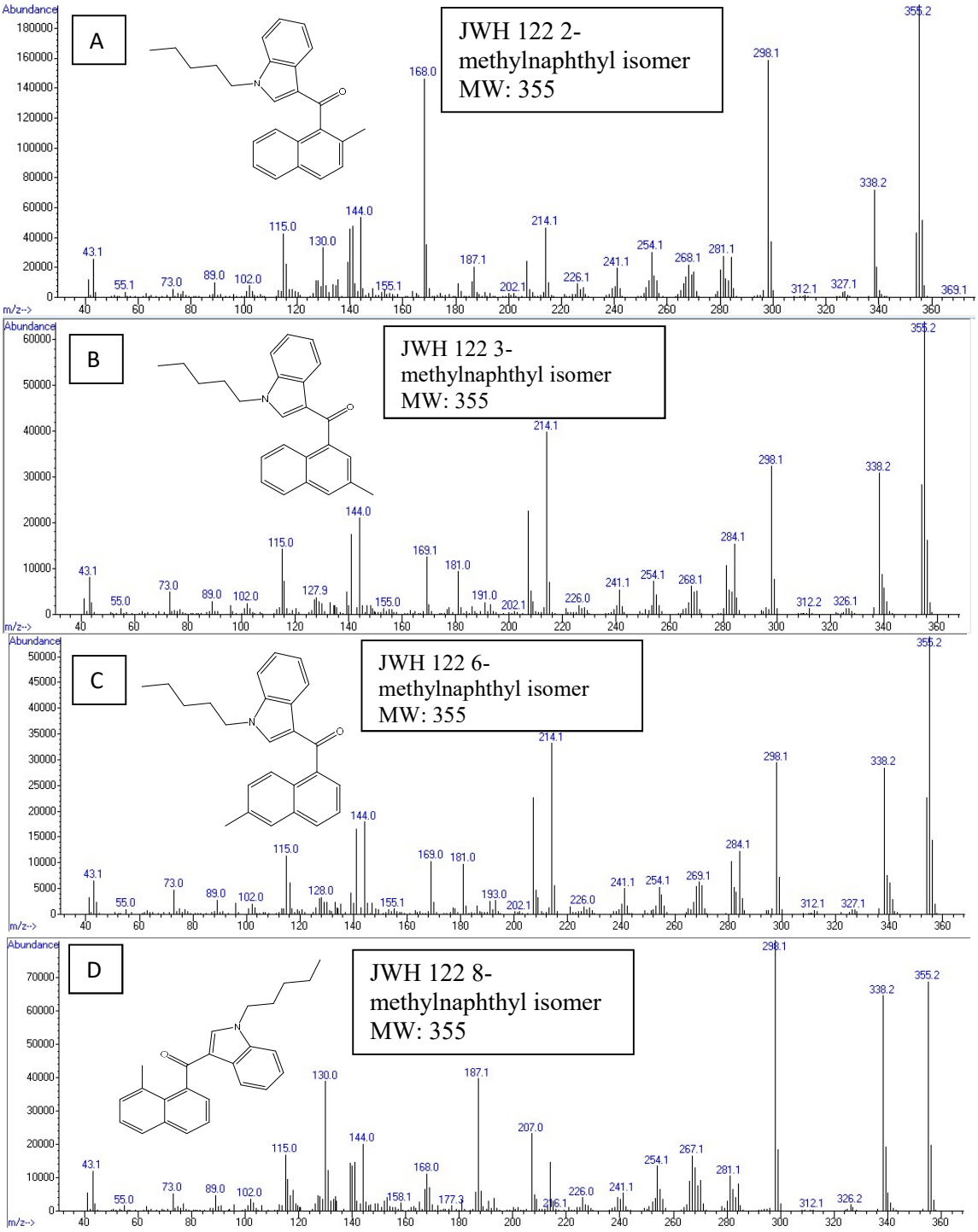

Figure 28. Mass spectra of JWH 122 (A) 2-methylphanthyl (B) 3-methylnaphthyl (C) 6-methylnaphtyl (D) 8-methylnahphtyl isomers.

2.4.4. JWH 081 isomers

The synthetic cannabinoid JWH 081 3, 6, and 7 methoxynaphthyl isomers were analyzed by GC-MS. The fragmentation of all 3 positional isomers analyzed yielded similar *m/z* ions but in different abundances. The JWH 081 3-methoxynaphthyl isomer had *m/z* ions had 371, 214, and 354 as the most abundant. The JWH 081 6-methoxynaphthyl isomer had the *m/z* ions 371, 214, and 354 as the most abundant. The JWH 081 7-methoxylnaphthyl isomer had the *m/z* ions 371, 214, and 144 as the most abundant.

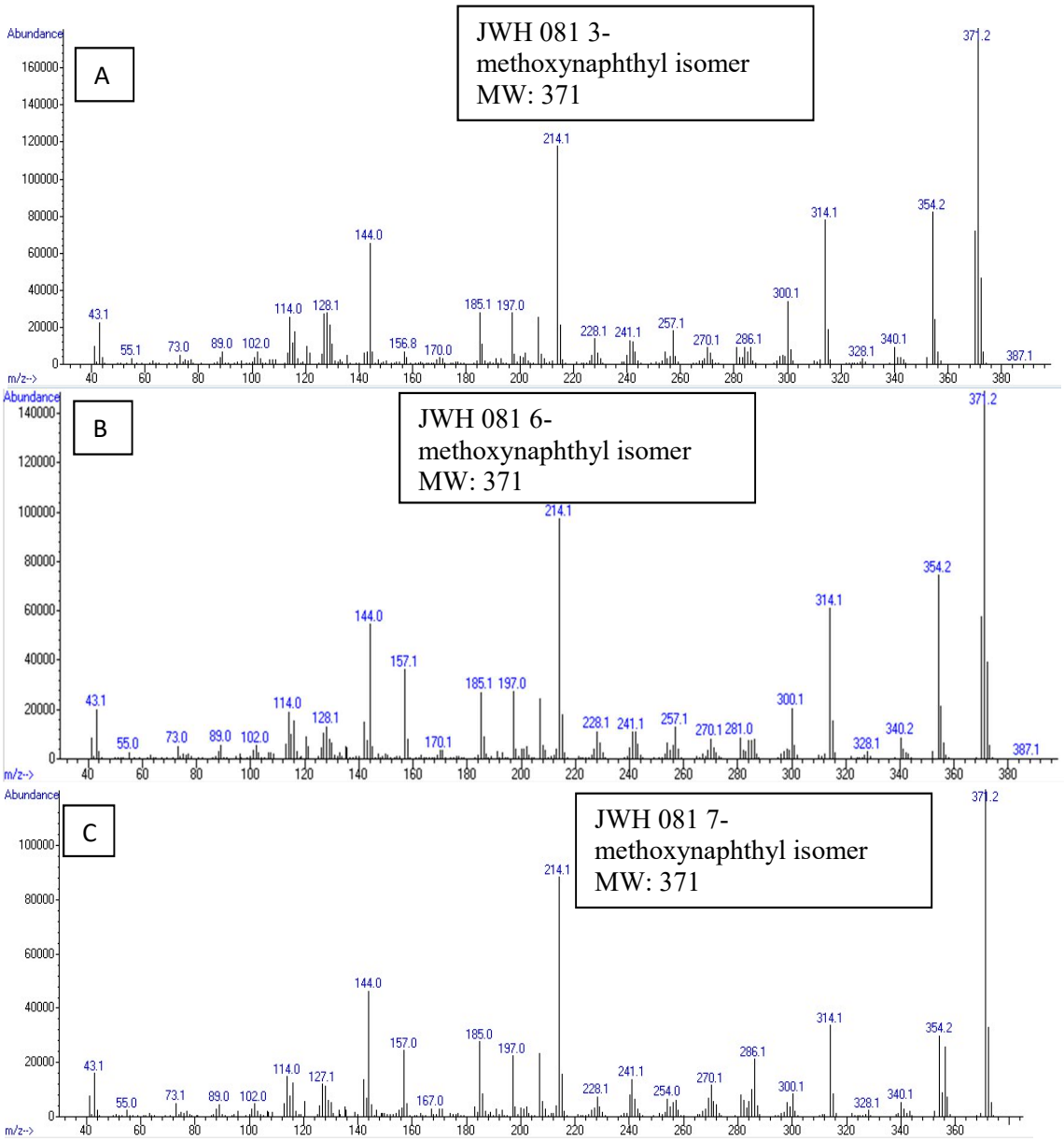

Figure 29. Mass spectra of JWH 081 (A) 3-methoxynaphthyl (B) 6-methoxynaphthyl and (C) 7-methoxynaphthyl isomers.

7.2.3. Utility of GC-IR in differentiation of synthetic cannabinoids

Though both sets of isomers analyzed contained another isomer with similar mass spectra, they were not misidentified in all cases. A search of all these isomers against the database created resulted in the correct identification of all isomeric compounds except JWH 122 3-methylnaphthyl isomer which yielded the JWH 122 6-methylnaphthyl isomer as its match in all three searches. As a result, the GC-IR library was searched to see if it provided a better means of correctly identifying the compound in question.

The GC-IR analysis yielded the spectra produced in **Figure 30** of JWH 122 3-methylnaphthyl and JWH 122 6-methylnaphthyl isomers. There is commonality in the ~3000 cm^{-1} region which is indicative of the presence of C-H bonds evident in the aliphatic chain and methyl group common to both. Additionally there is a sharp peak in the ~1600 cm^{-1} region indicative of a carbonyl group contained in both structures. The majority of the differences is seen in the fingerprint region highlighted by the red rectangle.

A search of cannabinoid database yielded 100% accurate identification of all synthetic cannabinoids analyzed. This improvement in correct identification of otherwise difficult to differentiate positional isomers is confirmatory that GC-IR is also useful for synthetic cannabinoids just as they are for the fentany isomers explained earlier.

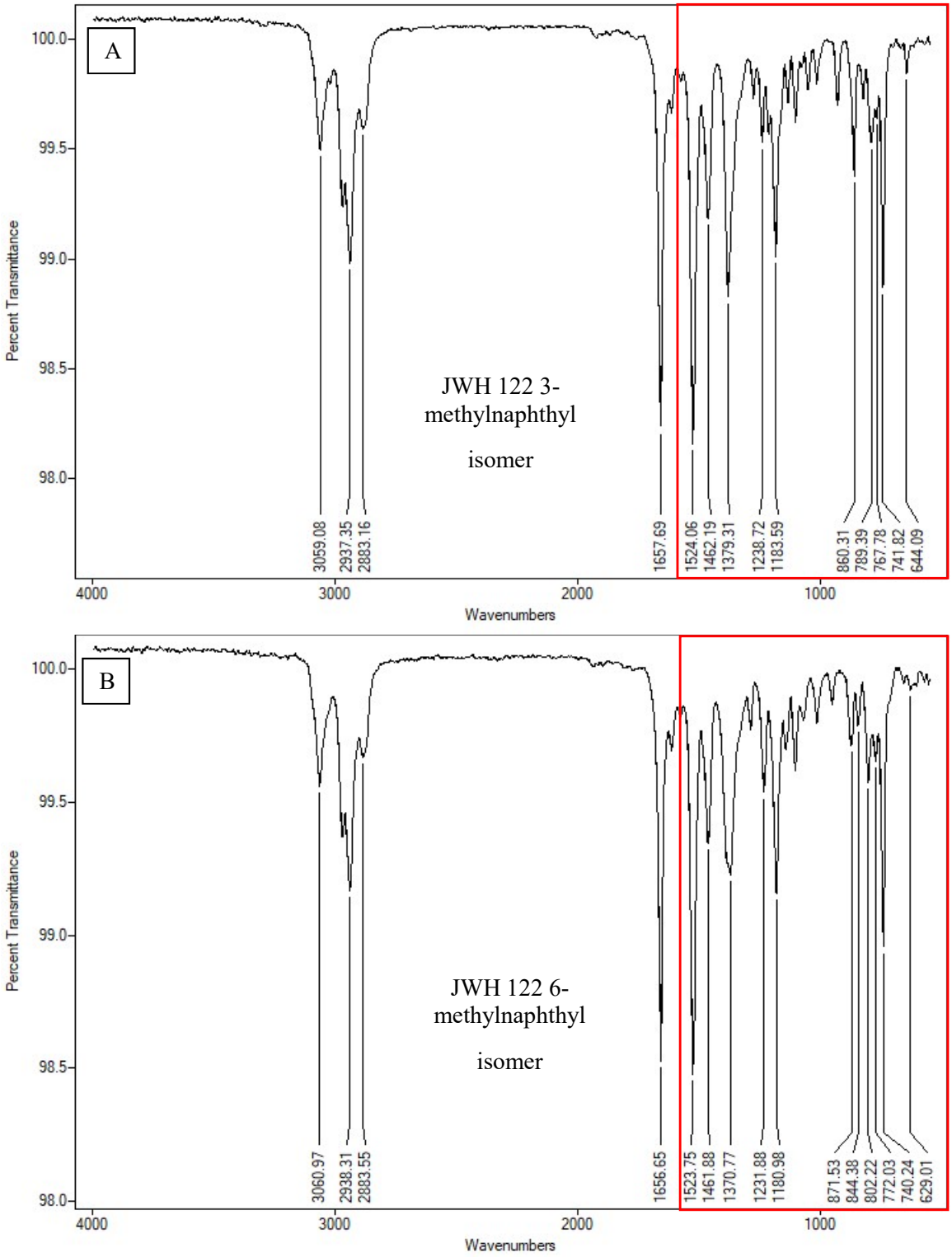

Figure 30. GC-IR spectra of JWH 122 (A) 3-methylnaphthyl isomer and (B) 6-methylnaphthyl isomer.

7.3. Conclusion and Future Directions

In conclusion, the GC-IR is a useful complement to GC-MS for the analysis of cannabinoids. The phytocannabinoids fragment by GC-MS to produce easy to differentiate mass spectra. However, isomeric compounds of the synthetic cannabinoids resulted in some isomers being misidentified as the other which has a similar mass spectra. This problem was resolved with the utilization of the GC-IR spectra which provided a more useful method of differentiating the hard to differentiate isomers. This use of GC-IR can be expanded for the differentiation of isomeric forms of other controlled substances such as cathinones and other emerging NPS.

8. THE ANALYSIS OF FENTANYL-RELATED SUBSTANCES OBTAINED FROM QUADRUPOLE GC-MS DATA USING CERNO BIOSCIENCE MASSWORKS™ AND ITS COMPARISON TO HIGH RESOLUTION MASS SPECTROMETRY ANALYSIS

8.1. Introduction

Mass spectrometry (MS) is heavily relied upon in forensic analysis, with its main advantages being high sensitivity and provision for structural information. In modern MS, the acquired raw data are reduced to the well-known stick spectrum, or centroid, in a process known as centroiding [89]. Since this process reduces data file size, centroiding the MS data results in information loss, including noise characteristics, mass spectral interfering ions, isotopic fine features, and linearity of the ion signal. [89]. For example, **Figure 31** shows a comparison of the spectra for $C_{25}H_{22}N_2OS^{+\cdot}$ for (A) calculated theoretical isotope distribution, (B) measured profile mode response, and (C) measured MS data after centroiding [89].

MS spectral peaks arise from a combination of different ratios of elemental isotopes, with the monoisotopic peak having the complete combination of the lightest isotopes of all elements [89]. Centroiding of the data has the least impact on the monoisotopic peak of an ion and therefore there is very little ambiguity brought on from the combination of other elemental isotopes.

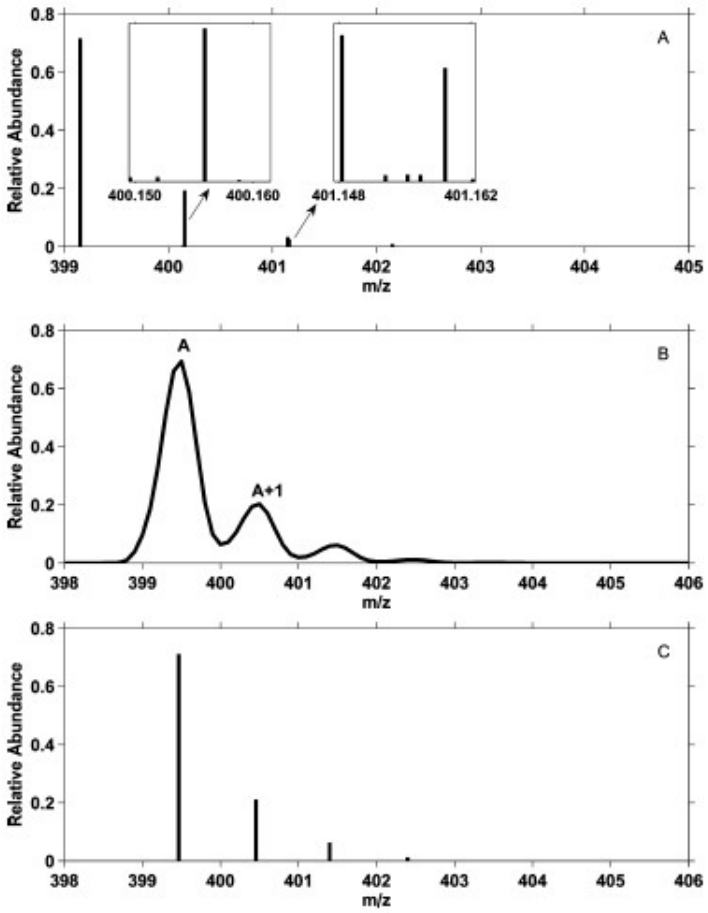

Figure 31. Figure showing (A) calculated theoretical isotope distribution, (B) measured profile mode response, and (C) measured data after centroiding $C_{25}H_{22}N_2OS^+$ (Figure obtained from [89]).

8.1.1. Mass Accuracy, Spectral Accuracy and Elemental Composition Determination

Unit resolution monoisotopic ion peak*s* typically have a mass error of ± 0.2-0.5 Daltons (Da), as a result of the errors associated with the centroiding process. In high resolution MS systems, the mass accuracy is improved to parts per million (ppm) mass error, with mass error of <5 ppm considered accurate enough for high confidence molecular formula confirmation [89].

This high accuracy is relevant only to the monoisotopic peak. While the other isotope clusters of the same ion are more complex and susceptible to errors from the centroiding process, they do contain more information on the ion and the elemental compositions, which aids in determining the correct formula. In order to eliminate errors from centroiding, the clusters are run in raw scan mode or profile mode. Raw scan mode data signal is sampled continuously at some interval of time or other variable prior to conversion to *m/z*. This ensures that all isotopes related to the ion of interest are accurately represented in an attempt at spectral accuracy.

Data obtained in raw scan mode is similar to that seen in **Figure 32B**, which is a mathematical convolution between the theoretical isotope distribution in **Figure 32A** and the continuous function called the peak shape function. This complete profile of the peak shape function provides more information on the ion dispersion in the mass spectrometer and other information about the dispersion inside the ion source. The peak shape function is unique to the mass spectrometer and is specific to the instrument under a given set of MS tune conditions. The full width half maximum (FWHM) parameter elucidates the resolving power while the shift in the position of the peak shape function defines the mass accuracy.

The profile mode mass spectrum is undefined and variable as a result of its typically undefined MS peak shape function. This variability makes it difficult to determine the spectral accuracy of a mass spectral measurement. The uncertainty from the MS peak shape can be calibrated through a process which involves both the *m/z* and the peak shape [89]. Here, the calibration is accomplished though the measurement of standards whose

elemental composition is known; e.g., using perfluorotributylamine (PFTBA) in a GC-MS system.

Figure 32 details the process of mass spectral calibration. The calibration standard and the sample are run in raw scan mode and the calibration filter ensures that all isotope information is preserved through the process. This calibrated spectrum now has a definable peak function and this allows the possibility of convoluting the theoretical isotope distribution for a specific formula with this peak shape function to generate a theoretical MS (in profile mode). A theoretical mass spectral vector is then compared to the calibrated mass spectral vector to measure the spectral accuracy through a spectral error calculation.

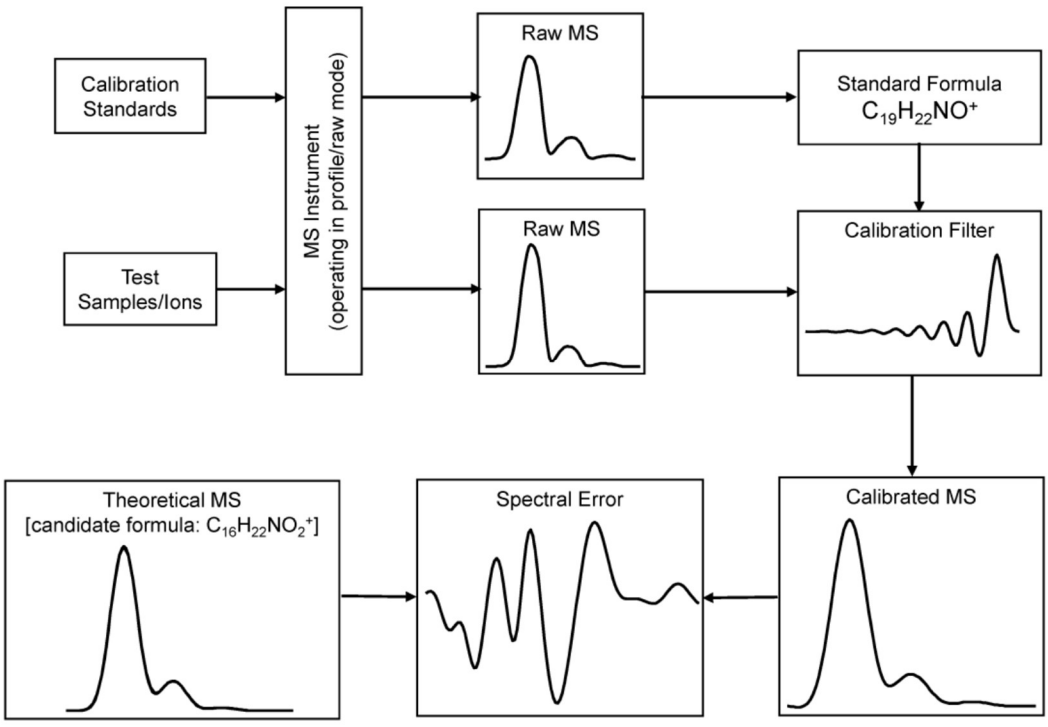

Figure 32. The details of the mass spectral calibration and the spectral accuracy calculation at unit mass resolution [89].

The compound analyzed in raw scan mode (profile mode) and calibrated using a perfluorotributylamine (PFTBA) standard corrects for the uncertainty and variability of the spectra produced in profile mode [89], [90]. As a result, low-resolution data can be refined to give greater mass accuracy and ideal peak shape, which allows comparison of simulated isotopic peak data to the experimental result for each fragment ion produced [89], [91]. This is achieved through the analysis of the data using an algorithm known as the Calibrated Lineshape Isotope Profile Search (CLIPS) to generate a possible formula for an ion and which utilizes the isotopic peak shape to assess the quality of fit for each proposed formula [91], [92], with higher quality having a higher percent spectral accuracy. Since elemental composition is usually obtained using high resolution MS instruments, this method is useful for improving the mass accuracy of low resolution data like those obtained from single quadrupole GC-MS.

8.1.2. Application of Spectral Accuracy Optimization using MassWorks™

Spectral accuracy experiments using spectral data obtained by single quadrupole GC-MS and high resolution instruments with the use of MassWorks™ software have been reported in literature [91], [93]. MassWorks™ software analyzes the single quadrupole GC-MS data generated in profile mode and converts it to high resolution data which provides chemical formula data for fragments and molecular ions. The main use of the use of this software in conjunction with single quadrupole GC-MS data is for molecular formula and elemental composition determination of those molecular ions or fragments in question, particularly for those determined to be “unknown” when searched by a spectral library.

In one experiment, quadrupole GC-MS data from analyzed dye molecules were calibrated by the method detailed above and analyzed using MassWorks™ [91]. The analytical method was validated and the CLIPS function of the software was used to obtain the chemical formulae for molecular and fragment ions for known dye molecules and the identification of unknowns.

In another experiment, restricted spectral accuracy (RSA) was used, whereby only the A+2 profile was fitted and analyzed using self-Calibrated Line-shape Isotope Profile Search (sCLIPS) of Orbitrap data. The A+2 profile was selected due to its having greater differentiating power arising from the much richer fine structure than the A+1 or the monoisotopic form. Obtaining accurate elemental composition using MassWorks with high-resolution data demonstrates its applicability for both high- and low-resolution data. This analytical method also produces accurate mass data, consistent with that of high-resolution mass spectrometry. High-resolution mass spectrometry (HRMS). HRMS is widely utilized in drug and toxicological analysis in forensic science by means of orbitrap and time of flight (TOF) MS instrumentation [94]. Such high-resolution data would be useful for the differentiation of the incorrectly identified FRS discussed in Chapter 5. In this study, a sample of these FRS were analyzed using the recommended methods by Cerno Bioscience and analyzed using the MassWorks software. These results were then compared to those obtained from analysis using a high-resolution QTOF-MS analytical instrument.

8.2. Results and Discussion

8.2.1. The use of MassWorks for exploration of FRS

A sample list of FRS which were found to contain closely related common fragment ions by GC-MS are contained in **Table 18**. Out of this group, there are two sets of positional isomers in the form of 2'-methyl Acetyl fentanyl and 3'-methyl Acetyl fentanyl, as well as 2'-methyl Fentanyl and 3'-methyl Fentanyl. Since these were also present in the list of FRS which were incorrectly identified using the library search, the use of high-resolution MS to differentiate them was explored. The software can predict the formula of the fragment selected by means of its CLIPS feature. This will be explored for fragments produced by the isomers as well as those which produced a molecular ion.

Table 18. Table of select FRS which were previously misidentified by GC-MS.

Name	Nominal Mass	Major Fragment Ions	Average Retention Time (min)	Structure
2'-methyl Acetyl fentanyl	336	231, 230, 146	20.811	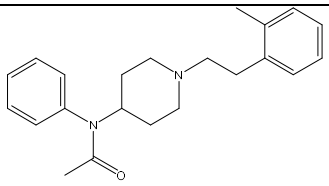
3'-methyl Acetyl fentanyl	336	231, 230, 146	20.657	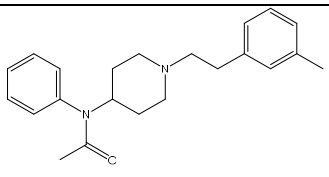

N-DOBU fentanyl	466	259, 258, 260	27.170	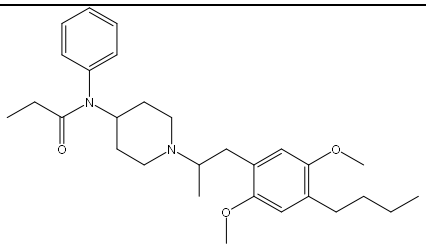
N-DOET fentanyl	438	259, 258, 260	24.825	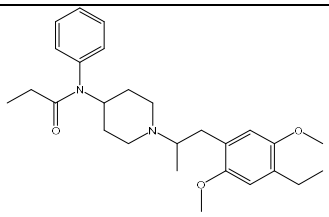
N-DOB fentanyl	488	259, 258, 260	27.896	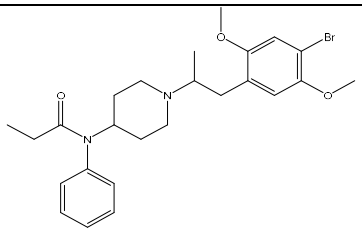
N-DOC fentanyl	444	259, 258, 260	26.185	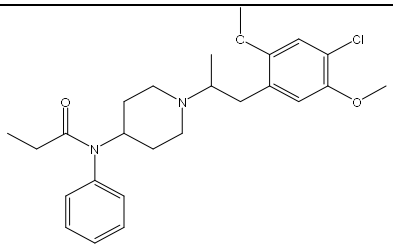
N-DOM fentanyl	424	259, 258, 260	24.287	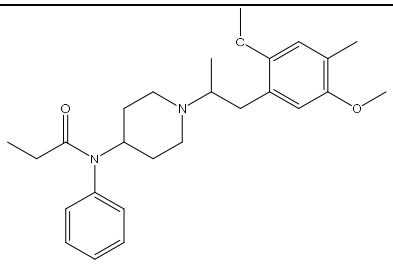

N-(3,4,5-TMA) Fentanyl	441	259, 258 260	25.969	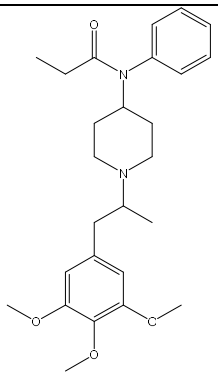
N-(3C-B-fly) fentanyl	512	259, 258, 260	40.623	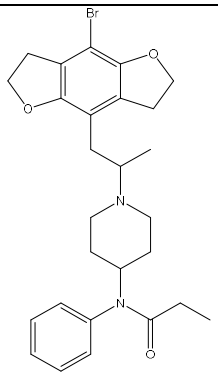
N-(DOI) fentanyl	536	259, 258, 260	30.304	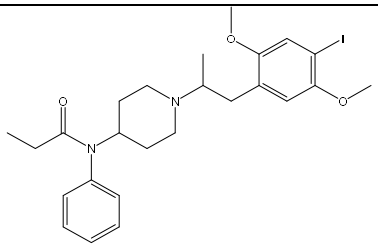
N-(2,5-DMA) fentanyl	410	259, 258, 260	23.907	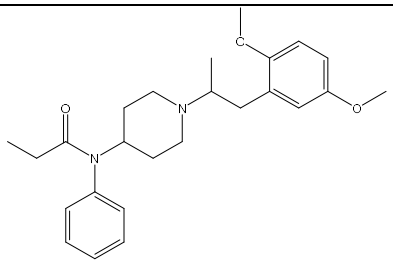
2'-methyl fentanyl	350	245, 244, 146	21.149	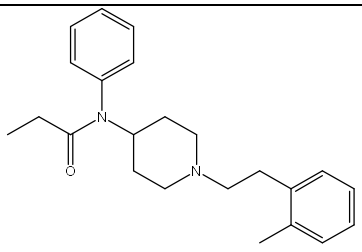

3'-methyl fentanyl	350	245, 244, 146	20.970	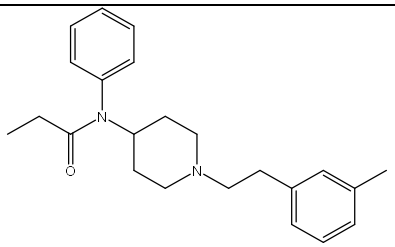
N-(2C-I) fentanyl	522	245, 244, 146	30.129	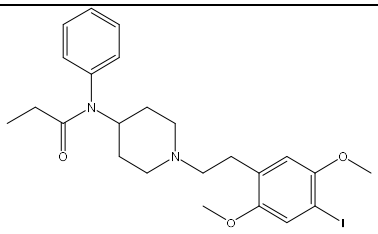
N-(2C-iP) fentanyl	438	245, 244, 146	24.779	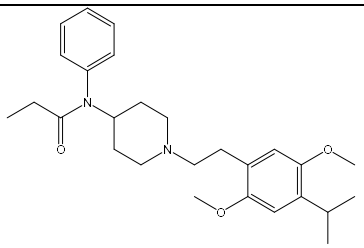
N-(2C-T-7) fentanyl	470	245, 244, 146	31.872	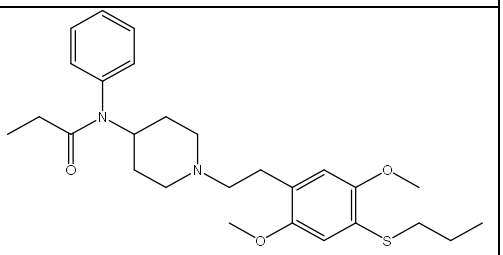

The FIU MS Fentanyl library search (library generated using centroid data) of the profile mode generated data of these select fentanyl analogs resulted in incorrect identification for all the compounds analyzed, returning no match to any content in the library. This result may be explained by the fact that the profile mode data contains more information than the spectra generated using centroid mode data present in the library, so a match cannot be established with any content in the library. The search of a centroid data generated library is not appropriate for the profile mode data.

The 2'-methyl Acetyl fentanyl and 3'-methyl Acetyl fentanyl spectra that were compared using the MassWorks software are shown in **Figure 33**.

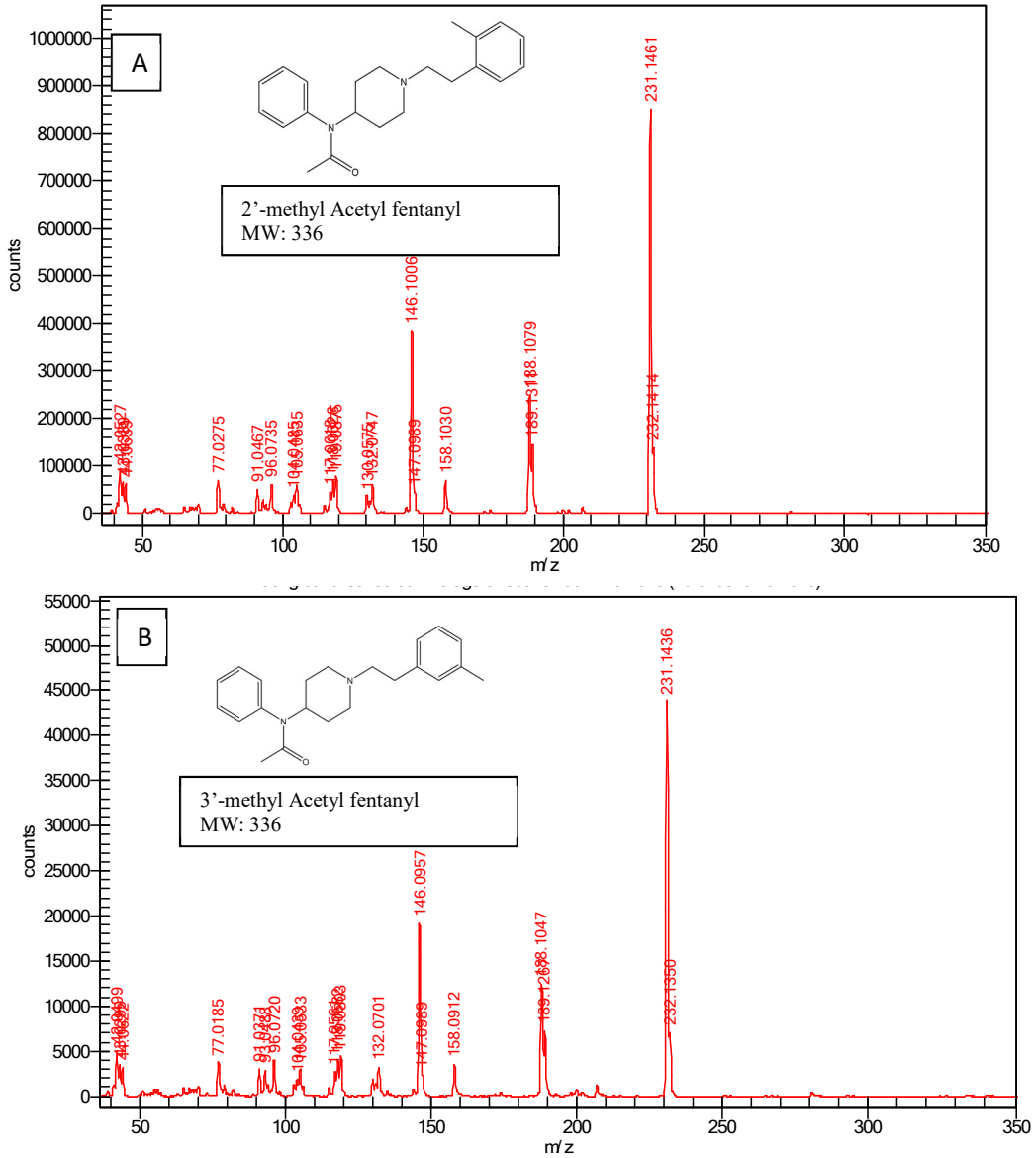

Figure 33. GC-MS spectra of 2'-methyl Acetyl fentanyl and 3'-methyl Acetyl fentanyl analyzed in MassWorks.

In both spectra, there is a lack of the molecular ion characteristic of fentanyls. Additionally, in both cases, the base peak ion is produced as a result of the cleavage between the α (alpha)

and β (beta) carbon of the phenethyl linker, producing the base peak ion of 231.1461 and 231.1436 m/z for 2'-methyl Acetyl fentanyl and 3'-methyl Acetyl fentanyl respectively.

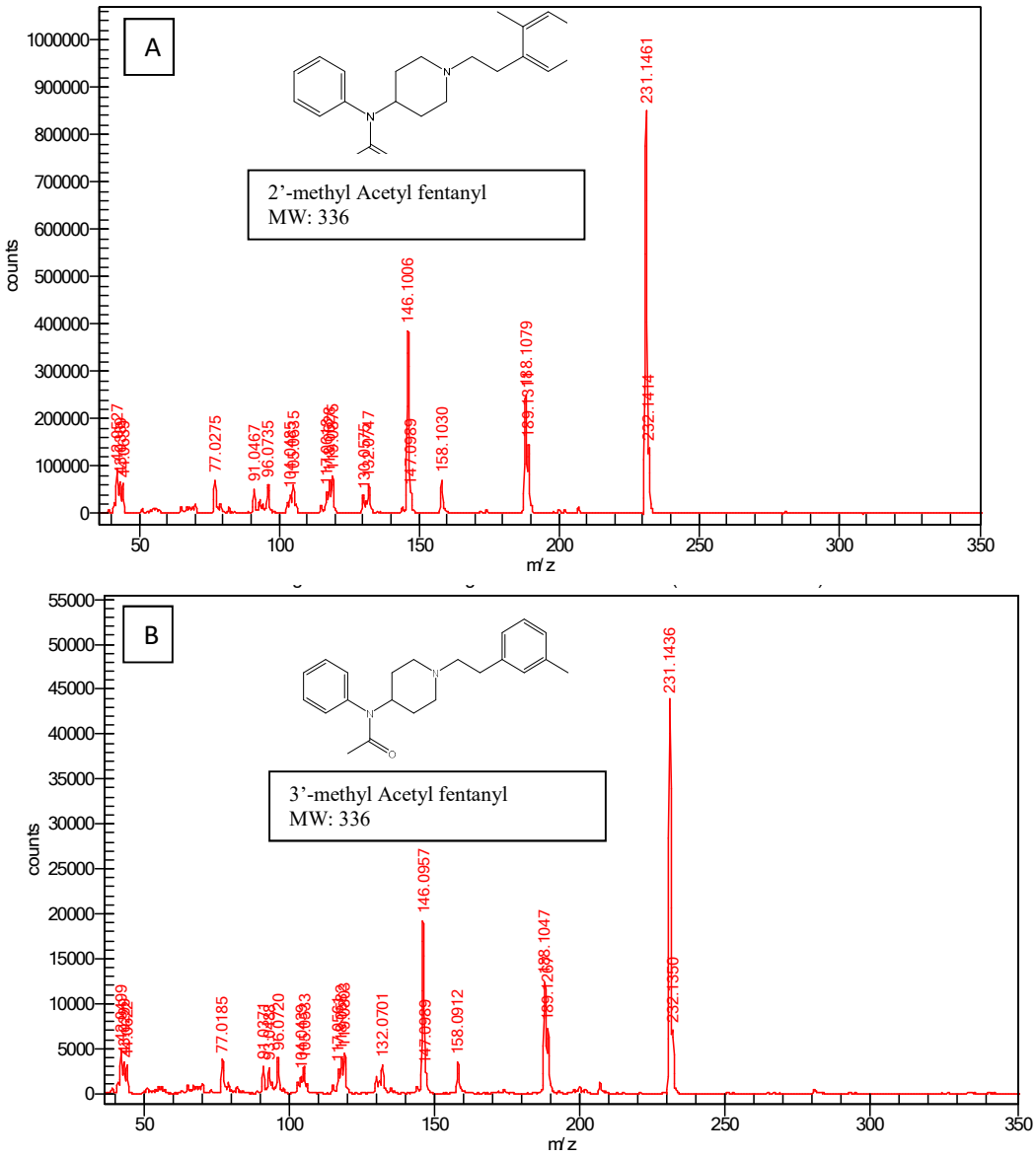

Figure 34. The GC-MS spectra generated from the analysis of 2'-methyl Fentanyl and 3'-methyl Fentanyl and then analyzed by MassWorks software.

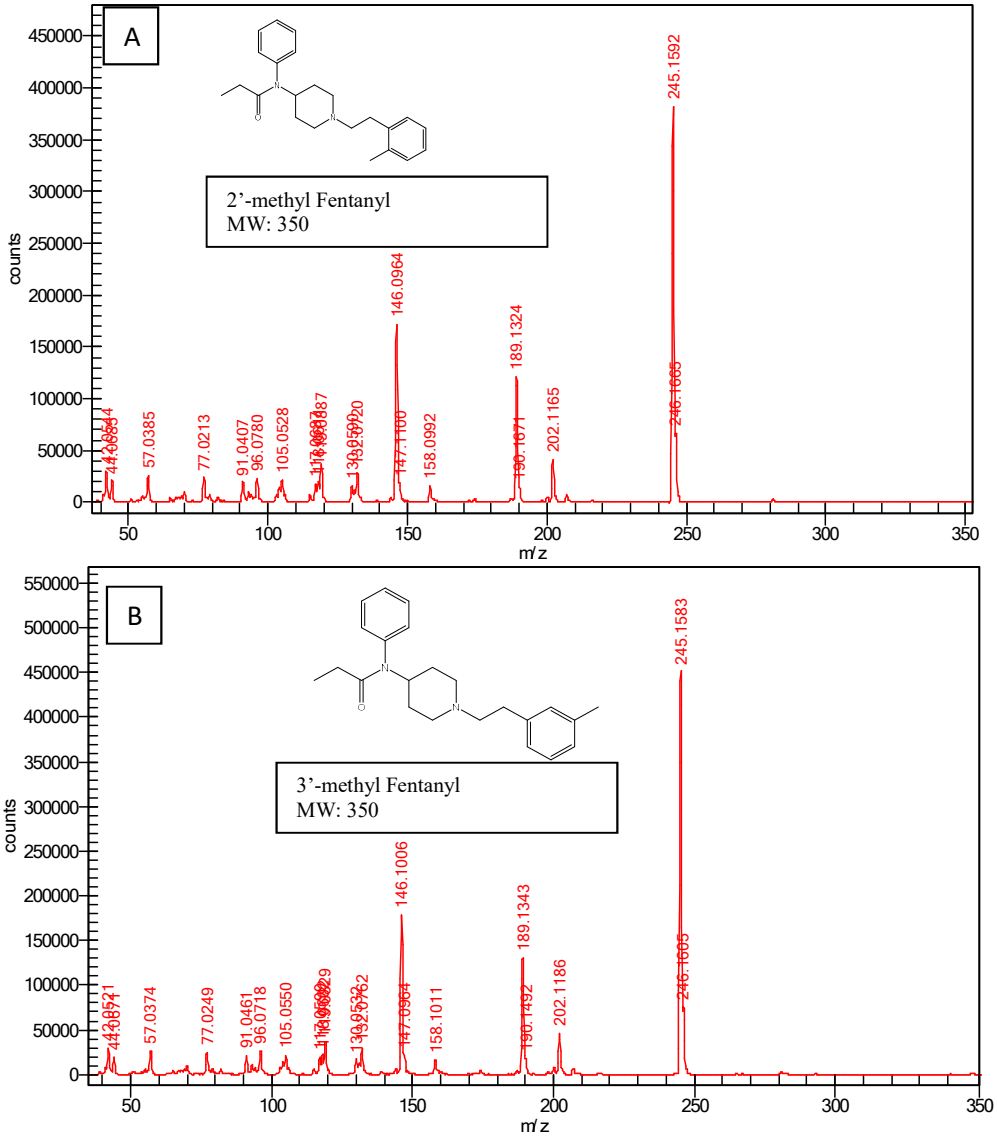

Figure 35. GC-MS spectra of 2'-methyl Fentanyl and 3'-methyl Fentanyl analyzed by MassWorks software.

The 2'-methyl Fentanyl and the 3'-methyl Fentanyl fragment to produce the same base peak ions of 245.1592 and 245.1589 m/z, respectively. This is also the result of the alpha cleavage of the bond at the N-alkyl chain bond. They also had major ions 146.0964, 189.1324 m/z and 146.1006, 189.1343, respectively.

As described previously, the CLIPS search feature of MassWorks using single quadrupole GC-MS data was found to be useful for the identification of dyes in a forensic study [91]. The ability to accurately calculate the molecular formulae based on the spectra in question was assessed. The fragments of the isomers analyzed in the previous section as well as those FRS from the list which retained their molecular ion were assessed.

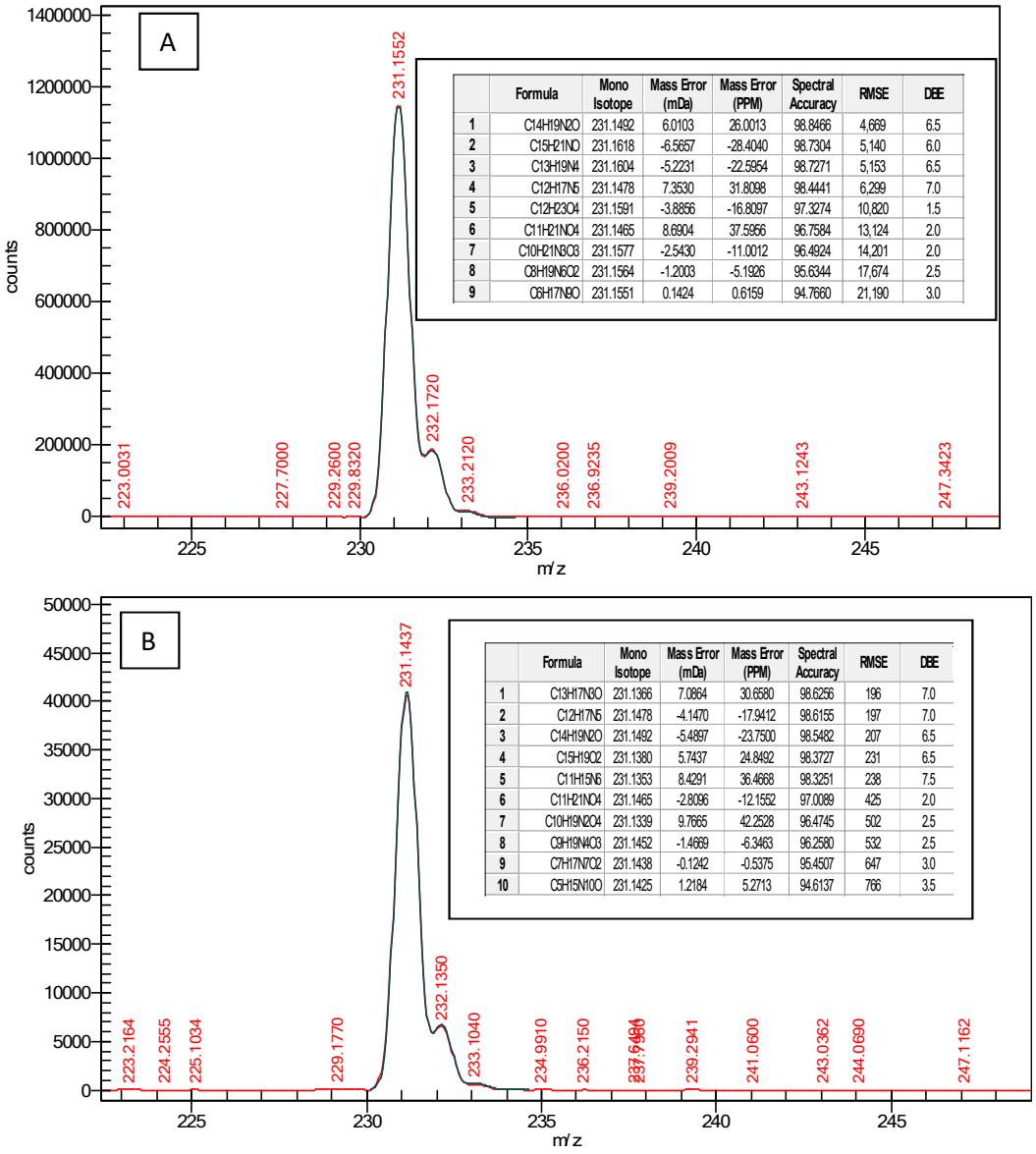

	Formula	Mono Isotope	Mass Error (mDa)	Mass Error (PPM)	Spectral Accuracy	RMSE	DBE
1	C14H19N2O	231.1492	6.0103	26.0013	98.8466	4,669	6.5
2	C15H21NO	231.1618	-6.5657	-28.4040	98.7304	5,140	6.0
3	C13H19N4	231.1604	-5.2231	-22.5954	98.7271	5,153	6.5
4	C12H17N5	231.1478	7.3530	31.8098	98.4441	6,299	7.0
5	C12H23O4	231.1591	-3.8856	-16.8097	97.3274	10,820	1.5
6	C11H21NO4	231.1465	8.6904	37.5956	96.7584	13,124	2.0
7	C10H21N3O3	231.1577	-2.5430	-11.0012	96.4924	14,201	2.0
8	C8H19N6O2	231.1564	-1.2003	-5.1926	95.6344	17,674	2.5
9	C8H17N8O	231.1551	0.1424	0.6159	94.7660	21,190	3.0

	Formula	Mono Isotope	Mass Error (mDa)	Mass Error (PPM)	Spectral Accuracy	RMSE	DBE
1	C13H17N3O	231.1366	7.0864	30.6580	98.6256	196	7.0
2	C12H17N5	231.1478	-4.1470	-17.9412	98.6155	197	7.0
3	C14H19N2O	231.1492	-5.4897	-23.7500	98.5482	207	6.5
4	C15H19O2	231.1380	5.7437	24.8492	98.3727	231	6.5
5	C11H15N6	231.1353	8.4291	36.4668	98.3251	238	7.5
6	C11H21NO4	231.1465	-2.8096	-12.1552	97.0089	425	2.0
7	C10H19N2O4	231.1339	9.7665	42.2528	96.4745	502	2.5
8	C9H19N4O3	231.1452	-1.4669	-6.3463	96.2580	532	2.5
9	C7H17N7O2	231.1438	-0.1242	-0.5375	95.4507	647	3.0
10	C9H15N10O	231.1425	1.2184	5.2713	94.6137	766	3.5

Figure 36. CLIPS search of the base peak ions of 231 m/z for (A) 2'-methyl Acetyl fentanyl and (B) 3'-methyl Acetyl fentanyl.

Both compounds fragment to produce the base peak ion 231 m/z, which corresponds to the formula $C_{14}H_{19}N_2O$. The 2'-methyl Acetyl fentanyl data search resulted in the first formula, which had a 26.0013 ppm mass error and spectral accuracy score of 98.8466. When the 3'-methyl Acetyl fentanyl data was searched, the third formula, which had a -

23.7500 ppm mass error and spectral accuracy score of 98.5482 was found. The fit of the proposed spectra is shown in blue as a smooth curve over the original spectra. The results are shown in **Figure 36**.

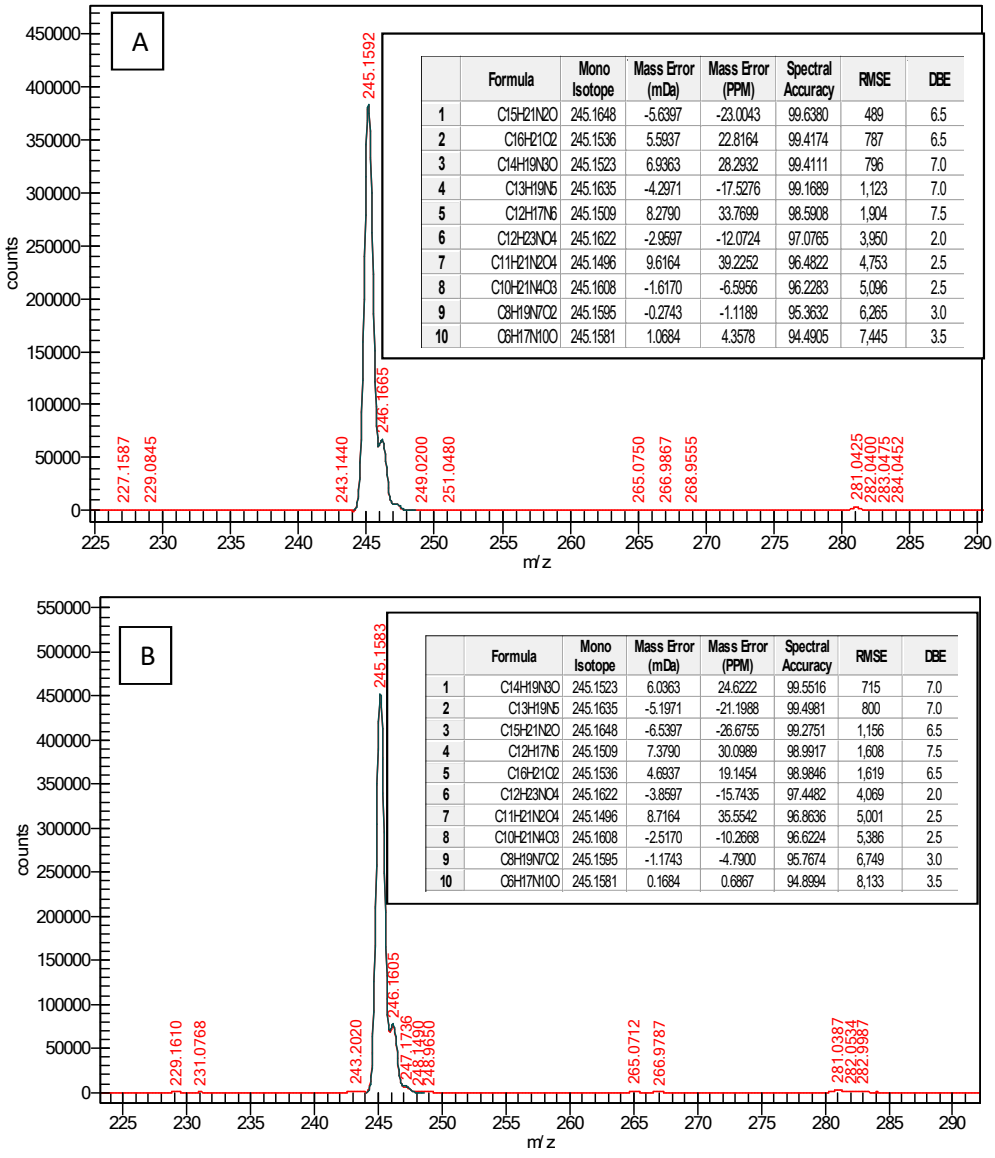

	Formula	Mono Isotope	Mass Error (mDa)	Mass Error (PPM)	Spectral Accuracy	RMSE	DBE
1	C15H21N2O	245.1648	-5.6397	-23.0043	99.6380	489	6.5
2	C16H21O2	245.1536	5.5937	22.8164	99.4174	787	6.5
3	C14H19N3O	245.1523	6.9363	28.2932	99.4111	796	7.0
4	C13H19N5	245.1635	-4.2971	-17.5276	99.1689	1,123	7.0
5	C12H17N6	245.1509	8.2790	33.7699	98.5908	1,904	7.5
6	C12H23NO4	245.1622	-2.9597	-12.0724	97.0765	3,950	2.0
7	C11H21N2O4	245.1496	9.6164	39.2252	96.4822	4,753	2.5
8	C10H21N4O3	245.1608	-1.6170	-6.5956	96.2283	5,096	2.5
9	C8H19N7O2	245.1595	-0.2743	-1.1189	95.3632	6,265	3.0
10	C6H17N10O	245.1581	1.0684	4.3578	94.4905	7,445	3.5

	Formula	Mono Isotope	Mass Error (mDa)	Mass Error (PPM)	Spectral Accuracy	RMSE	DBE
1	C14H19N3O	245.1523	6.0363	24.6222	99.5516	715	7.0
2	C13H19N5	245.1635	-5.1971	-21.1988	99.4981	800	7.0
3	C15H21N2O	245.1648	-6.5397	-26.6755	99.2751	1,156	6.5
4	C12H17N6	245.1509	7.3790	30.0989	98.9917	1,608	7.5
5	C16H21O2	245.1536	4.6937	19.1454	98.9846	1,619	6.5
6	C12H23NO4	245.1622	-3.8597	-15.7435	97.4482	4,069	2.0
7	C11H21N2O4	245.1496	8.7164	35.5542	96.8636	5,001	2.5
8	C10H21N4O3	245.1608	-2.5170	-10.2668	96.6224	5,386	2.5
9	C8H19N7O2	245.1595	-1.1743	-4.7900	95.7674	6,749	3.0
10	C6H17N10O	245.1581	0.1684	0.6867	94.8994	8,133	3.5

Figure 37. CLIPS search of the base peak ions of 245 m/z of (A) 2'-methyl Fentanyl and (B) 3'-methyl Fentanyl.

The 2'-methyl Fentanyl and 3'-methyl Fentanyl both have a base peak ion of 245 m/z. This corresponds to a formula of $C_{15}H_{21}N_2O$, and results can be seen in **Figure 37**. The 2'-

methyl Fentanyl resulted in the first ranked formula, with a mass error of 24.6222 ppm and a spectral accuracy score of 99.5516. A CLIPS search of the 3'-methyl Fentanyl yielded the third ranking formula, with a mass error of -26.6755 ppm and spectral accuracy score of 99.2751.

All other compounds were searched for the presence of a molecular ion; however, only N-(2C-iP) Fentanyl and N-(2C-T-7) Fentanyl had these in their spectra at low intensity, at 438.2866 and 470.2271 m/z, respectively. A CLIPS search was conducted and the results are shown in **Figures 38 and 39**.

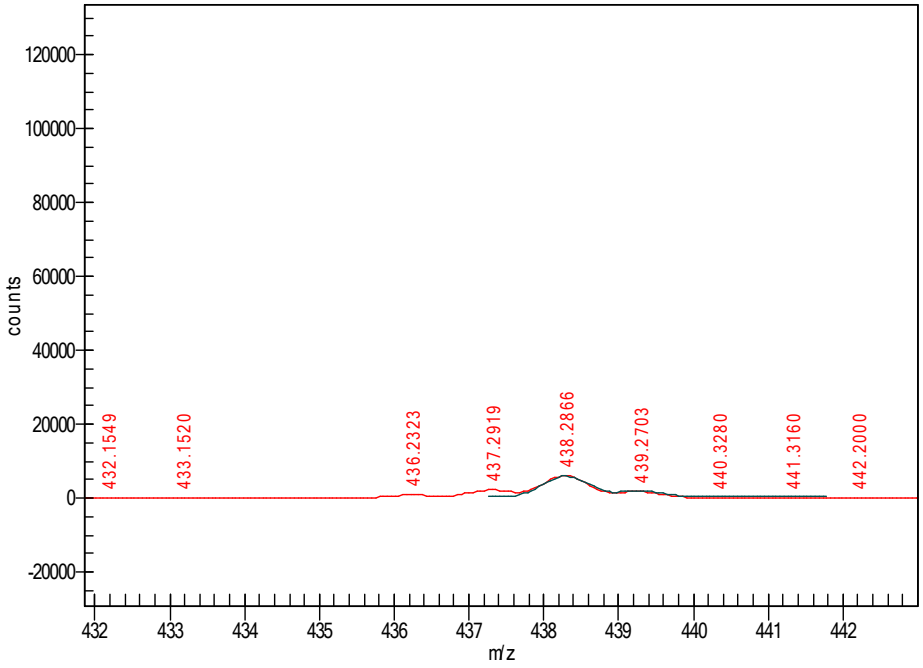

	Formula	Mono Isotope	Mass Error (mDa)	Mass Error (PPM)	Spectral Accuracy	RMSE	DBE
1	C13H30N18	438.2895	-2.9345	-6.6953	77.3202	522	8.0
2	C14H30N16O	438.2783	8.2989	18.9349	77.2489	524	8.0
3	C15H32N15O	438.2909	-4.2771	-9.7588	77.2147	524	7.5
4	C16H32N13O2	438.2796	6.9562	15.8714	77.1320	526	7.5
5	C10H32N17O3	438.2869	-0.2544	-0.5804	77.0808	527	3.5
6	C17H34N12O2	438.2922	-5.6198	-12.8222	77.0770	528	7.0
7	C12H34N14O4	438.2882	-1.5971	-3.6439	77.0719	528	3.0
8	C14H36N11O5	438.2895	-2.9397	-6.7074	77.0308	529	2.5
9	C13H34N12O5	438.2770	9.6363	21.9863	77.0204	529	3.0
10	C18H34N10O3	438.2810	5.6136	12.8080	76.9830	530	7.0
11	C15H36N9O6	438.2783	8.2936	18.9229	76.9679	530	2.5
12	C16H38N8O6	438.2909	-4.2824	-9.7708	76.9575	530	2.0
13	C19H36N9O3	438.2936	-6.9625	-15.8857	76.9075	531	6.5
14	C17H38N6O7	438.2796	6.9510	15.8594	76.8833	532	2.0
15	C18H40N5O7	438.2922	-5.6251	-12.8343	76.8521	533	1.5
16	C20H36N7O4	438.2823	4.2709	9.7445	76.8025	534	6.5
17	C19H40N3O8	438.2810	5.6083	12.7960	76.7665	535	1.5
18	C20H42N2O8	438.2936	-6.9678	-15.8977	76.7146	536	1.0
19	C21H38N6O4	438.2949	-8.3052	-18.9492	76.7068	536	6.0
20	C21H32N11	438.2837	2.9335	6.6931	76.6848	537	11.5
21	C21H42O9	438.2823	4.2656	9.7325	76.6179	538	1.0
22	C22H38N4O5	438.2837	2.9282	6.6811	76.5908	539	6.0
23	C22H34N10	438.2962	-9.6426	-22.0006	76.5466	540	11.0
24	C6H34N18O5	438.2954	-8.8077	-20.0958	76.5391	540	-1.0
25	C7H34N16O6	438.2842	2.4257	5.5344	76.5333	540	-1.0
26	C23H40N3O5	438.2962	-9.6478	-22.0126	76.4752	541	5.5
27	C23H34N8O	438.2850	1.5908	3.6296	76.4124	543	11.0
28	C24H40NO6	438.2850	1.5856	3.6176	76.3487	544	5.5
29	C25H36N5O2	438.2864	0.2482	0.5662	76.1112	550	10.5
30	C27H38N2O3	438.2877	-1.0945	-2.4973	75.7821	557	10.0
31	C29H34N4	438.2778	8.8015	20.0815	75.1786	571	15.0
32	C30H36N3	438.2904	-3.7746	-8.6122	74.9449	577	14.5
33	C31H36NO	438.2791	7.4588	17.0181	74.7638	581	14.5
34	C32H38O	438.2917	-5.1173	-11.6756	74.5150	587	14.0

Figure 38. CLIPS search of the molecular ion 438 m/z of N-(2C-iP) Fentanyl.

The molecular formula of the N-(2C-iP) Fentanyl is $C_{27}H_{38}N_2O_3$, which corresponds to the 438.2866 m/z ion seen in the figure. The search of the molecular ion in CLIPS resulted in the thirtieth ranked molecular formula, corresponding to a mass error of -2.4973 ppm and spectral accuracy score of 75.7821. This represents a rather low accuracy as can be seen in the overlay of that particular match over the actual spectra, where some regions did not smoothly fit on the spectra. This can be attributed to the low intensity of the molecular ion produced.

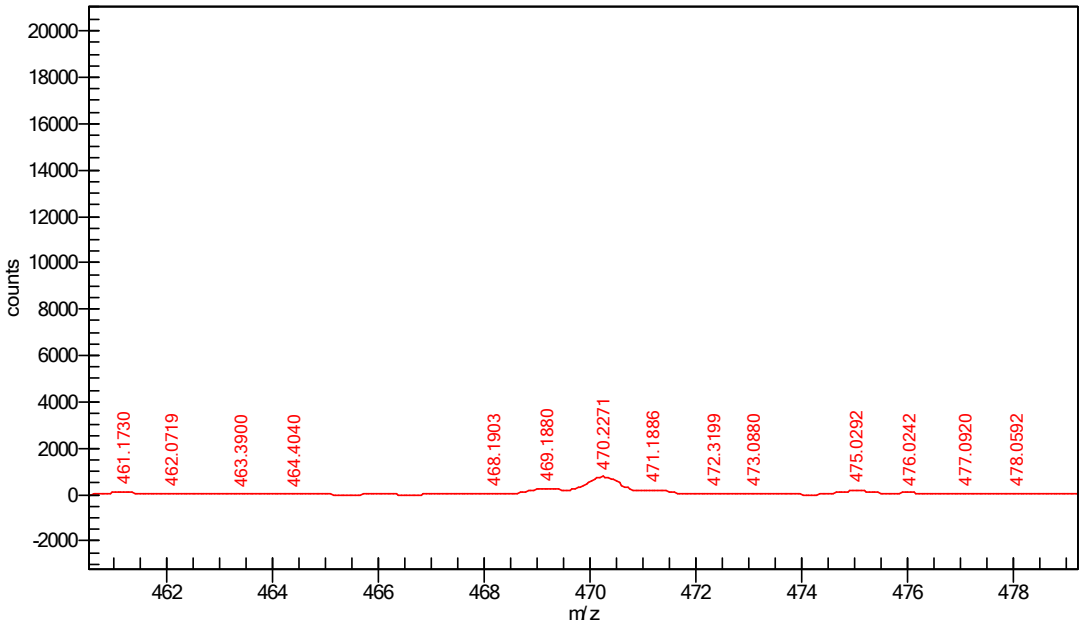

Figure 39. Molecular ion of 470 m/z of N-(2C-T-7) Fentanyl.

The molecular formula of the N-(2C-T-7) Fentanyl is $C_{27}H_{38}N_2O_3S$, which corresponds to the 470.2271 m/z ion seen in the figure. The molecular ion was rather weak and when searched in the CLIPS, did not yield any matching formula.

8.2.2. Analysis of fentanyl using ESI-QTOF-MS/MS

In an effort to compare the high-resolution capabilities of the MassWorks software, the analysis of the same FRS was compared with data from an actual high-resolution instrument, in the form of the QTOF-MS/MS.

The molecular ions of 14 of the 16 FRS analyzed in the GC-MS experiment were not generated; the 2 that did have a low intensity molecular ion that ranked very low in the CLIPS search for the spectral match. Meanwhile, when the samples were analyzed by QTOF-MS/MS, they all produced a molecular ion the 0-30 eV collision induced dissociation (CID) energy range. This can be explained by the fact that GC-MS utilizes electron impact ionization, which is regarded as a 'hard' ionization technique that produces extensive fragmentation. In contrast, electrospray ionization (ESI) is considered a 'soft' ionization technique which preserves the molecular ion [95].

An example of the effect of the collision energies is seen in **Figure 40**. For 2'-methyl Acetyl fentanyl, as the collision energy increases there is a gradual decrease in the presence of the molecular ion from 0 eV until it can no longer be seen at 60 eV.

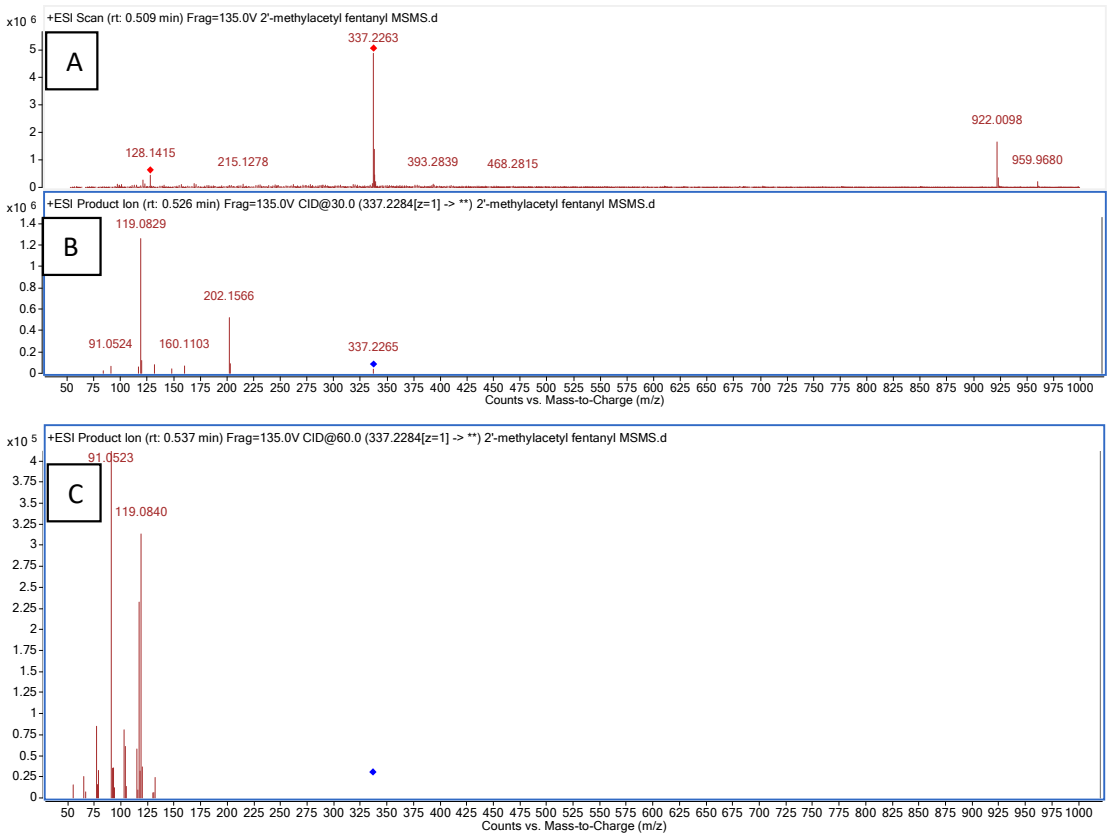

Figure 40. Fragmentation of 2'-methyl acetyl fentanyl at (A) 0 eV, (B) 30 eV, and (C) 60 eV.

The fragment ions which were produced by the isomers were also investigated. In **Figure 41**, the spectra obtained at 30 eV of 2'-methyl Acetyl fentanyl, 3'-methyl Acetyl fentanyl, 2'-methyl Fentanyl, and 3'-methyl fentanyl are shown.

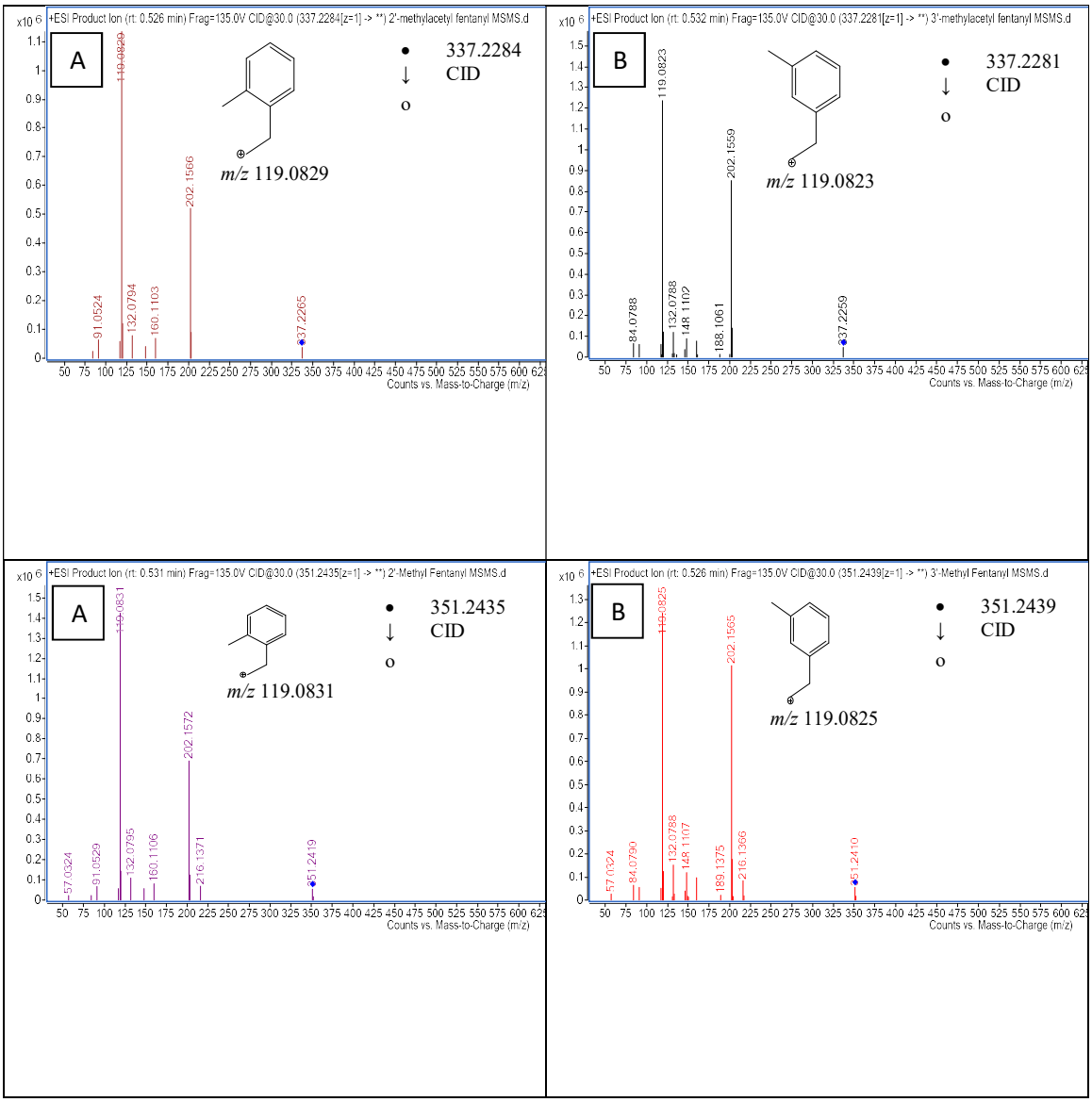

Figure 41. The spectra of product ions produced at 30 eV CE for (A) 2'-methyl Acetyl fentanyl (B) 3'-methyl Acetyl fentanyl (C) 2'-methyl Fentanyl and (D) 3'-methyl Fentanyl.

Both sets of isomers produced the same major product ions in their spectra. The primary base peak ions of 119 m/z are dominant in all spectra. This is due to the fragmentation between the nitrogen and the α-carbon of the phethyl linker. This easily further fragments to produce the $C_7H_7^+$ tropylium ion, which is seen at 91 m/z. The other dominant ion, 202

m/z ($C_{14}H_{20}N$), was formed by the fragmentation of the bond between the nitrogen of the amide group and the piperidine moiety. This fragmentation pattern demonstrates a consistency in fragmentation based on regions of substitution. In all cases, the substitution was present on at least the phenethyl moiety. This is consistent with findings in the trends of fentanyl fragmentation being conserved using QTOF-MS/MS for fentanyl analysis as detailed in [96], based on the region of substitution. In **Table 19,** the mass errors of <5 ppm indicate the confirmation of the proposed structures of the molecular ion with high certainty.

Table 19. Protonated precursor ion mass-to-charge ions, product ions in decreasing order of abundance, and mass error of each FRS analyzed by Q-TOF MS/MS instrument.

Compound Name	Chemical Formula	$[M+H]^+$ (m/z)	Product ions (m/z) at 30eV	Mass error (ppm)
2'-methyl Acetyl fentanyl	$C_{22}H_{28}N_2O$	337	119, 202, 120, 203	3.38
3'-methyl Acetyl fentanyl	$C_{22}H_{28}N_2O$	337	119, 202, 203, 120	-1.96
N-DOBU fentanyl	$C_{29}H_{42}N_2O_3$	467	235, 220, 220, 207	-0.81
N-DOET fentanyl	$C_{27}H_{38}N_2O_3$	439	207, 179, 192, 208	-1.55

N-DOB fentanyl	$C_{25}H_{33}BrN_2O_3$	489	259, 257, 228, 230	-3.82
N-DOC fentanyl	$C_{25}H_{33}ClN_2O_3$	445	213, 185, 215, 187	-0.79
N-DOM fentanyl	$C_{26}H_{36}N_2O_3$	425	193, 165, 178, 194	5.1
N-(3,4,5-TMA) fentanyl	$C_{26}H_{36}N_2O_4$	441	209, 181, 146, 194	3.82
N-(3C-B-fly) fentanyl	$C_{27}H_{33}BrN_2O_3$	513	283, 281, 202, 513	-0.91
N-(DOI) fentanyl	$C_{25}H_{33}IN_2O_3$	537	305, 276, 388, 178	0.49
N-(2,5-DMA) fentanyl	$C_{25}H_{34}N_2O_3$	411	151, 179, 164, 262	4.42
2'-methyl fentanyl	$C_{23}H_{30}N_2O$	351	119, 202, 120, 203	-1.17
3'-methyl fentanyl	$C_{23}H_{30}N_2O$	351	119, 202, 203, 120	-2.31
N-(2C-I) fentanyl	$C_{24}H_{31}IN_2O_3$	523	290, 374, 275, 375	0.6
N-(2C-iP) fentanyl	$C_{27}H_{38}N_2O_3$	439	207, 192, 208, 291	-1.55

N-(2C-T-7) fentanyl	$C_{27}H_{38}N_2O_3S$	471	239, 240, 332, 241	0.62

8.3. Comparison of Accurate Mass of Fragment Ions Analyzed by MassWorks and QTOF-MS/MS

High-resolution instrumentation such as QTOF-MS/MS and Orbitrap are unique in their ability to generate accurate mass fragment ions. The conversion of EI-MS mass data, generated from a single quadrupole GC-MS, to accurate mass data by way of MassWorks is a unique means of generating accurate mass data without using the more expensive high-resolution mass spectra instrumentation like the ESI-QTOF-MS/MS. In this section, the accurate mass of the designated high (≥200 m/z), medium (100-199.9 m/z), and low m/z (≤ 99.9 m/z) ions obtained through MassWorks and QTOF-MS/MS were compared to those generated using 70 eV energy, to determine if the two analytical methods produced ions of the same accurate mass.

Each spectrum generated was compared for similar fragment ions produced. The most common fragment ion produced was 91 m/z, found in all the QTOF-MS/MS analyses and in 14 of the 16 EI-MS generated and MassWorks analyzed data (N-[3,4,5-TMA fentanyl] and N-[2C-T-7] fentanyl did not produce the ion in question). This 91 m/z ion, in the context of FRS, is often an indicator of the presence of a phenethyl linker attached to the piperidine ring [23].

Nine (9) of the sixteen (16) compounds analyzed produced at least one other ion in addition to the 91 m/z that was common in both ESI-QTOF-MS/MS and the EI-MS MassWorks

data (**Table 20**). Furthermore, only the N-(2C-I) fentanyl contained high, medium, and low molecular weight ions to be compared.

Table 20. Common mass fragmentations (m/z values) of FRS based on EI-MS and ESI-QTOF-MS/MS.

Compound Name	$[M+H]^+$ (m/z)	Common mass fragmentations (m/z)
N-DOBU fentanyl	467	207, 93, 91, 84, 77
N-DOET fentanyl	439	207,91
N-DOB fentanyl	489	132, 91
N-(3,4,5-TMA) fentanyl	441	110, 93
N-(3C-B-fly) fentanyl	513	202, 91
N-(DOI) fentanyl	537	132, 91
N-(2C-I) fentanyl	523	290, 146, 91, 57
N-(2C-iP) fentanyl	439	207, 93, 91
N-(2C-T-7) fentanyl	471	132, 93, 77

Figure 42 shows the comparison of the spectra of N-(2C-I) fentanyl, which has all the required high, medium, and low m/z fragment ions for comparison. As described previously, soft ionization methods such as ESI produce spectra with more abundant higher mass fragments and fewer number of fragments than those from harder EI methods. This is evident in the spectra shown in **Figure 42**. The $[M+H]^+$ precursor at 523.1449 m/z (expected at 523.1452; 0.6 ppm mass error) fragments to produce the ions of interest. The

290 m/z ion had an accurate mass of 290.9582 m/z in the EI-MS data converted by MassWorks and 290.9877 m/z in the ESI-QTOF-MS/MS data (expected at 290.9876 m/z for $C_{10}H_{12}IO_2$; -101.0 ppm and 0.3 ppm mass errors, respectively). The 146 m/z ion had an accurate mass of 146.0870 m/z in the EI-MS data converted by MassWorks and 146.0965 m/z in the ESI-QTOF-MS/MS data (expected at 146.0964 m/z for $C_{10}H_{12}N$; -64.5 ppm and 0.5 ppm errors, respectively). The 91 m/z ion had an accurate mass of 91.0292 m/z in the EI-MS data converted by MassWorks and 91.0546 m/z in the ESI-QTOF-MS/MS data (expected at 91.0417 m/z for C_7H_7; -274.9 ppm and 4.1 ppm mass errors, respectively). Finally, the 57 m/z ion had an accurate mass of 57.0232 m/z in the EI-MS data converted by MassWorks and 57.0348 m/z in the ESI-QTOF-MS/MS data (expected at 57.0335 m/z for C_3H_5O; -180.4 and 23.0 ppm errors, respectively). All the mass error data fall into the acceptable range of <5 ppm except for the 57.0348 m/z ion obtained in the ESI-QTOF-MS/MS data. It should be noted that, although this number was out of acceptable range, the accurate mass of those determined by ESI-QTOF-MS/MS were often just a fraction higher than expected, while those generated by MassWorks were often a fraction lower than the expected value.

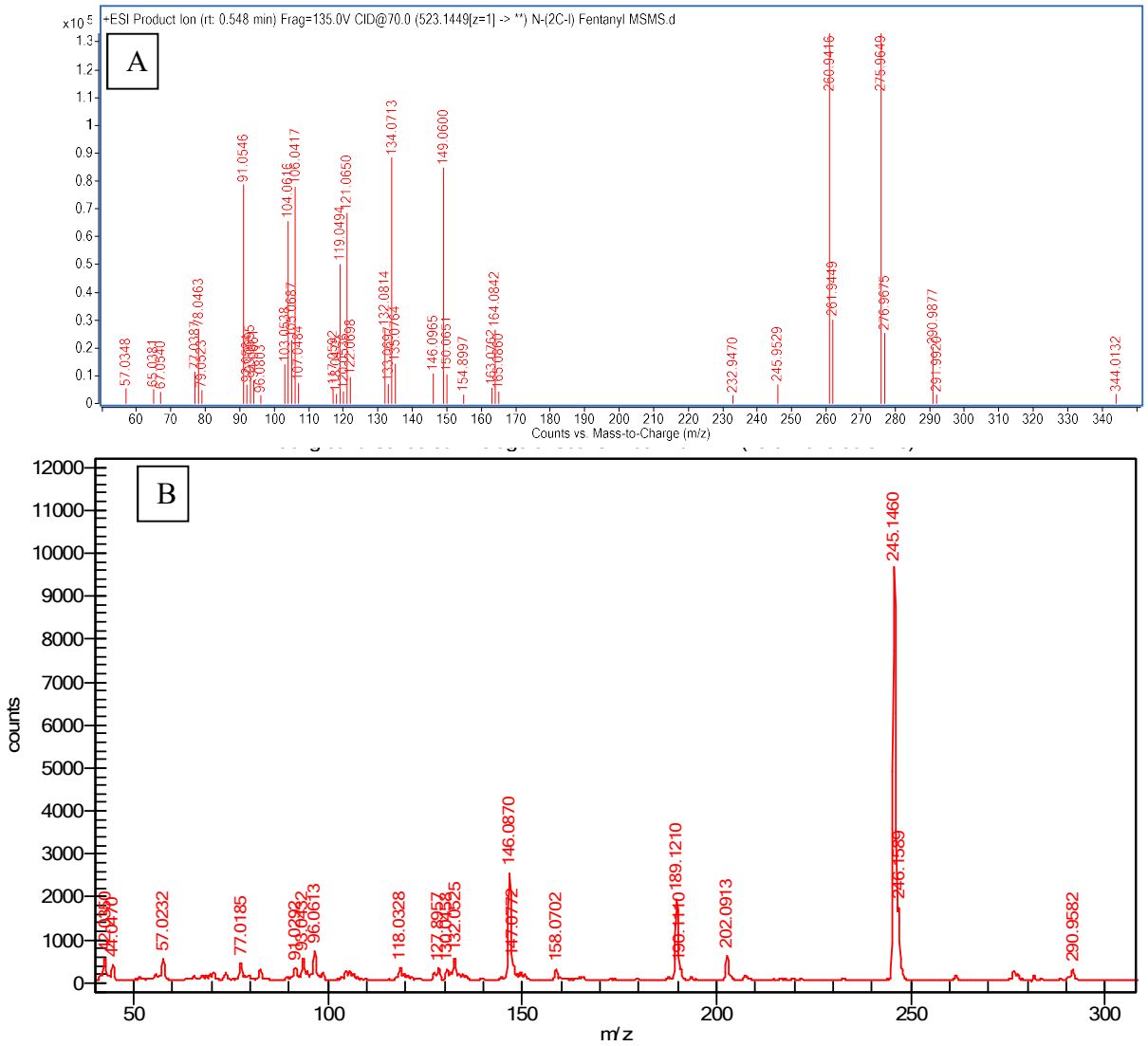

Figure 42. Comparison of the mass spectra of N-(2C-I) fentanyl generated by (A) ESI-QTOF-MS/MS and (B) EI-MS converted by MassWorks

*Mass error calculations not accomplished using the MassHunter or MassWorks software were done using mass calculator at https://warwick.ac.uk/fac/sci/chemistry/research/barrow/barrowgroup/calculators/mass_errors/

Table 21. Table of N-(2C-I) fentanyl fragment formula, expected mass of fragments, and the accurate mass obtained from MassWorks™ and ESI-QTOF-MS/MS.

Fragment Formula	Expected Mass (m/z)	MassWorks™		ESI-QTOF-MS/MS	
		Accurate Mass (m/z)	Mass Error (ppm)	Accurate Mass (m/z)	Mass Error (ppm)
$C_{10}H_{12}IO_2$	290.9876	290.9582	-101.0000	290.9877	0.3000
$C_{10}H_{12}N$	146.0964	146.0870	-64.5000	146.0965	0.5000
C_7H_7	91.0417	91.0292	-274.9000	91.0546	4.1000
C_3H_5O	57.0335	57.0232	-180.4000	57.0348	23.000

8.4. Conclusion and Future Directions

Analyzing single quadrupole GC-MS data using profile mode data and analyzing using MassWorks is an alternative to high-resolution instruments like QTOF-MS/MS. However, fragmentation patterns differ due to the difference in ionization methodologies employed. Electron impact ionization results in greater fragmentation than does the ESI employed in the ESI-QTOF-MS/MS analysis. There is similar mass error associated with the analysis of fentanyl using the MassWorks software versus the actual high-resolution data of ESI-QTOF-MS/MS. However, it should be noted that the accurate mass reported for the MassWorks data is often a fraction less than the actual value; while those generated by the high-resolution instrument are often a fraction more than the actual value. Finally, since the FRS are notorious for the lack of the production of a molecular ion using EI methods, the conversion of this type of data from single quadrupole generated from hard ionization makes it still rather difficult to get an accurate understanding of the structure. In the future, a comparison study of QTOF data and ion trap data can be done with a more extensive variety of substituted fentanyl.

9. OVERALL CONCLUSIONS AND FUTURE DIRECTIONS

9.1. Overall Conclusions

9.1.1. Development of a GC-IR and GC-MS Spectral Library

For the first time, new GC-MS and GC-IR libraries were created with authentic reference standards, with each reference standard acquired in triplicate, for 212 FRS and are now freely available [67] to the forensic science community. Seventy-nine, or approximately 37% of the 212 analogs, did not produce a molecular ion with electron impact ionization mass spectrometry and, as expected, positional isomers of FRS produce similar fragmentation in their mass spectra when using electron impact GC-MS.

9.1.2. Validation of Libraries for Identification of FRS

The second aim was to validate the libraries for their identification of FRS. GC-MS alone may not be sufficient for the identification of FRS; however, GC-IR provides an *orthogonal* confirmatory technique that differentiates between positional isomers of FRS. A library search of each of the 212 FRS using the NIST library produced 4.7% matches to the correct compound, which is not unexpected as most of the FRS were not included the NIST library. Only 89.6% of the searches resulted in the correct compound within the top five candidates when using the newly created GC-MS library. An existing GC-IR database (EUCLiD) that contained only 32 of the 212 FRS was also searched with 15.1% correct correlation. When the new GC-IR library containing all 212 FRS was searched, 100% identification was achieved. The three laboratories in this study searched 20 blind FRS samples using the FIU FRS Library with 100% correctly identified.

The LODs and LOQs were also calculated for the GC-IR methods used by the three laboratories ranging in LODs between 0.10 mg/mL to 0.19 mg/mL and the LOQs from 0.30 mg/mL to 0.57 mg/mL.

This study strongly supports the use of GC- IR in the analysis of unknown compounds, especially FRS.

9.1.3. Interlaboratory Study to Evaluate the Utility of GC-IR for the Forensic Analysis of FRS

The third aim was to conduct an interlaboratory to evaluate the utility of GC-IR for the analysis of FRS. The GC-IR is a useful confirmatory complementary technique when used with GC-MS analysis for the differentiation of FRS. Results of the interlaboratory study show 100% positive identification of FRS when using GC-MS only in conjunction with vapor phase GC-IR analysis. Solid phase IR analysis produces spectra with less detail than vapor phase IR, affecting the ability for solid phase IR spectra to be correctly searched against a vapor phase IR library. Thus, solid phase IR analysis generated spectra should be searched using a solid phase IR library; vapor phase IR spectra searched with a vapor phase IR library for identification. The results of this study are being used in the development of an ASTM International standard test method for the analysis of fentanyl (and fentanyl-related substances) using GC-IR.

9.1.4. GC-IR and GC-MS Analysis of Phytocannabinoids and Synthetic Cannabinoids

The fourth aim was to evaluate the utility of GC-IR for differentiation of positional isomers of cannabinoids. This involved both GC-MS and GC-IR analysis of the cannabinoids. The GC-IR is a useful complement to GC-MS for the analysis of cannabinoids. The

phytocannabinoids fragment by GC-MS to produce easy to differentiate mass spectra. However, isomeric compounds of the synthetic cannabinoids resulted in some isomers being misidentified as the other which has a similar mass spectra. This problem was resolved with the utilization of the GC-IR spectra which provided a more useful method of differentiating the hard to differentiate isomers.

9.1.5. Use of Cerno Bioscience's MassWorks™ Software to Convert Single Quadrupole GC-MS Data of FRS to High Resolution Data Capable for Use in Spectral Accuracy

Finally, our last aim was the conversion of single quadrupole GC-MS data of FRS to high resolution data capable of providing spectral information. This was done in an effort to improve single quadrupole data in a manner that allowed for the differentiation of those which were difficult to differentiate in the library by GC-MS. This results obtained were compared to those generated from an actual HRMS instrument – the ESI-QTOF-MS. For the first time there is a report of the conversion of fentanyl data from single quadrupole GC-MS to high-resolution mass spectrometry data, which is compare to data produced by an actual high-resolution ESI-QTOF-MS/MS. The data is useful; however, the use of high-resolution offers a greater opportunity for the production of the molecular ion and closer values to the exact mass.

There were plans to include other classes of drugs and a wider variety of positional isomers of the drugs included in the experiments previously described; however, further experiments were precluded by the commencement of construction in the laboratory whereby all operations had to be shut down.

9.2. Overall Findings

A GC-IR library of FRS containing 212 FRS was created and validated. GC-IR shows improvement in the differentiation of the difficult to differentiate by GC-MS positional isomers contained in the library. Furthermore, GC-IR also demonstrates to be effective for the differentiation of the difficult to differentiate by GC-MS positional isomers of synthetic cannabinoids. Finally, the use of MassWorks™ software for the conversion of single quadrupole GC-MS data to HRMS data showed comparable results to the ESI-QTOF-MS/MS data; however, the ESI-QTOF-MS/MS offers a greater opportunity for the production of the molecular ion and closer values to the exact mass.

9.3. Future Directions

Future analysis includes adding a wider selection of positional isomers from other NPS categories e.g. cathinones and collect their mass spectra and infrared spectra. This can then be compared to see if GC-IR is more effective for their differentiation than GC-MS. Additionally, the exploration of high-resolution methods of mass spectrometry using cannabinoids which produced similar spectra in this study as well as other hard to differentiate NPS. Furthermore, experiments can be designed for the high-resolution analysis of fentanyls using ESI-QTOF-MS/MS and orbitrap analysis to investigate if there is conservation of fragmentation across the instruments considering different levels of substitution across the FRS.

Finally, the results of the inter-laboratory study forges a path to create a standard method of analysis via the American Society for Testing and Materials (ASTM) International for the use of GC-IR for the analysis of fentanyl and FRS. The intention is to start with FRS

and as time progresses other NPS can be included and other inter-laboratory studies created which can assist in the development of an ASTM method.

9.3. Recommendations

It is recommended that when using the IRD3 detector to wait at least 30 minutes after the instrument indicates “ready” status. This is to allow the optics to fully reach alignment and results in better quality spectral acquisition.

REFERENCES

[1] US Department of Justice Drug Enforcement Administration, "Special NFLIS Drug 2021 Annual Report," 2022. [Online]. Available: https://www.nflis.deadiversion.usdoj.gov/publicationsRedesign.xhtml. [Accessed: 30-Sep-2022].

[2] "Overdose Death Rates," *National Institute on Drug Abuse*, 2022. [Online]. Available: https://www.drugabuse.gov/related-topics/trends-statistics/overdose-death-rates. [Accessed: 04-Apr-2022].

[3] Center for Disease Control and Prevention, "Provisional Drug Overdose Death Counts," 2022. [Online]. Available: https://www.cdc.gov/nchs/nvss/vsrr/drug-overdose-data.htm?te=1&nl=the-morning&emc=edit_nn_20220520. [Accessed: 14-Jul-2022].

[4] J. Knestrick, "Impact of the Opioid Crisis," *J. Nurse Pract.*, vol. 13, no. 9, p. A18, 2017.

[5] M. R. Spencer, M. Warner, B. A. Bastian, J. P. Trinidara, and H. Hedegaard, "Drug overdose deaths involving fentanyl, 2011-2016," *Natl. Vital Stat. Reports*, vol. 68, no. 3, 2019.

[6] L. N. Rodda, J. L. Pilgrim, M. Di Rago, K. Crump, D. Gerostamoulos, and O. H. Drummer, "A cluster of fentanyl-laced heroin deaths in 2015 in Melbourne, Australia," *J. Anal. Toxicol.*, vol. 41, no. 4, pp. 318–324, 2017.

[7] D. Ciccarone, "Fentanyl in the US heroin supply: A rapidly changing risk environment," *Int. J. Drug Policy*, vol. 46, pp. 107–111, 2017.

[8] J. M. Stogner, "The Potential Threat of Acetyl Fentanyl: Legal Issues, Contaminated Heroin, and Acetyl Fentanyl 'Disguised' as Other Opioids," *Ann. Emerg. Med.*, vol. 64, no. 6, pp. 637–639, 2014.

[9] M. L.J. and E. B.J., "A series of forensic toxicology and drug seizure cases involving illicit fentanyl alone and in combination with heroin, cocaine or heroin and cocaine," *J. Anal. Toxicol.*, vol. 38, no. 8, pp. 592–598, 2014.

[10] P. Armenian, K. T. Vo, J. Barr-Walker, and K. L. Lynch, "Fentanyl, fentanyl analogs and novel synthetic opioids: A comprehensive review," *Neuropharmacology*, vol. 134, pp. 121–132, 2018.

[11] J. F. Casale, J. R. Mallette, and E. M. Guest, "Analysis of illicit carfentanil : Emergence of the death dragon," *Forensic Chem.*, vol. 3, pp. 74–80, 2017.

[12] E. Sisco, J. Verkouteren, J. Staymates, and J. Lawrence, “Rapid detection of fentanyl, fentanyl analogues, and opioids for on-site or laboratory based drug seizure screening using thermal desorption DART-MS and ion mobility spectrometry,” *Forensic Chem.*, vol. 4, pp. 108–115, 2017.

[13] V. W. Weedn, M. Elizabeth Zaney, B. McCord, I. Lurie, and A. Baker, “Fentanyl-related substance scheduling as an effective drug control strategy,” *J. Forensic Sci.*, no. March, pp. 1186–1200, 2021.

[14] N. Fairbairn, P. O. Coffin, and A. Y. Walley, “Naloxone for heroin, prescription opioid, and illicitly made fentanyl overdoses: Challenges and innovations responding to a dynamic epidemic,” *Int. J. Drug Policy*, vol. 46, pp. 172–179, 2017.

[15] T. Awad, T. Belal, J. DeRuiter, K. Kramer, and C. R. Clark, “Comparison of GC-MS and GC-IRD methods for the differentiation of methamphetamine and regioisomeric substances,” *Forensic Sci. Int.*, 2009.

[16] The Center for Forensic Science Research & Education, “Trend Reports 2018-2022,” 2022. [Online]. Available: https://www.cfsre.org/nps-discovery/trend-reports. [Accessed: 02-Apr-2023].

[17] T. S. Belal *et al.*, “Differentiation of methylated indole ring regioisomers of JWH-007: GC–MS and GC–IR studies,” *Forensic Chem.*, vol. 7, pp. 1–9, 2018.

[18] L. N. Sacco, “Drug enforcement in the United States: History, policy, and trends,” 2015.

[19] US Drug Enforcement Administration, “Drug Scheduling.” [Online]. Available: https://www.dea.gov/drug-information/drug-scheduling. [Accessed: 16-Aug-2022].

[20] US Drug Enforcement Administration, “Control of immediate precursor used in the illicit manufacture of fentanyl as schedule II controlled substances,” *Fed. Regist.*, vol. 75, no. 124, pp. 37295–37299, 2010.

[21] D. C. D. DEA, “Fentanyl (Trade Names: Actiq®, Fentora TM , Duragesic®),” 2018.

[22] K. Kuczyńska, P. Grzonkowski, Ł. Kacprzak, and J. B. Zawilska, “Abuse of fentanyl: An emerging problem to face,” *Forensic Sci. Int.*, vol. 289, pp. 207–214, 2018.

[23] H. Grenke Pierzynski, L. Neubauer, C. Choi, R. Franckowski, S. D. Augustin, and D. M. Iula, “Tips for interpreting GC-MS fragmentation of unknown substituted fentanyls,” *Cayman Curr.*, no. 28, 2017.

[24] C. A. Valdez, “Gas Chromatography-Mass Spectrometry Analysis of Synthetic Opioids Belonging to the Fentanyl Class: A Review,” *Crit. Rev. Anal. Chem.*, vol. 52, no. 8, pp. 1938–1968, 2022.

[25] S. Jickells and A. Negrusz, Eds., *Clarke’s Analytical Forensic Toxicology*. Pharmaceutical Press, 2008.

[26] J. Suzuki and S. El-Haddad, “A review: Fentanyl and non-pharmaceutical fentanyls,” *Drug Alcohol Depend.*, vol. 171, pp. 107–116, 2017.

[27] M. Wilde *et al.*, “Metabolic Pathways and Potencies of New Fentanyl Analogs,” *Front. Pharmacol.*, vol. 10, no. April, pp. 1–16, 2019.

[28] UNODC, *Rapid testing methods of drugs of abuse*. 1994.

[29] J. Siegel, “Forensic Chemistry: Fundamentals and Applications.” p. 560, 2015.

[30] P. Allan, K. Phillip, B. Ms, and E. Canonico, “Fentanyl as a potential false positive with color tests commonly used for presumptive cocaine identification,” *J. Forensic Sci.*, no. April, pp. 1–7, 2022.

[31] R. E. Wharton, J. Casbohm, R. Hoffmaster, B. N. Brewer, M. G. Finn, and R. C. Johnson, “Detection of 30 Fentanyl Analogs by Commercial Immunoassay Kits,” *J. Anal. Toxicol.*, vol. 45, no. 2, pp. 111–116, 2021.

[32] J. E. Goldman, K. M. Waye, K. A. Periera, M. S. Krieger, J. L. Yedinak, and B. D. L. Marshall, “Perspectives on rapid fentanyl test strips as a harm reduction practice among young adults who use drugs: A qualitative study 11 Medical and Health Sciences 1117 Public Health and Health Services 17 Psychology and Cognitive Sciences 1701 Psychology,” *Harm Reduct. J.*, vol. 16, no. 1, pp. 1–11, 2019.

[33] S.-N. Lin, T.-P. F. Wang, R. M. Caprioli, and B. P. N. Mo, “Determination of Plasma Fentanyl by GC-Mass Spectrometry and Pharmacokinetic Analysis,” *J. Pharm. Sci.*, vol. 70, no. 11, pp. 1276–1279, 1981.

[34] W. Feeney, A. S. Moorthy, and E. Sisco, “Spectral Trends in GC-EI-MS Data Obtained from the SWGDRUG Library and Literature: A Resource for the Identification of Unknown Compounds,” *Forensic Chem.*, vol. 31, no. September, p. 100459, 2022.

[35] A. S. Moorthy, A. J. Kearsley, W. G. Mallard, and W. E. Wallace, “Mass spectral similarity mapping applied to fentanyl analogs,” *Forensic Chem.*, vol. 19, no. March, p. 100237, 2020.

[36] M. A. ElSohly, Ed., *Marijuana and the Cannabinoids*. Totowa, New Jersey: Human Press Inc., 2007.

[37] V. L. Alves, J. L. Gonçalves, J. Aguiar, H. M. Teixeira, and J. S. Câmara, "The synthetic cannabinoids phenomenon: from structure to toxicological properties. A review," *Crit. Rev. Toxicol.*, vol. 50, no. 5, pp. 359–382, 2020.

[38] The Center for Forensic Science Research & Education, "Synthetic Cannabinoids in the United States - Trend Report: Q4 2021," 2022. [Online]. Available: https://www.npsdiscovery.org/wp-content/uploads/2022/02/2021-Q4_Synthetic-Cannabinoids_Trend-Report.pdf.

[39] UNODC, *Recommended Methods for the Identification and Analysis of Cannabis and Cannabis Products*, vol. 1, no. of 55. 2013.

[40] SWGDRUG, "Construction of an Analytical Scheme - Supplemental Document SD-7," 2019. [Online]. Available: https://swgdrug.org/supplemental.htm. [Accessed: 09-Sep-2022].

[41] X. Guo and E. Lankmayr, "Hyphenated Techniques in Gas Chromatography," in *Advanced Gas Chromatography - Progress in Agricultural, Biomedical and Industrial Applications*, 2012, pp. 3–26.

[42] R. Leibrand, Ed., *Basics of GCIRD*. USA: Hewlett Packard, 1993.

[43] D. L. Pavia, G. M. Lampman, G. S. Kriz, and J. R. Vyvyan, *Introduction to Spectroscopy*, 5th ed. Cengage Learning, 2015.

[44] "Spectra Analysis - Solid phase deposition FTIR-DISCOVIR-LC." [Online]. Available: https://www.dksh.com/global-en/products/ins/spectra-analysis-discovir-lc. [Accessed: 20-Sep-2022].

[45] L. Jones, L. Fambro, B. M. Allred, and N. Thomas, "Isomer Differentiation of Novel Psychoactive Substances Using Gas Chromatography Solid Phase Infrared Spectroscopy (GC / IR)," *US Department of Justice, Office of Justice Programs*, 2022. [Online]. Available: https://www.ojp.gov/ncjrs/virtual-library/abstracts/isomer-differentiation-novel-psychoactive-substances-using-gas?mc_cid=9068a490df&mc_eid=75b46123e6. [Accessed: 03-May-2022].

[46] M. Donahue, Botonjic-Sehic, D. Wells, and C. W. Brown, "Understanding Infrared and Raman Spectra of Pharmaceutical Polymorphs," *Am. Pharm. Rev.*, vol. 14, no. 2, 2011.

[47] PerkinElmer, "FT-IR Spectroscopy Attenuated Total Reflectance (ATR)," *PerkinElmer Life and Analytical Sciences*, 2005. [Online]. Available: http://www.utsc.utoronto.ca/~traceslab/ATR_FTIR.pdf.

[48] A. Winokur, L. Kaufman, and J. Almirall, “Differentiation and identification of fentanyl analogues using GC-IRD,” *Forensic Chem.*, vol. 20, p. 100255, 2020.

[49] H. Ohta, S. Suzuki, and K. Ogasawara, “Studies on fentanyl and related compounds IV. Chromatographic and spectrometric discrimination of fentanyl and its derivatives,” *J. Anal. Toxicol.*, vol. 23, no. 4, pp. 280–285, 1999.

[50] T. Belal, T. Awad, J. DeRuiter, and C. R. Clark, “GC-IRD methods for the identification of isomeric ethoxyphenethylamines and methoxymethcathinones,” *Forensic Sci. Int.*, vol. 184, no. 1–3, pp. 54–63, 2009.

[51] K. M. Abdel-Hay, T. Awad, J. DeRuiter, and C. R. Clark, “Differentiation of methylenedioxybenzylpiperazines (MDBPs) and methoxymethylbenzylpiperazines (MMBPs) By GC-IRD and GC-MS,” *Forensic Sci. Int.*, vol. 210, no. 1–3, pp. 122–128, 2011.

[52] T. A. Sasaki and C. L. Wilkins, “Gas chromatography with Fourier transform infrared and mass spectral detection,” *J. Chromatogr. A*, vol. 842, no. 1–2, pp. 341–349, 1999.

[53] J. F. Casale, J. R. Mallette, G. Claro, P. A. Hays, M. Frisch, and K. T. Chan, “Synthesis and Characterization of Benzoylfentanyl and Benzoylbenzylfentanyl Synthesis and Characterization of Benzoylfentanyl and Benzoylbenzylfentanyl [email address withheld at the primary author ’ s request .] Largo , Maryland 20774 6880 Koll Center P,” *Microgram J.*, vol. 15, no. February, 2018.

[54] U.S. Department of Justice, “NFLIS-Drug 2020 Mid-Year Report.” 2020.

[55] “Scientific Working Group for the Analysis of Seized Drugs (SWGDURG) Recommendations,” 2016.

[56] National Institute of Standards and Technology (NIST), “Forensic Database Chemistry & Toxicology Table,” 2017. [Online]. Available: https://www.nist.gov/oles/forensic-database-chemistry-toxicology-table. [Accessed: 22-Mar-2021].

[57] A. Urbas, T. Schoenberger, C. Corbett, K. Lippa, F. Rudolphi, and W. Robien, “NPS Data Hub: A web-based community driven analytical data repository for new psychoactive substances,” *Forensic Chem.*, vol. 9, pp. 76–81, 2018.

[58] S. Stein, “Mass spectral reference libraries: An ever-expanding resource for chemical identification,” *Anal. Chem.*, vol. 84, no. 17, pp. 7274–7282, 2012.

[59] “ASAP Analytical EUCLiD Database.” Covington, KY, 2021.

[60] “Overdose Death Rates,” *National Institute on Drug Abuse*, 2021. [Online]. Available: https://nida.nih.gov/research-topics/trends-statistics/overdose-death-rates.

[61] National Institute on Drug Abuse (NIDA), “DrugFacts: Fentanyl,” no. February 2019. pp. 1–6, 2019.

[62] U.S. Department of Justice, “Special NFLIS Drug Maps Release: Tracking Fentanyl and Fentanyl-Related Compounds Reported in NFLIS Drug by State, 2018-2019,” no. December, 2020.

[63] E. Sisco, A. Burns, and A. S. Moorthy, “Development and evaluation of a synthetic opioid targeted gas chromatography mass spectrometry (GC-MS) method,” *J. Forensic Sci.*, vol. 66, no. 6, pp. 2369–2380, 2021.

[64] T. Awad, T. Belal, J. DeRuiter, K. Kramer, and C. R. Clark, “Comparison of GC-MS and GC-IRD methods for the differentiation of methamphetamine and regioisomeric substances,” *Forensic Sci. Int.*, vol. 185, no. 1–3, pp. 67–77, 2009.

[65] Agilent Technologies, “GC/MSD Libraries for the MSD ChemStation MSD ChemStation General-Purpose Libraries.” 2000.

[66] J. Miller, J. Miller, and R. Miller, *Statistics and Chemometrics for Analytical Chemistry*, 7th Editio. Harlow, UK, 2018.

[67] J. Almirall and K. Ferguson, “FIU Mass Spectrometry and Infrared Libraries of Fentanyl Related Substances.” FIU Research Data Portal, V2, 2022.

[68] K. Ferguson, S. L. Tupik, H. Haddad, J. Perr, M. Gilbert, and R. Newman, “Utility of gas chromatography infrared spectroscopy (GC-IR) for the differentiation of positional isomers of fentanyl related substances,” *Forensic Chem.*, vol. 29, p. 100425, 2022.

[69] J. K. L. D. Field, S. Sternhell, *Organic Structures From Spectra*, Fourth Edi. 2008.

[70] T. M. G. Salerno, P. Donato, G. Frison, L. Zamengo, and L. Mondello, “Gas Chromatography—Fourier Transform Infrared Spectroscopy for Unambiguous Determination of Illicit Drugs: A Proof of Concept,” *Front. Chem.*, vol. 8, no. July, pp. 1–12, 2020.

[71] T. S. Belal *et al.*, “Differentiation of methylated indole ring regioisomers of JWH-007: GC–MS and GC–IR studies,” *Forensic Chem.*, vol. 7, pp. 1–9, 2018.

[72] P. Rosner and T. Junge, “Investigation of the alkylamino group of aliphatic amines by collision-induced dissociation mass spectra of C4H1ON+ immonium ions,” *J. Mass Spectrom.*, vol. 31, pp. 1047–1053, 1996.

[73] S. Borth, W. Hänsel, P. Rösner, and T. Junge, “Synthesis of 2,3- and 3,4-methylenedioxyphenylalkylamines and their regioisomeric differentiation by mass spectral analysis using GC-MS-MS,” *Forensic Sci. Int.*, vol. 114, no. 3, pp. 139–153, 2000.

[74] S. Borth, W. Hänsel, P. Rösner, and T. Junge, “Regioisomeric differentiation of 2,3- and 3,4-methylenedioxy ring-substituted phenylalkylamines by gas chromatography/tandem mass spectrometry,” *J. Mass Spectrom.*, vol. 35, no. 6, pp. 705–710, 2000.

[75] F. Westphal, P. Rösner, and T. Junge, “Differentiation of regioisomeric ring-substituted fluorophenethylamines with product ion spectrometry,” *Forensic Sci. Int.*, vol. 194, no. 1–3, pp. 53–59, 2010.

[76] S. D. Brandt *et al.*, “Separating the wheat from the chaff: Observations on the analysis of lysergamides LSD, MIPLA, and LAMPA,” *Drug Test. Anal.*, vol. 14, no. 3, pp. 545–556, 2022.

[77] F. Westphal and T. Junge, “Ring positional differentiation of isomeric N-alkylated fluorocathinones by gas chromatography/tandem mass spectrometry,” *Forensic Sci. Int.*, vol. 223, no. 1–3, pp. 97–105, 2012.

[78] A. J. Almalki, L. Smith, C. R. Clark, and J. DeRuiter, “Vapor phase GC-IR identification of regioisomeric N-methoxybenzyl-4-substituted-2,5-dimethoxyphenethylamines (NBOMe),” *Forensic Chem.*, vol. 16, no. August, p. 100181, 2019.

[79] A. J. Almalki, L. Smith, Y. Abiedalla, C. R. Clark, and J. DeRuiter, “Vapor phase infrared identification of regioisomeric N-(dimethoxybenzyl)-4-iodo- and 4-bromo-2,5-dimethoxyphenethylamines,” *Forensic Chem.*, vol. 19, no. January, p. 100239, 2020.

[80] Y. Abiedalla, A. J. Almalki, J. Deruiter, and C. R. Clark, “GC – MS and GC – IR analysis of substituted N -benzyl 4-bromo-2,5-dimethoxyphenylisopropylamines,” *Forensic Chem.*, vol. 24, no. December 2020, p. 100326, 2021.

[81] Y. Abiedalla, A. J. Almalki, J. DeRuiter, and C. R. Clark, “GC–MS and GC–IR analysis of methylenedioxyphenylalkylamine analogues of the psychoactive 25X-NBOMe drugs,” *Forensic Chem.*, vol. 23, no. November 2020, p. 100314, 2021.

[82] F. W. Mclafferty, D. a Stauffer, and S. Y. Loh, "Unknown Identification Using Reference Mass Spectra. Quality Evaluation of Databases," *Am. Soc. Mass Spectrom.*, vol. 0305, no. 99, 1999.

[83] J. Heseltine, "Hydrogen as a Carrier Gas for GC and GC-MS," *LCGC North America*, 2010. [Online]. Available: https://www.chromatographyonline.com/view/hydrogen-carrier-gas-gc-and-gc-ms. [Accessed: 19-Apr-2023].

[84] R. Bramston-Cook and E. Bramston-Cook, "Unintended consequences with conversion to hydrogen carrier in gas chromatography," *Air and Waste Management Association - Air Quality Measurement Methods and Technology Conference 2013*, 2013. [Online]. Available: http://lotusinstruments.com/wp/wp-content/uploads/Unintended-Consequences-with-Conversion-to-Hydrogen-Carrier.pdf. [Accessed: 20-Apr-2022].

[85] "Using Hydrogen Carrier Gas with Mass Spectrometric Detection," *Crawford Scientific*, 2019. [Online]. Available: https://www.crawfordscientific.com/chromatography-blog/post/hydrogen-carrier-gas-ms-detection. [Accessed: 21-Apr-2023].

[86] R. Shipman, T. Conti, T. Tighe, and E. Buel, "Forensic Drug Identification by Gas Chromatography-Infrared Spectroscopy," *US Department of Justice*, 2013. [Online]. Available: https://www.ncjrs.gov/pdffiles1/nij/grants/242698.pdf. [Accessed: 31-May-2022].

[87] H. Z. Shirley Lee *et al.*, "Identification of closely related new psychoactive substances (NPS) using solid deposition gas-chromatography infra-red detection (GC–IRD) spectroscopy," *Forensic Sci. Int.*, vol. 299, pp. 21–33, 2019.

[88] H. Z. S. Lee, J. Y. J. Ng, M. C. Ong, J. L. W. Lim, and T. W. A. Yap, "Technical note: Unequivocal identification of 5-methoxy-DiPT with NOESY NMR and GC-IRD," *Forensic Sci. Int.*, vol. 316, p. 110537, 2020.

[89] Y. Wang and M. Gu, "The concept of spectral accuracy for MS," *Anal. Chem.*, vol. 82, no. 17, pp. 7055–7062, 2010.

[90] Cerno Bioscience, "MassWorks Rx GC / ID Experimental Guidelines MassWorks Rx GC / ID Experimental Guidlenes." pp. 1–6, 2020.

[91] R. J. Abel, "Identification of unknown compounds from quadrupole GC-MS data using Cerno Bioscience MassWorks™," *J. Can. Soc. Forensic Sci.*, vol. 47, no. 2, pp. 74–98, 2014.

[92] Cerno Bioscience, "Spectral Accuracy Analysis of an Ion Series for Structural Elucidation and Elemental Composition Determination," 2021.

[93] R. J. Strife, Y. Wang, and D. Kuehl, “Restricted spectral accuracy analysis to identify the single correct organic compound elemental-composition from Orbitrap accurate mass data lists obtained at very high resolution,” *J. Mass Spectrom.*, vol. 53, no. 10, pp. 921–926, 2018.

[94] I. Ojanperä, M. Kolmonen, and A. Pelander, “Current use of high-resolution mass spectrometry in drug screening relevant to clinical and forensic toxicology and doping control,” *Anal. Bioanal. Chem.*, vol. 403, no. 5, pp. 1203–1220, 2012.

[95] E. De Hoffman and V. Stroobant, *Mass Spectrometry: Principles and Applications*, Third Edit. John Wiley & Sons, Ltd, 2012.

[96] J. T. Davidson, Z. J. Sasiene, and G. P. Jackson, “The influence of chemical modifications on the fragmentation behavior of fentanyl and fentanyl-related compounds in electrospray ionization tandem mass spectrometry,” *Drug Test. Anal.*, vol. 12, no. 7, pp. 957–967, 2020.

APPENDIX

Table 22. Table of components of Plate 1 of the Cayman Chemical Fentanyl Analog Screening Kit

Plate Location	Fentanyl Analog Chemical Name	Formal Chemical Name
A2	α-Methyl Acetyl Fentanyl	N-[1-(1-methyl-2-phenylethyl)-4-piperidinyl]-N-phenyl-acetamide
A3	Acetyl Norfentanyl	N-phenyl-N-4-piperidinyl-acetamide
A4	*ortho*-methoxy Furanyl Fentanyl	N-(2-methoxyphenyl)-N-[1-(2-phenylethyl)-4-piperidinyl]-2-furancarboxamide
A5	*ortho*-methyl Furanyl Fentanyl	N-(2-methylphenyl)-N-[1-(2-phenylethyl)-4-piperidinyl]-2-furancarboxamide
A6	4'-methyl Acetyl Fentanyl	N-[1-[2-(4-methylphenyl)ethyl]-4-piperidinyl]-N-phenyl-acetamide
A7	Thiophene Fentanyl	N-phenyl-N-[1-(2-phenylethyl)-4-piperidinyl]-2-thiophenecarboxamide
A8	*para*-chloro Cyclobutyl Fentanyl	N-(4-chlorophenyl)-N-[1-(2-phenylethyl)-4-piperidinyl]-cyclobutanecarboxamide
A9	N-methyl Cyclopropyl Norfentanyl	N-(1-methyl-4-piperidinyl)-N-phenyl-cyclopropanecarboxamide
A10	β-methyl Acetyl Fentanyl	N-phenyl-N-[1-(2-phenylpropyl)-4-piperidinyl]-acetamide
A11	4-ANPP	N-phenyl-1-(2-phenylethyl)-4-piperidinamine
B2	*para*-methyl Acrylfentanyl	N-(4-methylphenyl)-N-[1-(2-phenylethyl)-4-piperidinyl]-2-propenamide
B3	*ortho*-methyl Cyclopropyl Fentanyl	N-(2-methylphenyl)-N-[1-(2-phenylethyl)-4-piperidinyl]-cyclopropanecarboxamide
B4	Fentanyl	N-phenyl-N-[1-(2-phenylethyl)-4-piperidinyl]-propanamide
B5	Norfentanyl	N-phenyl-N-4-piperidinyl-propanamide

B6	Cyclopropyl Fentanyl	N-(1-phenethylpiperidin-4-yl)-N-phenylcyclopropanecarboxamide
B7	Butyryl Norfentanyl	N-phenyl-N-4-piperidinyl-butanamide
B8	*ortho*-methyl Acetyl Fentanyl	N-(2-methylphenyl)-N-[1-(2-phenylethyl)-4-piperidinyl]-acetamide
B9	α'-methyl Butyryl Fentanyl	2-methyl-N-phenyl-N-[1-(2-phenylethyl)-4-piperidinyl]-butanamide
B10	Methacrylfentanyl	2-methyl-N-phenyl-N-[1-(2-phenylethyl)-4-piperidinyl]-2-propenamide
B11	α-methyl Butyryl Fentanyl	N-[1-(1-methyl-2-phenylethyl)-4-piperidinyl]-N-phenyl-butanamide
C2	*para*-fluoro Crotonyl Fentanyl	(E)-N-(4-fluorophenyl)-N-(1-phenethylpiperidin-4-yl)but-2-enamide
C3	α-Methyl Fentanyl	N-[1-(1-methyl-2-phenylethyl)-4-piperidinyl]-N-phenyl-propanamide
C4	Crotonyl Fentanyl	(2E)-N-phenyl-N-[1-(2-phenylethyl)-4-piperidinyl]-2-butenamide
C5	*para*-methyl Cyclopropyl Fentanyl	N-(4-methylphenyl)-N-[1-(2-phenylethyl)-4-piperidinyl]-cyclopropanecarboxamide
C6	*para*-Methoxyfentanyl	N-(4-methoxyphenyl)-N-[1-(2-phenylethyl)-4-piperidinyl]-propanamide
C7	Cyclobutyl Fentanyl	N-phenyl-N-[1-(2-phenylethyl)-4-piperidinyl]-cyclobutanecarboxamide
C8	*ortho*-methyl Acrylfentanyl	N-(2-methylphenyl)-N-[1-(2-phenylethyl)-4-piperidinyl]-2-propenamide
C9	(+/-)-Cis-3-methyl Fentanyl	*cis*-N-[3-methyl-1-(2-phenylethyl)-4-piperidinyl]-N-phenyl-propanamide
C10	Ocfentanil	N-(2-fluorophenyl)-2-methoxy-N-[1-(2-phenylethyl)-4-piperidinyl]-acetamide

C11	*meta*-Methylfentanyl	N-(3-methylphenyl)-N-[1-(2-phenylethyl)-4-piperidinyl]-propanamide

Table 23. Table of components of Plate 1 of the Cayman Chemical Fentanyl Analog Screening Kit

Plate Location	Fentanyl Analog Chemical Name	Formal Chemical Name
D2	*ortho*-fluoro Acrylfentanyl	N-(2-fluorophenyl)-N-[1-(2-phenylethyl)-4-piperidinyl]-2-propenamide
D3	*para*-Chlorofentanyl	N-(4-chlorophenyl)-N-[1-(2-phenylethyl)-4-piperidinyl]-propanamide
D4	*para*-fluoro Cyclopropyl Fentanyl	N-(4-fluorophenyl)-N-[1-(2-phenylethyl)-4-piperidinyl]-cyclopropanecarboxamide
D5	Butyryl Fentanyl	N-phenyl-N-[1-(2-phenylethyl)-4-piperidinyl]-butanamide
D6	Fentanyl Carbamate	phenyl[1-(2-phenylethyl)-4-piperidinyl]-carbamic acid, ethyl ester
D7	Isobutyryl Fentanyl	2-methyl-N-phenyl-N-[1-(2-phenylethyl)-4-piperidinyl]-propanamide
D8	*ortho*-methyl Methoxyacetyl Fentanyl	2-methoxy-N-(2-methylphenyl)-N-[1-(2-phenylethyl)-4-piperidinyl]-acetamide
D9	Benzyl Carfentanil	4-[(1-oxopropyl)phenylamino]-1-(phenylmethyl)-4-piperidinecarboxylic acid, methyl ester
D10	α-methyl Thiofentanyl	N-[1-[1-methyl-2-(2-thienyl)ethyl]-4-piperidinyl]-N-phenyl-propanamide
D11	*para*-methoxy Butyryl Fentanyl	N-(4-methoxyphenyl)-N-[1-(2-phenylethyl)-4-piperidinyl]-butanamide
E2	*para*-chloro Cyclopropyl Fentanyl	N-(4-chlorophenyl)-N-[1-(2-phenylethyl)-4-piperidinyl]-cyclopropanecarboxamide

E3	*ortho*-Fluorobutyryl Fentanyl	N-(2-fluorophenyl)-N-[1-(2-phenylethyl)-4-piperidinyl]-butanamide
E4	*para*-fluoro Acrylfentanyl	N-(4-fluorophenyl)-N-[1-(2-phenylethyl)-4-piperidinyl]-2-propenamide
E5	Cyclopentyl Fentanyl	N-phenyl-N-[1-(2-phenylethyl)-4-piperidinyl]-cyclopentanecarboxamide
E6	Phenyl Fentanyl	N-phenyl-N-[1-(2-phenylethyl)-4-piperidinyl]-benzamide
E7	Tetrahydrofuran Fentanyl	tetrahydro-N-phenyl-N-[1-(2-phenylethyl)-4-piperidinyl]-2-furancarboxamide
E8	Methoxyacetyl Fentanyl	2-methoxy-N-phenyl-N-[1-(2-phenylethyl)-4-piperidinyl]-acetamide
E9	*ortho*-Fluoroisobutyryl Fentanyl	N-(2-fluorophenyl)-2-methyl-N-[1-(2-phenylethyl)-4-piperidinyl]-propanamide
E10	*para*-fluoro Furanyl Fentanyl – 3-Furancarboxamide	N-(4-fluorophenyl)-N-[1-(2-phenylethyl)-4-piperidinyl]-3-furancarboxamide
E11	*para*-Fluorobutyryl Fentanyl	N-(4-fluorophenyl)-N-[1-(2-phenylethyl)-4-piperidinyl]-butanamide
F2	*para*-methyl Tetrahydrofuran Fentanyl	tetrahydro-N-(4-methylphenyl)-N-[1-(2-phenylethyl)-4-piperidinyl]-2-furancarboxamide
F3	Phenylacetyl Fentanyl	N-phenyl-N-[1-(2-phenylethyl)-4-piperidinyl]-benzeneacetamide
F4	*para*-Chloroisobutyryl Fentanyl	N-(4-chlorophenyl)-2-methyl-N-[1-(2-phenylethyl)-4-piperidinyl]-propanamide
F5	*meta*-Fluorobutyryl Fentanyl	N-(3-fluorophenyl)-N-[1-(2-phenylethyl)-4-piperidinyl]-butanamide
F6	*ortho*-fluoro Furanyl Fentanyl	N-(2-fluorophenyl)-N-[1-(2-phenylethyl)-4-piperidinyl]-2-furancarboxamide
F7	*meta*-Fluoroisobutyryl Fentanyl	N-(3-fluorophenyl)-2-methyl-N-[1-(2-phenylethyl)-4-piperidinyl]-propanamide

F8	*para*-chloro Methoxyacetyl Fentanyl	N-(4-chlorophenyl)-2-methoxy-N-[1-(2-phenylethyl)-4-piperidinyl]-acetamide
F9	Alfentanil	N-[1-[2-(4-ethyl-4,5-dihydro-5-oxo-1H-tetrazol-1-yl)ethyl]-4-(methoxymethyl)-4-piperidinyl]-N-phenyl-propanamide
F10	β'-Phenyl Fentanyl	N-phenyl-N-[1-(2-phenylethyl)-4-piperidinyl]-benzenepropanamide
F11	Benzodioxole Fentanyl	N-phenyl-N-[1-(2-phenylethyl)-4-piperidinyl]-1,3-benzodioxole-5-carboxamide

Table 24. Table of components of Plate 2 of the Cayman Chemical Fentanyl Analog Screening Kit

Plate Location	Fentanyl Analog Chemical Name	Formal Chemical Name
A2	*para*-methyl Acetyl Fentanyl	N-(4-methylphenyl)-N-[1-(2-phenylethyl)-4-piperidinyl]-acetamide
A3	*para*-methyl Isobutyryl Fentanyl	2-methyl-N-(4-methylphenyl)-N-[1-(2-phenylethyl)-4-piperidinyl]-propanamide
A4	4'-methyl Fentanyl	N-[1-[2-(4-methylphenyl)ethyl]-4-piperidinyl]-N-phenyl-propanamide
A5	*para*-Fluoroacetyl Fentanyl	N-(4-fluorophenyl)-N-[1-(2-phenylethyl)-4-piperidinyl]-acetamide
A6	β-Hydroxythiofentanyl	N-[1-[2-hydroxy-2-(2-thienyl)ethyl]-4-piperidinyl]-N-phenyl-propanamide
A7	Pivaloyl Fentanyl	2,2-dimethyl-N-phenyl-N-[1-(2-phenylethyl)-4-piperidinyl]-propanamide
A8	*para*-Methylfentanyl	N-(4-methylphenyl)-N-[1-(2-phenylethyl)-4-piperidinyl]-propanamide
A9	Furanyl Fentanyl 3-Furancarboxamide isomer	N-phenyl-N-[1-(2-phenylethyl)-4-piperidinyl]-3-furancarboxamide
A10	*para*-chloro Acrylfentanyl	N-(4-chlorophenyl)-N-[1-(2-phenylethyl)-4-piperidinyl]-2-propenamide

A11	Valeryl Fentanyl	N-phenyl-N-[1-(2-phenylethyl)-4-piperidinyl]-pentanamide
B2	(+/-)-trans-3-methyl Fentanyl	*trans*-N-[3-methyl-1-(2-phenylethyl)-4-piperidinyl]-N-phenyl-propanamide
B3	*meta*-Fluorofentanyl	N-(3-fluorophenyl)-N-[1-(2-phenylethyl)-4-piperidinyl]-propanamide
B4	*para*-fluoro Methoxyacetyl Fentanyl	N-(4-fluorophenyl)-2-methoxy-N-[1-(2-phenylethyl)-4-piperidinyl]-acetamide
B5	Isovaleryl Fentanyl	3-methyl-N-phenyl-N-[1-(2-phenylethyl)-4-piperidinyl]-butanamide
B6	*ortho*-Methylfentanyl	N-(2-methylphenyl)-N-[1-(2-phenylethyl)-4-piperidinyl]-propanamide
B7	*para*-Fluorofentanyl	N-(4-fluorophenyl)-N-[1-(2-phenylethyl)-4-piperidinyl]-propanamide
B8	Tetrahydrofuran Fentanyl 3-Tetrahydrofurancarboxamide	tetrahydro-N-phenyl-N-[1-(2-phenylethyl)-4-piperidinyl]-3-furancarboxamide
B9	(+/-)-cis-3-methyl Butyryl Fentanyl	cis-N-[3-methyl-1-(2-phenylethyl)-4-piperidinyl]-N-phenyl-butanamide
B10	β-methyl Fentanyl	N-phenyl-N-[1-(2-phenylpropyl)-4-piperidinyl]-propanamide
B11	(+/-)-cis-3-methyl Thiofentanyl	cis-N-[3-methyl-1-(2-thienyl)ethyl]-4-piperidinyl]-N-phenyl-propanamide
C2	*para*-methoxy Acrylfentanyl	N-(4-methoxyphenyl)-N-[1-(2-phenylethyl)-4-piperidinyl]-2-propenamide
C3	*ortho*-methoxy Butyryl Fentanyl	N-(2-methoxyphenyl)-N-[1-(2-phenylethyl)-4-piperidinyl]-butanamide
C4	*meta*-methyl Methoxyacetyl Fentanyl	2-methoxy-N-(3-methylphenyl)-N-[1-(2-phenylethyl)-4-piperidinyl]-acetamide

C5	*ortho*-Fluorofentanyl	N-(2-fluorophenyl)-N-[1-(2-phenylethyl)-4-piperidinyl]-propanamide
C6	Remifentanil	4-(methoxycarbonyl)-4-[(1-oxopropyl)phenylamino]-1-piperidinepropanoic acid, methyl ester
C7	*para*-Chlorobutyryl Fentanyl	N-(4-chlorophenyl)-N-[1-(2-phenylethyl)-4-piperidinyl]-butanamide
C8	Ethoxyacetyl Fentanyl	2-ethoxy-N-phenyl-N-[1-(2-phenylethyl)-4-piperidinyl]-acetamide
C9	(+/-)-trans-3-methyl Thiofentanyl	trans-N-3-methyl-1-(2-(thiophen-2-yl)ethyl)piperidin-4-yl)-N-phenylpropionamide
C10	*meta*-fluoro Methoxyacetyl Fentanyl	N-(3-fluorophenyl)-2-methoxy-N-[1-(2-phenylethyl)-4-piperidinyl]-acetamide
C11	*para*-fluoro Furanyl Fentanyl	N-(4-fluorophenyl)-N-[1-(2-phenylethyl)-4-piperidinyl]-2-furancarboxamide

Table 25. Table of components of Plate 2 of the Cayman Chemical Fentanyl Analog Screening Kit

Plate Location	Fentanyl Analog Chemical Name	Formal Chemical Name
D2	FIBF	N-(4-fluorophenyl)-2-methyl-N-[1-(2-phenylethyl)-4-piperidinyl]-propanamide
D3	*para*-fluoro Cyclopentyl Fentanyl	N-(4-fluorophenyl)-N-[1-(2-phenylethyl)-4-piperidinyl]-cyclopentanecarboxamide
D4	*ortho*-methyl Phenyl Fentanyl	N-(2-methylphenyl)-N-[1-(2-phenylethyl)-4-piperidinyl]-benzamide
D5	*para*-fluoro Valeryl Fentanyl	N-(4-fluorophenyl)-N-[1-(2-phenylethyl)-4-piperidinyl]-pentanamide
D6	*para*-methyl Methoxyacetyl Fentanyl	2-methoxy-N-(4-methylphenyl)-N-[1-(2-phenylethyl)-4-piperidinyl]-acetamide

D7	Cyclohexyl Fentanyl	N-phenyl-N-[1-(2-phenylethyl)-4-piperidinyl]-cyclohexanecarboxamide
D8	*para*-methoxy Valeryl Fentanyl	N-(4-methoxyphenyl)-N-[1-(2-phenylethyl)-4-piperidinyl]-pentanamide
D9	Sufentanil	N-[4-(methoxymethyl)-1-[2-(2-thienyl)ethyl]-4-piperidinyl]-N-phenyl-propanamide
D10	α'-Methoxy Fentanyl	2-methoxy-N-phenyl-N-[1-(2-phenylethyl)-4-piperidinyl]-propanamide
D11	*para*-chloro Furanyl Fentanyl	N-(4-chlorophenyl)-N-[1-(2-phenylethyl)-4-piperidinyl]-2-furancarboxamide
E2	*para*-methyl Furanyl Fentanyl	N-(4-methylphenyl)-N-[1-(2-phenylethyl)-4-piperidinyl]-2-furancarboxamide
E3	4'-fluoro, *para*-fluoro (+/-)-trans-3-methyl Fentanyl	*trans*-N-1-(4-fluorophenethyl)-3-methylpiperidin-4-yl)-N-(4-fluorophenyl)propionamide
E4	*para*-methoxy Tetrahydrofuran Fentanyl	tetrahydro-N-(4-methoxyphenyl)-N-[1-(2-phenylethyl)-4-piperidinyl]-2-furancarboxamide
E5	*para*-methoxy Furanyl Fentanyl	N-(4-methoxyphenyl)-N-[1-(2-phenylethyl)-4-piperidinyl]-2-furancarboxamide
E6	*meta*-methyl Furanyl Fentanyl	N-(3-methylphenyl)-N-[1-(2-phenylethyl)-4-piperidinyl]-2-furancarboxamide
E7	*para*-chloro Cyclopentyl Fentanyl	N-(4-chlorophenyl)-N-[1-(2-phenylethyl)-4-piperidinyl]-cyclopentanecarboxamide
E8	Norcarfentanil	4-[(1-oxopropyl)phenylamino]-4-piperidinecarboxylic acid, methyl ester
E9	*para*-fluoro Tetrahydrofuran Fentanyl	N-(4-fluorophenyl)tetrahydro-N-[1-(2-phenylethyl)-4-piperidinyl]-2-furancarboxamide
E10	2,2,3,3-tetramethyl Cyclopropyl Fentanyl	2,2,3,3-tetramethyl-N-phenyl-N-[1-(2-phenylethyl)-4-piperidinyl]-cyclopropanecarboxamide

E11	Furanylethyl Fentanyl	N-[1-[2-(2-furanyl)ethyl]-4-piperidinyl]-N-phenyl-propanamide
F2	Benzyl Fentanyl	N-phenyl-N-[1-(phenylmethyl)-4-piperidinyl]-propanamide
F3	Thienyl Fentanyl	N-phenyl-N-[1-(2-thienylmethyl)-4-piperidinyl]-propanamide
F4	Acrylfentanyl	N-phenyl-N-[1-(2-phenylethyl)-4-piperidinyl]-2-propenamide
F5	*ortho*-Isopropyl Furanyl Fentanyl	N-[2-(1-methylethyl)phenyl]-N-[1-(2-phenylethyl)-4-piperidinyl]-2-furancarboxamide
F6	*para*-chloro Valeryl Fentanyl	N-(4-chlorophenyl)-N-[1-(2-phenylethyl)-4-piperidinyl]-pentanamide
F7	Thiofentanyl	N-phenyl-N-[1-[2-(2-thienyl)ethyl]-4-piperidinyl]-propanamide
F8	N-Benzyl Furanyl Norfentanyl	N-phenyl-N-[1-(phenylmethyl)-4-piperidinyl]-2-furancarboxamide
F9	N-Methyl Norcarfentanil	1-methyl-4-[(1-oxopropyl)phenylamino]-4-piperidinecarboxylic acid, methyl ester
F10	Benzyl Acrylfentanyl	N-phenyl-N-[1-(phenylmethyl)-4-piperidinyl]-2-propenamide
F11	2'-fluoro *ortho*-Fluorofentanyl	N-(2-fluorophenyl)-N-[1-[2-(2-fluorophenyl)ethyl]-4-piperidinyl]-propanamide

Table 26. Table of components of the Emergent Panel Version 1 of the Cayman Chemical Fentanyl Analog Screening Kit

Plate Location	Fentanyl Analog Chemical Name	Formal Chemical Name
A2	Acetyl Fentanyl	N-phenyl-N-[1-(2-phenylethyl)-4-piperidinyl]-acetamide
A3	U-47700	*trans*-3,4-dichloro-N-[2-(dimethylamino)cyclohexyl]-N-methyl-benzamide

A4	U-49900	*trans*-3,4-dichloro-N-[2-(diethylamino)cyclohexyl]-N-methyl-benzamide
A5	*meta*-methyl Cyclopropyl Fentanyl	N-(3-methylphenyl)-N-[1-(2-phenylethyl)-4-piperidinyl]-cyclopropanecarboxamide
A6	*para*-methyl Cyclopentyl Fentanyl	N-(4-methylphenyl)-N-[1-(2-phenylethyl)-4-piperidinyl]-cyclopentanecarboxamide
A7	*para*-methoxy Acetyl Fentanyl	N-(4-methoxyphenyl)-N-[1-(2-phenylethyl)-4-piperidinyl]-acetamide
A8	Furanyl Norfentanyl	N-phenyl-N-4-piperidinyl-2-furancarboxamide
A9	Fentanyl Methyl Carbamate	methyl (1-phenethylpiperidin-4-yl)(phenyl)carbamate
A10	Cyclopentenyl Fentanyl	N-phenyl-N-[1-(2-phenylethyl)-4-piperidinyl]-1-cyclopentene-1-carboxamide
A11	U-48800	*trans*-2-(2,4-dichlorophenyl)-N-2-(dimethylamino)cyclohexyl)-N-methylacetamide
B2	4'-Fluorofentanyl	N-[1-[2-(4-fluorophenyl)ethyl]-4-piperidinyl]-N-phenyl-propanamide
B3	β-Hydroxy Fentanyl	N-[1-(2-hydroxy-2-phenylethyl)-4-piperidinyl]-N-phenyl-propanamide
B4	MT-45	1-cyclohexyl-4-(1,2-diphenylethyl)-piperazine
B5	*para*-methyl Butyryl Fentanyl	N-(1-phenethylpiperidin-4-yl)-N-(p-tolyl)butyramide
B6	Norsufentanil	N-[4-(methoxymethyl)-4-piperidinyl]-N-phenyl-propanamide
B7	β-Hydroxythioacetylfentanyl	N-[1-[2-hydroxy-2-(2-thienyl)ethyl]-4-piperidinyl]-N-phenyl-acetamide
B8	Senecioylfentanyl	3-methyl-N-phenyl-N-[1-(2-phenylethyl)-4-piperidinyl]-2-butenamide
B9	Isopropyl U-47700	*trans*-3,4-dichloro-N-2-(dimethylamino)cyclohexyl)-N-isopropylbenzamide
B10	N,N-Dimethylamido-despropionyl Fentanyl	N,N-dimethyl-N'-phenyl-N'-[1-(2-phenylethyl)-4-piperidinyl]-urea

B11	AH-7921	3,4-dichloro-N-[[1-(dimethylamino)cyclohexyl]methyl]-benzamide
C2	*para*-methoxy Methoxyacetyl Fentanyl	2-methoxy-N-(4-methoxyphenyl)-N-[1-(2-phenylethyl)-4-piperidinyl]-acetamide
C3	Heptanoyl Fentanyl	N-(1-phenethylpiperidin-4-yl)-N-phenylheptanamide
C4	Tetrahydrothiophene Fentanyl	tetrahydro-N-phenyl-N-[1-(2-phenylethyl)-4-piperidinyl]-2-thiophenecarboxamide
C5	4-Phenyl Fentanyl	N-phenyl-N-[4-phenyl-1-(2-phenylethyl)-4-piperidinyl]-propanamide
C6	Phenoxyacetyl Fentanyl	2-phenoxy-N-phenyl-N-[1-(2-phenylethyl)-4-piperidinyl]-acetamide
C7	2-Fluoro MT-45	1-cyclohexyl-4-[1-(2-fluorophenyl)-2-phenylethyl]-piperazine
C8	Furanyl Fentanyl	N-phenyl-N-[1-(2-phenylethyl)-4-piperidinyl]-2-furancarboxamide
C9	2,3-Seco-Fentanyl	N-[1-methyl-3-[methyl(2-phenylethyl)amino]propyl]-N-phenyl-propanamide
C10	N-(3-Ethylindole) Norfentanyl	N-[1-[2-(1H-indol-3-yl)ethyl]-4-piperidinyl]-N-phenyl-propanamide
C11	Hexanoyl Fentanyl	N-phenyl-N-[1-(2-phenylethyl)-4-piperidinyl]-hexanamide

Table 27. Table of components of the Emergent Panel Version 2 of the Cayman Chemical Fentanyl Analog Screening Kit

Plate Location	Fentanyl Analog Chemical Name	Formal Chemical Name
A2	U-48520	*trans*-4-chloro-N-[2-(dimethylamino)cyclohexyl]-N-methyl-benzamide
A3	3'-methyl Acetyl Fentanyl	N-[1-[2-(3-methylphenyl)ethyl]-4-piperidinyl]-N-phenyl-acetamide
A4	4-Phenyl U-51754	N-[2-(dimethylamino)cyclohexyl]-N-methyl-*trans*-[1,1'-biphenyl]-4-acetamide

A5	2'-methyl Acetyl Fentanyl	N-[1-[2-(2-methylphenyl)ethyl]-4-piperidinyl]-N-phenyl-acetamide
A6	(±)-cis-3-methyl Norfentanyl	*cis*-N-(3-methyl-4-piperidinyl)-N-phenyl-propanamide
A7	*meta*-methyl Acetyl Fentanyl	N-(3-methylphenyl)-N-[1-(2-phenylethyl)-4-piperidinyl]-acetamide
A8	U-51754	*trans*-3,4-dichloro-N-[2-(dimethylamino)cyclohexyl]-N-methyl-benzeneacetamide
A9	(±)-cis-Isofentanyl	*cis*-N-[3-methyl-1-(phenylmethyl)-4-piperidinyl]-N-phenyl-propanamide
A10	U-47931E	*trans*-4-bromo-N-2-(dimethylamino)cyclohexyl]-benzamide
A11	U-48753E	*trans*-N-(3,4-dichlorophenyl)-N-[(1R,2R)-2-(dimethylamino)cyclopentyl]-propanamide, 2Z-butenedioate
B2	*meta*-fluoro Furanyl Fentanyl	N-(3-fluorophenyl)-N-(1-phenethylpiperidin-4-yl)furan-2-carboxamide
B3	3,4-Methylenedioxy U-47700	*trans*-N-2-(dimethylamino)cyclohexyl)-N-methylbenzo[d][1,3]dioxole-5-carboxamide
B4	3,4-Ethylenedioxy U-51754	*trans*-2-(2,3-dihydrobenzo[b][1,4]dioxin-6-yl)-N-(2-(dimethylamino)cyclohexyl)-N-methylacetamide
B5	3,4-Ethylenedioxy U-47700	*trans*-N-2-(dimethylamino)cyclohexyl)-N-methyl-2,3-dihydrobenzo[b][1,4]dioxine-6-carboxamide
B6	N-methyl U-47931E	*trans*-4-bromo-N-[2-(dimethylamino)cyclohexyl]-N-methyl-benzamide
B7	2'-methyl Fentanyl	N-[1-[2-(2-methylphenyl)ethyl]-4-piperidinyl]-N-phenyl-propanamide, monohydrochloride

B8	Propyl U-47700	*trans*-3,4-dichloro-N-2-((dimethylamino)cyclohexyl)-N-propylbenzamide
B9	N-Desmethyl U-47700	*trans*-3,4-dichloro-N-methyl-N-[2-(methylamino)cyclohexyl]-benzamide
B10	3'-methyl Fentanyl	N-[1-[2-(3-methylphenyl)ethyl]-4-piperidinyl]-N-phenyl-propanamide
B11	N,N-Didesmethyl U-47700	*trans*-N-2-(aminocyclohexyl)-3,4-dichloro-N-methylbenzamide 2,2,2-trifluoroacetate
C2	Remifentanil Acid	4-(methoxycarbonyl)-4-[(1-oxopropyl)phenylamino]-1-piperidinepropanoic acid, 2,2,2-trifluoroacetate
C3	N-Benzyl Phenyl Norfentanyl	N-phenyl-N-[1-(phenylmethyl)-4-piperidinyl]-benzamide
C4	*para*-fluoro 4-ANBP	N-(4-fluorophenyl)-1-(phenylmethyl)-4-piperidinamine
C5	Despropionyl *para*-Fluorofentanyl	N-(4-fluorophenyl)-1-(2-phenylethyl)-4-piperidinamine
C6	Despropionyl *meta*-Methylfentanyl	N-(3-methylphenyl)-1-(2-phenylethyl)-4-piperidinamine
C7	N-Benzyl *para*-fluoro Norfentanyl	N-(4-fluorophenyl)-N-[1-(phenylmethyl)-4-piperidinyl]-propanamide
C8	Despropionyl 2'-fluoro *ortho*-Fluorofentanyl	1-(2-fluorophenethyl)-N-(2-fluorophenyl)piperidin-4-amine
C9	U-50488	*trans*-3,4-dichloro-N-methyl-N-[(1R,2R)-2-(1-pyrrolidinyl)cyclohexyl]-benzeneacetamide
C10	N-methyl Norfentanyl	N-(1-methyl-4-piperidinyl)-N-phenyl-propanamide
C11	N-Benzyl *para*-fluoro Cyclopropyl Norfentanyl	N-(4-fluorophenyl)-N-[1-(phenylmethyl)-4-piperidinyl]-cyclopropanecarboxamide
D2	*para*-Bromofentanyl	N-(4-bromophenyl)-N-[1-(2-phenylethyl)-4-piperidinyl]-propanamide
D3	*para*-Toluoyl Fentanyl	4-methyl-N-(1-phenethylpiperidin-4-yl)-N-phenylbenzamide

Table 28. Table of components of the Emergent Panel Version 3 of the Cayman Chemical Fentanyl Analog Screening Kit

Plate Location	Fentanyl Analog Chemical Name	Formal Chemical Name
F2	N-(MDA) Fentanyl	N-(1-(1-(benzo[d][1,3]dioxol-5-yl)propan-2-yl)piperidin-4-yl)-N-phenylpropionamide
F3	N-(Phentermine) Fentanyl	N-(1-(2-methyl-1-phenylpropan-2-yl)piperidin-4-yl)-N-phenylpropionamide
F4	N-(6-APB) Fentanyl	N-(1-(1-(benzofuran-6-yl)propan-2-yl)piperidin-4-yl)-N-phenylpropionamide
F5	N-(6-APDB) Fentanyl	N-(1-(1-(2,3-dihydrobenzofuran-6-yl)propan-2-yl)piperidin-4-yl)-N-phenylpropionamid
F6	N-(2-APB) Fentanyl	N-(1-(1-(benzofuran-2-yl)propan-2-yl)piperidin-4-yl)-N-phenylpropionamide
F7	2',5'-Dimethoxy Fentanyl	N-(1-(2,5-dimethoxyphenethyl)piperidin-4-yl)-N-phenylpropionamide
F8	N-(2C-E) Fentanyl	N-(1-(4-ethyl-2,5-dimethoxyphenethyl)piperidin-4-yl)-N-phenylpropionamide
F9	N-(2C-B) Fentanyl	N-(1-(4-bromo-2,5-dimethoxyphenethyl)piperidin-4-yl)-N-phenylpropionamide
F10	N-(2C-C) Fentanyl	N-(1-(4-chloro-2,5-dimethoxyphenethyl)piperidin-4-yl)-N-phenylpropionamide
F11	N-(2C-P) Fentanyl	N-(1-(2,5-dimethoxy-4-propylphenethyl)piperidin-4-yl)-N-phenylpropionamide
G2	N-(2C-T-7) Fentanyl	N-(1-(2,5-dimethoxy-4-(propylthio)phenethyl)piperidin-4-yl)-N-phenylpropionamide
G3	N-(2C-D) Fentanyl	N-(1-(2,5-dimethoxy-4-methylphenethyl)piperidin-4-yl)-N-phenylpropionamide

G4	N-(2C-G) Fentanyl	N-(1-(2,5-dimethoxy-3,4-dimethylphenethyl)piperidin-4-yl)-N-phenylpropionamide
G5	N-(2C-I) Fentanyl	N-(1-(4-iodo-2,5-dimethoxyphenethyl)piperidin-4-yl)-N-phenylpropionamide
G6	N-(2C-iP) Fentanyl	N-(1-(4-isopropyl-2,5-dimethoxyphenethyl)piperidin-4-yl)-N-phenylpropionamide
G7	N-(2C-N) Fentanyl	N-(1-(2,5-dimethoxy-4-nitrophenethyl)piperidin-4-yl)-N-phenylpropionamide
G8	N-(2C-T) Fentanyl	N-(1-(2,5-dimethoxy-4-(methylthio)phenethyl)piperidin-4-yl)-N-phenylpropionamide
G9	N-(2C-T-2) Fentanyl	N-(1-(4-(ethylthio)-2,5-dimethoxyphenethyl)piperidin-4-yl)-N-phenylpropionamide
G10	N-(2C-T-4) Fentanyl	N-(1-(4-(isopropylthio)-2,5-dimethoxyphenethyl)piperidin-4-yl)-N-phenylpropionamide
G11	N-(2C-TFM) Fentanyl	N-(1-(2,5-dimethoxy-4-(trifluoromethyl)phenethyl)piperidin-4-yl)-N-phenylpropionamide
H2	N-(2C-B-fly) Fentanyl	N-(1-(2-(8-bromo-2,3,6,7-tetrahydrobenzo[1,2-b:4,5-b']difuran-4-yl)ethyl)piperidin-4-yl)-N-phenylpropionamide
H3	N-(3C-B-fly) Fentanyl	N-(1-(1-(8-bromo-2,3,6,7-tetrahydrobenzo[1,2-b:4,5-b']difuran-4-yl)propan-2-yl)piperidin-4-yl)-N-phenylpropionamide
H4	N-(3,4,5-TMA) Fentanyl	N-phenyl-N-(1-(1-(3,4,5-trimethoxyphenyl)propan-2-yl)piperidin-4-yl)propionamide
H5	N-(2,5-DMA) Fentanyl	N-(1-(1-(2,5-dimethoxyphenyl)propan-2-yl)piperidin-4-yl)-N-phenylpropionamide
H6	N-(DOC) Fentanyl	N-(1-(1-(4-chloro-2,5-dimethoxyphenyl)propan-2-

		yl)piperidin-4-yl)-N-phenylpropionamide
H7	N-(DOB) Fentanyl	N-(1-(1-(4-bromo-2,5-dimethoxyphenyl)propan-2-yl)piperidin-4-yl)-N-phenylpropionamide
H8	N-(DOI) Fentanyl	N-(1-(1-(4-iodo-2,5-dimethoxyphenyl)propan-2-yl)piperidin-4-yl)-N-phenylpropionamide
H9	N-(DOM) Fentanyl	N-(1-(1-(2,5-dimethoxy-4-methylphenyl)propan-2-yl)piperidin-4-yl)-N-phenylpropionamide
H10	N-(DOET) Fentanyl	N-(1-(1-(4-ethyl-2,5-dimethoxyphenyl)propan-2-yl)piperidin-4-yl)-N-phenylpropionamide
H11	N-(DOBU) Fentanyl	N-(1-(1-(4-butyl-2,5-dimethoxyphenyl)propan-2-yl)piperidin-4-yl)-N-phenylpropionamide

Table 29. Table of components of the Emergent Panel Version 4 of the Cayman Chemical Fentanyl Analog Screening Kit

Plate Location	Fentanyl Analog Chemical Name	Formal Chemical Name
A2	Despropionyl *ortho*-Fluorofentanyl	N-(2-fluorophenyl)-1-(2-phenylethyl)-4-piperidinamine
A3	4-Piperidone	4-piperidinone
A4	2',4' – dimethoxy Fentanyl	N-(1-(2,4-dimethoxyphenethyl)piperidin-4-yl)-N-phenylpropionamide
A5	O-Desmethyl-cis-tramadol	*el*-3-[(1R,2R)-2-[(dimethylamino)methyl]-1-hydroxycyclohexyl]-phenol
A6	3',4' – dimethoxy Fentanyl	N-(1-(3,4-dimethoxyphenethyl)piperidin-4-yl)-N-phenylpropionamide
A7	2-methyl AP-237	1-[2-methyl-4-(3-phenyl-2-propen-1-yl)-1-piperazinyl]-1-butanone
A8	Tianeptine	7-[(3-chloro-6,11-dihydro-6-methyl-5,5-

		dioxidodibenzo[c,f][1,2]thiazepin-11-yl)amino]-heptanoic acid
A9	Piperidylthiambutene	1-(1-methyl-3,3-di-2-thienyl-2-propen-1-yl)-piperidine
A10	Isotonitazene	N,N-diethyl-2-[[4-(1-methylethoxy)phenyl]methyl]-5-nitro-1H-benzimidazole-1-ethanamine
A11	*meta*-fluoro Valeryl fentanyl	N-(3-fluorophenyl)-N-(1-phenethylpiperidin-4-yl)pentanamide
B2	*meta*-fluoro Acrylfentanyl	N-(3-fluorophenyl)-N-[1-(2-phenylethyl)-4-piperidinyl]-2-propenamide
B3	Metonitazene	N,N-diethyl-2-[(4-methoxyphenyl)methyl]-5-nitro-1H-benzimidazole-1-ethanamine
B4	4-Anilino-1-benzylpiperidine	N-phenyl-1-(phenylmethyl)-4-piperidinamine
B5	4-Anilino-1-Boc-piperidine	4-(phenylamino)-1-piperidinecarboxylic acid, 1,1-dimethylethyl ester
B6	*para*-chloro Furanyl fentanyl 3-furancarboxamide	N-(4-chlorophenyl)-N-[1-(2-phenylethyl)-4-piperidinyl]-3-furancarboxamide
B7	Thiophene fentanyl 3-thiophenecarboxamide	N-phenyl-N-[1-(2-phenylethyl)-4-piperidinyl]-3-thiophenecarboxamide
B8	3'-Fluorofentanyl	N-[1-[2-(3-fluorophenyl)ethyl]-4-piperidinyl]-N-phenyl-propanamide
B9	*ortho*-fluoro Valeryl fentanyl	N-(2-fluorophenyl)-N-[1-(2-phenylethyl)-4-piperidinyl]-pentanamide
B10	4-methyl Fentanyl	N-(4-methyl-1-phenethylpiperidin-4-yl)-N-phenylpropionamide
B11	Cyclopropaneacetyl fentanyl	2-cyclopropyl-N-(1-phenethylpiperidin-4-yl)-N-phenylacetamide
C2	Etinotazene	2-[(4-ethoxyphenyl)methyl]-N,N-diethyl-5-nitro-1H-benzimidazole-1-ethanamine

C3	*para*-Chloroacetyl fentanyl	N-(4-chlorophenyl)-N-(1-phenethylpiperidin-4-yl)acetamide
C4	2-fluoro Viminol	α-[[*bis*(1-methylpropyl)amino]methyl]-1-[(2-fluorophenyl)methyl]-1H-pyrrole-2-methanol
C5	*para*-hydroxy Butyryl fentanyl	N-(4-hydroxyphenyl)-N-[1-(2-phenylethyl)-4-piperidinyl]-butanamide
C6	2'-Fluorofentanyl	N-[1-[2-(2-fluorophenyl)ethyl]-4-piperidinyl]-N-phenyl-propanamide
C7	AP-237	1-[4-(3-phenyl-2-propen-1-yl)-1-piperazinyl]-1-butanone
C8	*meta*-methoxy Furanyl fentanyl	N-(3-methoxyphenyl)-N-[1-(2-phenylethyl)-4-piperidinyl]-2-furancarboxamide
C9	Brorphine	1-[1-[1-(4-bromophenyl)ethyl]-4-piperidinyl]-1,3-dihydro-2H-benzimidazol-2-one
C10	2,3-Benzodioxole fentanyl	N-(1-phenethylpiperidin-4-yl)-N-phenylbenzo[d][1,3]dioxole-4-carboxamide
C11	3'-fluoro *ortho*-Fluorofentanyl	N-(2-fluorophenyl)-N-[1-[2-(3-fluorophenyl)ethyl]-4-piperidinyl]-propanamide
D2	Tigloyl fentanyl	(E)-2-methyl-N-(1-phenethylpiperidin-4-yl)-N-phenylbut-2-enamide
D3	2',3'-dimethoxy Fentanyl	N-(1-(2,3-dimethoxyphenethyl)piperidin-4-yl)-N-phenylpropionamide
D4	N-Benzyl-4-piperidone	1-(phenylmethyl)-4-piperidinone
D5	2',6'-dimethoxy Fentanyl	N-(1-(2,6-dimethoxyphenethyl)piperidin-4-yl)-N-phenylpropionamide
D6	NPP	1-(2-phenylethyl)-4-piperidinone
D7	3',5'-dimethoxy Fentanyl	N-(1-(3,5-dimethoxyphenethyl)piperidin-4-yl)-N-phenylpropionamide
D8	AP-238	1-(4-cinnamyl-2,6-dimethylpiperazin-1-yl)propan-1-one

D9	4-Anilinopiperidine	N-phenyl-4-piperidinamine
D10	Unused	
D11	Unused	

Figure 43. The GC-MS and GC-IR fentanyl spectral libraries published in the FIU Research Data Portal, 2022. Available at doi.org/10.34703/gzx1-9v95/A68TVK

Table 30. Table of description of chemical description of cannabinoids used in the study.

Cannabinoid Name	Molecular Weight	IUPAC Name
CBD	314	2-[1R-3-methyl-6R-(1-methylethenyl)-2-cyclohexen-1-yl]-5-pentyl-1,3-benzenediol
CBG	316	2-[(2E)-3,7-dimethyl-2,6-octadien-1-yl]-5-pentyl-1,3-benzenediol
CBN	310	6,6,9-trimethyl-3-pentyl-6H-dibenzo[b,d]pyran-1-ol
Δ^8-THC	314	6aR,7,10,10aR-tetrahydro-6,6,9-trimethyl-3-pentyl-6H-dibenzo[b,d]pyran-1-ol
Δ^9-THC	314	6aR,7,8,10aR-tetrahydro-6,6,9-trimethyl-3-pentyl-6H-dibenzo[b,d]pyran-1-ol
JWH122-2 methylnaphthyl isomer	355	(2-methylnaphthalen-1-yl)(1-pentyl-1H-indol-3-yl)methanone
JWH122-3 methylnaphthyl isomer	355	(3-methylnaphthalen-1-yl)(1-pentyl-1H-indol-3-yl)methanone
JWH122-6 methylnaphthyl isomer	355	(6-methylnaphthalen-1-yl)(1-pentyl-1H-indol-3-yl)methanone
JWH122-8 methylnaphthyl isomer	355	(8-methylnaphthalen-1-yl)(1-pentyl-1H-indol-3-yl)methanone
JWH 081-3 methoxynaphthyl isomer	371	(3-methoxynaphthalen-1-yl)(1-pentyl-1H-indol-3-yl)methanone
JWH 081-6 methoxynaphthyl isomer	371	(6-methoxynaphthalen-1-yl)(1-pentyl-1H-indol-3-yl)methanone
JWH 081-7 methoxynaphthyl isomer	371	(7-methoxynaphthalen-1-yl)(1-pentyl-1H-indol-3-yl)methanone

VITA

KIMIKO C. FERGUSON

Born: Belize City, Belize

2003	A.S., Biology and Chemistry St. John's College Junior College Belize City, Belize
2007	B.S, Biology University of Belize Belmopan, Belize
2007-2009	Lecturer St. John's College Junior College Belize City, Belize
2011	M.S., Biotechnology University at Buffalo Buffalo, New York
2012-2014	Teacher St. Catherine Academy Belize City, Belize
2014-2018	Assistant Director – Forensic Laboratory (Acting Executive Director 2017-2018) Belize National Forensic Science Service Ladyville, Belize
2021	M.S., Chemistry Florida International University Miami, Florida
2018-Present	Graduate Teaching/Research Assistant Florida International University Miami, Florida

PUBLICATIONS AND PRESENTATIONS (* Corresponding author)

1. K Ferguson, J Perr, S Tupik, M Gilbert, R Newman, A Winokur, I Vallejo, S Hokanson, M Pothier, B Knapp, M Icard, K Kramer, and JR Almirall*. An Interlaboratory Study to Evaluate the Utility of Gas Chromatography Mass

Spectrometry (GC-MS) and Gas Chromatography Infrared Spectroscopy (GC-IR) Spectral Libraries in the Forensic Analysis of Fentanyl Related Substances (FRS). *Journal of Forensic Science,* In press, 2023.

2. JR Almirall and K Ferguson, "FIU Mass Spectrometry and Infrared Libraries of Fentanyl Related Substances." *FIU Research Data Portal*, Version 2, 2022.

3. K Ferguson and JR Almirall. Utility of gas chromatography vapor-phase infrared spectroscopy (GC-VIR) for the identification of positional isomers of fentanyl related substances (FRS) and cannabinoids. *Southeastern Regional American Chemical Society (SERMACS) Meeting*. San Juan, Puerto Rico. October 19-22, 2022.

4. K Ferguson, J Perr, S Tupik, H Haddad, M Gilbert, R Newman and JR Almirall. Utility of Gas Chromatography Infrared Spectroscopy (GC-IR) for the Differentiation of Positional Isomers of Fentanyl Related Substances. *Center for Advanced Research in Forensic Science (CARFS) 10th Industry Advisory Board (IAB) Meeting*. Livermore, California. June 15-17 , 2022.

5. K Ferguson. Utility of Gas Chromatography Infrared Spectroscopy (GC-IR) for the Differentiation of Positional Isomers of Fentanyl Related Substances and Draft ASTM Method for Fentanyl Related Substances Analysis Using GC-IR. *Organization of Scienctific Area Committees (OSAC) Seized Drug Scientific Area Committee Meeting.* Orlando, Florida. June 13-17, 2022.

6. K Ferguson, J Perr, S L.Tupik, H Haddad, M Gilbert, R Newman and JR Almirall*. Utility of Gas Chromatography Infrared Spectroscopy (GC-IR) for the Differentiation of Positional Isomers of Fentanyl Related Substances. *Forensic Chemistry*.(2022) 29, 100425

7. K Ferguson, M Gilbert, R Newman and JR Almirall. Utility of Gas Chromatography Infrared Spectroscopy (GC-IR) for the Differentiation of Positional Isomers of Fentanyl Related Substances. *American Academy of Forensic Science Annual Conference*. Seattle, Washington. February 21-25, 2022.

8. K Ferguson and J Almirall. Development of a GC-IR Library for the Identification of Fentanyl Analogues. *Current Trends in Seized Drug Analysis* Online Symposium. January 20, 2021.

9. K Ferguson, A Yadav, S Morey, J Abdullah, G Hrysenko, J Ying Eng, M Sajjad, S Koury, K Rittenhouse-Olson*. Preclinical studies with JAA-F11 anti-Thomsen-Friedenreich monoclonal antibody for human breast cancer. *Future Oncology*. (2014) 10(3), 385-399.